University of Nottingham

UK | CHINA | MALAYSIA

The Role of the Calpain/Calpastatin System in Breast Cancer

Liam Cook

(BSc)

Thesis Submitted to the University of Nottingham for the Degree of Master of Research

September 2023

Acknowledgements

I would like to sincerely thank my supervisors Professor Stewart Martin and Dr Sarah Storr for their support and invaluable guidance throughout my study. I am grateful for their excellent supervision that kept motivated me every day.

I would like also to thank my colleagues Muazzez Yilmaz, Megan Greener, Tangkam Marak and Sophie Williams for the supportive and encouraging environment throughout my study and for making the days in the lab much more enjoyable.

I express my greatest gratitude to my parents, Mr Ian Cook and Mrs Deborah Cook, for their unconditional care and guidance. Their guidance inspired and motivated me to choose this path and to keep me going through times of self-doubt.

Abstract

Background: Breast cancer is the most prevalent cancer in the UK, with 55,000 cases every year, making up 15% of cases annually. The number of cases is estimated to rise to 69,900 cases per year by 2038-2040. Breast cancer can be classified into different subtypes which each have a different prognosis. Triple-Negative breast cancer has the worst prognosis when compared to other molecular subtypes of Luminal A/B and HER2+. A common treatment option of breast cancer is radiotherapy often used in conjunction with chemotherapy. Calpains are ubiquitously expressed proteases with various physiological functions. The calpain system has been reported to play a role in cancer including breast cancer. The effects of targeting the calpain system in breast cancer have been explored but need further assessment.

Method: The effect of commercially available calpain inhibitors were assessed in two triple negative breast cancer cell lines (MDA-MB-231 and MDA-MB-468) using clonogenic survival assays, with and without the added treatment of calcium ionophore to activate the calpain system. The IC50 dose for PD150606 was taken forward for a combination radiation and PD150606 to assess for any increase in radio response. RNAseq data of Calpastatin II (CASTII) overexpression cell lines (MDA-MB-231 and T47D) were also assessed. Differentially expressed genes (DEGs) were identified and analysed for any significant association with survival using the METABRIC cohort and assessed for correlation with Calpastatin (CAST) probes. DEGs of interest were shortlisted for validation.

Results: The effect of the calpain inhibitors, Calpeptin and PD150606, was shown to be cytotoxic to breast cancer cells as a single agent. There was a high increase in cell killing in cells treated with calcium ionophore prior to the treatment of the calpain inhibitors, with at the highest doses displayed around 80-90% cell killing. The combination of PD150606 and radiation was attempted but yielded erroneous results due to undetermined reasons and could not be repeated due to the time limitations. A large number of DEGs were identified and associated significantly with survival in the METABRIC cohort. A smaller number of these DEGs correlated with the CAST Probes. CACNA2D4, NONO and CEBPB were selected to take forward for verification with western blots and qRT-PCR, however time limitations meant this was not completed.

Conclusions: The calpain system as a target in breast cancer has shown interesting effects. The cytotoxicity as a result of the activation of the calpain system prior to treatment indicates that inhibiting the calpain system activate produces a significantly increased response. This can be applied to hypoxia where there is an increased level of calpain activity, potentially provided an option for tumours with hypoxic regions. DEGs affected by the calpastatin overexpression have been shown to be important in breast cancer specific survival, however, need further investigation to understand the mechanism by which the calpain system affects these genes.

Abbreviations

AC	Adenocarcinomas
ALCAM	Activated leukocyte cell adhesion molecule
AT1	Angiotensin II receptor type 1
ATG	Autophagy-related
ATP	Adeno triphosphate
BCT	Breast Conserving Therapy
BMI	Body Mass Index
BRCA1	Breast Cancer Gene 1
BRCA2	Breast cancer gene 2
C5ORF46	Chromosome 5 Open Reading Frame 46
CACNA2D4	Calcium Voltage-Gated Channel Auxiliary Subunit Alpha2delta 4
CAPN1	Calpain 1
CAPN2	Calpain 2
CAPNS1	Calpain 4
CASP3	Caspase 3
CAST	Calpastatin
CEBPA	CCAAT enhancer-binding protein alpha
CEBPB	CCAAT enhancer-binding protein beta
CHK1	Checkpoint Kinase 1
CRT	Conformal Radiation Therapy
CRUK	Cancer Research UK
CT	Computed Tomography
DCIS	Ductal Carcinoma in situ
DDX53	DEAD-Box Helicase 53
DEG	Differentially Expressed Genes
DMSO	Dimethyl-sulfoxide
DSB	Double Strand Break
E2F8	E2F Transcription Factor 8
EBRT	External Bean Radiotherapy
EGFR	Epidermal growth factor
EGR	Early Growth Response
EGR1	Early Growth Response 1
EMT	Epithelial-Mesenchymal Transition
EPHA3	Ephrin tyrosine kinase a3
ER	Estrogen Receptor
ERK	Extracellular signal-regulated kinase
ESBC	Early Stage Invasive Breast Cancer
FHL1	Four And A Half LIM Domains 1
FISH	Fluorescence in situ hybridization
FLRT2	Fibronectin Leucine Rich Transmembrane Protein 2
FN1	Fibronectin 1

GATA1	GATA Binding Protein 1
GSK3B	Glycogen Synthase Kinase 3 Beta
HDAC1	Histone deacetylase 1
HER	Human Epidermal Growth Factor
HER2	Human Epidermal Growth Factor 2
HR	Hormone Receptor
HRT	Hormone Replacement Therapy
HWBI	Hypofractionated Whole Breast Irradiation
IDC	Invasive Ductal Carcinoma
IHC	Immunohistochemistry
IL	Interleukin
IL13	Interleukin-13
IL6	Interleukin-6
ILC	Invasive Lobular Carcinoma
IPA	Ingenuity Pathway Analysis
IRF7	Interferon Regulatory Factor 7
ITM2A	Integral membrane protein 2A
LABC	Locally Advanced Breast Carcinoma
LAP	Liver-enriched transcriptional activator protein
LCIS	Lobular Carcinoma in Situ
LINC00200	Long Non coding RNA 00200
LINC02582	Long Non coding RNA 02582
LQ	Linear Quadratic
LRRC61	Leucine rich repeat containing 61
LVI	Lymphovascular invasion
MAGEB2	Melanoma-associated antigen B2
MAP	MUTYH-associated polyposis
MTC	Metronomic chemotherapy
MYC	MYC Proto-Oncogene
MYCL	MYC Proto-Oncogene - L
NHS	National Health Service
NLRP3	NLR Family Pyrin Domain Containing 3
NONO	Non-POU Domain Containing Octamer Binding
PAGE5	P Antigen Family Member 5
PAK5	P21 (RAC1) Activated Kinase
PARP	Poly [ADP-ribose] polymerase 1
PBS	Phosphate Buffered Saline
PCR	Polymerase Chain Reaction
PE	Plating Efficiency
PGM5	Phosphoglucomutase 5
PMRT	Postmastectomy radiation therapy
PR	Progesterone Receptor
ROS	Reactive Oxygen Species
SD	Standard Deviation

SF	Surviving Fraction
SF2	Surviving Fraction at 2 Gray
SH3BGRL	SH3 Domain Binding Glutamate Rich Protein Like
SIX2	SIX Homeobox 2
SMAD	Suppressor mother against decapentaplegic
SPARC	Secreted Protein Acidic And Cysteine Rich
SREBP	Sterol regulatory element binding proteins
STAT3	Signal Transducer And Activator Of Transcription 3
STR	Short tandem repeat
TAGLN	Transgelin
TFDP3	Transcription Factor Dp Family Member 3
TGF	Transforming growth factor
THBS2	Thrombospondin 2
TMA	Tissue Microarray
TN	Triple Negative
TNBC	Triple Negative Breast Cancer
TREML2	Triggering Receptor Expressed On Myeloid Cells Like 2
USP7	Ubiquitin specific peptidase 7
WBI	Whole Breast Irradiation
WNT5A	Wnt Family Member 5A

Table of Contents

List of Figures and Tables

Chapter 1: Introduction

1.1 Breast Cancer

Breast cancer is the most prevalent cancer in the UK, with 55,000 cases per year, making up 15% of cancer cases (Katsura *et al.,* 2022). It more commonly occurs in women than in men, with 99% compared to 1%, respectively (Cancer Research UK, 2022). Breast cancer is the second most common cause of death from cancer in women, with 5- and 10-year survival rates of 85% and 76% (Cancer Research UK, 2022). Projections of breast cancer estimate that between 2038-2040 there will be 69,900 new cases of breast cancer annually compared to 55,900 cases between 2016-2018 in the UK (CRUK, 2022).

There are various different risk factors associated with breast cancer, some of which can be reduced or avoided, others cannot be. Age has an important role in cancer in particularly breast cancer, in the UK 24% of breast cancer cases were in the 75+ age group. Whilst age plays a role in breast cancer for male and females there is a stronger association with females, incidence rates at the 30-34 age group are 2066 times higher in females compared to males. The rise in incidence rates is also affected by age and gender, with the steepest rise for females between ages 35 and 39 and 65 to 69 in males (Cancer Research UK, 2022). Gender is also a major risk factor in breast cancer, with women having the biggest risk of the disease. This is because of the higher chance of hormone irregularities and exposure to hormones that have been associated with breast cancer (NHS, 2022). Other hormone exposures can also increase the risk of breast cancer, post-menopausal women have twice the risk in comparison to those with the highest level of sex hormones compared to the lowest level (Stapelkamp *et al.*, 2011). Examples of sex hormones include oestrogen, progesterone and testosterone. Exposure to sex hormones is also through the use of the contraceptive pill, which uses a synthetic sex hormone which has been shown to increase the risk of breast cancer with continuous use. A 7% increase per 5 years of use and 14% increase per 10 years of use (Wu and Zhu, 2015). Hormone replacement therapy (HRT) is another route of exposure to sex hormones, increasing the risk of breast cancer. A study by the Collaborative Group on Hormonal Factors in Breast Cancer (2019) found that risk is 37% higher in oestrogen only HRT and is 112% higher in oestrogen-progesterone HRT compared to no HRT. Lifestyle factors are also a huge risk factor with breast

cancer, this includes obesity, alcohol consumption and smoking. Alcohol intake at a moderate level increases risk by 30-50%, it is believed that alcohol increases the level of oestrogen thereby increasing risk (McDonald, Goyal and Terry, 2013). Studies found that there was a 7-13% higher risk for current smokers and 6-9% increase for former smokers (Gaudet *et al.*, 2013). Obesity is also linked to breast cancer; this has differing risk factors depending on if a woman is post or pre-menopausal. Post-menopausal women have an increased risk of breast cancer the higher their body mass index is (BMI) 13% higher per 5-units of BMI. In contrast in the same study, Kyrgiou *et al.*, 2017, they found that breast cancer is 8% lower in pre-menopausal per 5-unit BMI. Genetic mutations have a vital role in the progression and risk of breast cancer, BRCA1 and BRCA2 mutations increase the risk of breast cancer. BRCA1 is a

tumour suppressor gene and has many different roles including DNA damage repair, transcription regulations and cell cycle control, the transcriptional targets of BRCA1 also exhibit tumour suppressor properties (Buckley and Mullan, 2012). BRCA2 is also tumour suppressor genes and has functions including homologous recombination, G2 checkpoint control, protection of stalled replication forks and promoting cellular resistance to DNA damage (Andreassen *et al*., 2021). Mutations in these genes increase the risk of breast cancer. With a BRCA1 mutation the risk of developing breast cancer by age 70 is between 44% to 78%, with BRCA2 this risk is between 31% to 56% (Casaubon, Kashyap and Regan, 2023).

Subtype	Description
Ductal Carcinoma in situ (DCIS)	Tumour is located in the ducts of the breast and is non-invasive but increases risk of invasive carcinoma
Lobular Carcinoma in situ (LCIS)	Tumour is located in the lobules, similar to DCIS, it is not invasive but does increase the risk
Invasive Ductal Carcinoma (IDC)	The tumour has spread from the from the ducts and is now considered invasive
Invasive Lobular Carcinoma (ILC)	The tumour originating in the lobules has spread and is now classified as an invasive carcinoma
Inflammatory Breast Cancer	A rarer form of breast cancer, caused by cancer cells blocking the lymph vessels making the breast inflamed
Angiosarcoma	Starts in cells that line the blood or lymph vessels
Paget Disease of Breast	The tumour starts in the milk ducts that spreads to the nipple then the areola

Table 1.1.1 Summary of breast cancer subtypes defined by the location the tumour originates in.

When diagnosing breast cancer different subtypes of the disease can be identified, with the histological subtypes being used as one classification system, and with each subtype having varying prognosis. 95% of breast cancers are adenocarcinomas (AC) and are the most common histological breast cancer group. Descriptions of the various subgroups are shown in Table 1.1.1

Invasive ductal carcinoma (IDC) is a malignant carcinoma and accounts for 55% of all invasive carcinomas (Makki, 2015). There is a high morphological variation with IDC, and they are also classified into subtypes with varying prevalence, some of these include medullary carcinoma, tubular carcinoma, and mucinous carcinoma. The other type of invasive carcinoma is invasive lobular carcinoma (ILC), usually associated with Lobular Carcinoma in situ (LCIS), it forms a single file structure making the surgical margins more difficult to find as the size of the tumour is not easy to determine (McCart Reed *et al.,* 2021).

Breast cancer can also be classified into four widely accepted molecular subtypes; Luminal A, luminal B, HER2+, and Triple-negative (Perou *et al.,* 2000). Each of the subtypes have a different prognosis and treatment options. Luminal A is the most common molecular subtype, accounting got 50-60% of breast cancers (Yersal and Baructa, 2014). Luminal A also shows the best survival after 10 years with a 70% survival rate (Kennecke *et al.,* 2010). Luminal A is associated with a low tumour grade and a good prognosis. It is defined by high expression of estrogen receptor (ER) and/or high progesterone receptor (PR) expression but is negative for human epidermal growth factor 2 (HER2). Luminal B has a higher grade and is more aggressive than luminal A and shares similar hormone expression of ER and PR this can also express HER2. ER and PR positivity is defined as the expression of ER and PR receptors on the tumour allowing the tumour to utilise these hormones. The prognosis of luminal B is significantly worse than luminal A, with recurrence rates being higher, 6.8% compared to 5.3% (Ahn *et al.,* 2015). Both of these subtypes can receive, as discussed below, antihormone treatments targeting the receptors present on the cancer cells. Triple negative (TN) is the most aggressive molecular subtype of breast cancer with the lowest survival rate of the molecular subtypes (Hennigs *et al.,* 2016). TN breast cancer does not express any hormone receptors therefore is resistant to hormone targeting therapy, and as it is also negative for HER2 expression anti-HER2 therapies are ineffective, limiting treatment to surgery, radiotherapy, and conventional

chemotherapy regimens, however some novel treatment options are under evaluation (e.g., PARP inhibitors, anti-PD-L1 immunotherapy etc).

While subtypes can be used for guidance in choosing the right therapy for a patient the clinical presentation of breast cancer can also influence the choice of treatments. The most common clinical presentation is early-stage invasive breast cancer (ESBC), accounting for 62% of cases (Vondeling *et al.,* 2018). It has an overall survival rate of 90% (NICE, 2018). Locally advanced breast cancer (LABC) is cancer that has not spread beyond the breast or local lymph nodes, it accounts for approximately 49% of cases and has a mortality rate of 41%-62% (Vondeling *et al.,* 2018). Metastatic breast cancer also affects the course of treatment for the patient. Metastatic cancer is described as a cancer that has spread to another region of the body; this drastically negatively affects prognosis. There are estimates of 57000 people living in England with metastatic breast cancer (Palmeri *et al.,* 2022), and has a 10-year survival rate of 6%-9% (Vondeling *et al.,* 2018). This presentation of breast cancer decreases the effectiveness of local therapies due to the cancer no longer being 'local', leaving systemic treatments to be the only effective option (Waks and Winer, 2019).

1.2 Breast Cancer Treatments

Local therapies for ESBC are commonly used. Breast conserving therapy (BCT) is an effective treatment strategy, involving a lumpectomy (wide local incision) followed by whole breast irradiation (WBI). This type of therapy aims to reduce cosmetic alterations, while also being effective in the treatment of breast cancer. This therapy is only effective if the patient can receive radiotherapy and attend follow-ups to detect any recurrence (Moo *et al.,* 2018). If the tumour size is not suitable for BCT neoadjuvant chemotherapy is used to reduce the size of the tumour before a lumpectomy. The adjuvant radiation given after the lumpectomy is used to eliminate any residual cancer cells. Mastectomy is another form of local therapy. The majority of mastectomies are classified into three distinct types. Standard mastectomies involve the removal of all of the breast tissue and the skin covering it. Skin-sparing mastectomies have all of the breast tissue and the nipple removed leaving most of the skin behind. Nipple-sparing mastectomies are the same as the skin-sparing procedure, but the

nipple is not removed (Nava *et al.,* 2009). A study conducted by Chen *et al.,* (2015) to compare the effectiveness of BCT+ radiotherapy (RT) with mastectomy ± RT, found that BCT with RT was more effective than a mastectomy without RT, however with radiotherapy there was a similar overall survival rate. Potentially following on from a mastectomy is postmastectomy radiation therapy (PMRT). It is used in the treatment of advanced breast cancer, the procedure is standard for patients with four or more positive auxiliary lymph nodes and/or a tumour size of greater than 5cm, as there is an increased risk of recurrence in these patients.

Radiotherapy is a fundamental part of breast cancer treatment; it involves using radiation either internally (brachytherapy) or externally (external beam radiotherapy, EBRT) to damage the DNA in the cancer cells, resulting in cell death. EBRT is by far the most common type of radiotherapy. In the UK, the conventional method of radiotherapy has historically been WBI (whole breast irradiation), delivered in 15 daily fractions over 3 weeks, to a total dose of 40Gy. Another form of radiotherapy is hypofractionated whole breast irradiation (HWBI) this differs slightly from conventional WBI in that it uses higher dosages and takes a smaller number of sessions. Wei *et al.,* (2020) conducted a review of clinical trials of HWBI and found it to be safer, more cost efficient, and reduce the time required while still being as effective as WBI. The FAST forward trials developed a quicker regimen of radiotherapy bringing down the dosage of 26 or 27Gy in 5 fractions over 1 week (Brunt *et al.,* 2020) and has, partially due to the global pandemic, been rapidly adopted across UK radiotherapy centres. These trials however have only had short terms effects observed long term studies are yet to be conducted for this regimen of radiotherapy. Internal radiotherapy includes brachytherapy. This treatment has radioactive material sealed in catheters or seeds and placed in the tumour or at the tumour bed after removal, allowing high doses of radiation to be delivered into small areas (Kauer-Dorner and Berger, 2018). A number of additional methods, and altered fractionation regimes, are under evaluation. Irrespective of the method, and regime, used with radiotherapy comes the possibility of healthy tissue also being irradiated causing side effects. Early responses to radiation mimic the response to wound healing, in contrast, late response to radiation can include vascular damage, induced fibrosis, and endocrine effects and can often be life-threatening (Bentzen, 2006).

Systemic therapy is the use of drugs that function throughout the whole body. These treatments include chemotherapy, hormone therapy, targeted therapy, and immunotherapy. Chemotherapy is the use of cytotoxic drugs to kill cancer cells, commonly used in metastatic breast cancer because of the systemic ability of chemotherapeutic drugs. Chemotherapy drugs are used singularly, in combination, or sequentially (Sachdev and Jahanzeb, 2016). Combination chemotherapy also known as polychemotherapy is the most established method of chemotherapy for breast cancer with an alkylating agent, such as cyclophosphamide, and an antimetabolite, such as 5-fluorouracil. Bonadonna *et al.,* (1976) found that polychemotherapy significantly reduced the recurrence of the tumour. A combination of cyclophosphamide, epirubicin and fluorouracil is given over a 21-day cycle with six cycles. In a day cyclophosphamide and fluorouracil is given in a dose of 500mg/m2, and epirubicin at 100mg/m2. Neoadjuvant chemotherapy is also proven to be an effective treatment option, docetaxel used before BCT showed an enhanced clinical response rate while also conserving more of the breast (Hey *et al.,* 2002). Along with combining different cytotoxic agents' chemotherapy can also be combined with targeting therapy. However, there are a varying number of potential side effects associated with chemotherapy, including nausea, hair loss, and fatigue. A major side effect of chemotherapy is the loss of white blood cells, this leads to a higher risk of infections in patients undergoing chemotherapy (Schirrmacher, 2018).

Targeting therapy involves drugs that target receptors that are expressed on the tumour such as HER2+. Trastuzumab is a monoclonal antibody against HER2 receptors, the creation of this drug significantly improved the prognosis of HER2+ patients when paired with chemotherapy as the initial course of treatment (Cameron *et al.,* 2017). The regimen for Trastuzumab in the UK is 6mg/kg through intravenous infusion and is then observed for the next 21 days to monitor for any adverse side effects. The possible side effects for HER2 targeted drugs are primarily mild but can cause cardiotoxicity which in turn may result in heart failure (Onitilo, Engel and Stankowski, 2014). The risk of this occurring can be reduced by clinicians monitoring the cardiovascular system of patients undergoing HER2+ targeting treatment. A number of next generation Traztumab based agents are becoming available (e.g., Trastuzumab-Deruxtucan, Trastuzumab-Duocarmazine, Margetuximab) (Mezni *et al.,* 2020). Targeting therapies are also used for patients with a mutated BRCA gene, an example of one class of

such drugs are the PARP inhibitors. These agents (e.g., Olaparib) prevent the PARP protein from repairing DNA (notably single strand breaks), which combined with the mutated BRCA gene (that causes defective double strand break (DSB) DNA repair) prevents full DNA repair and leads to cancer cell death (Cortesi, Rugo and Jackisch, 2021). As normal cells have functional DSB repair these agents are well tolerated and cause minimal side effects – use in such scenarios is termed a 'synthetic lethality' approach. The function of PARP inhibitors also sensitises the tumour to chemo- and radiotherapy providing another option for combination therapy. Olaparib is used clinically to effectively treat metastatic triple negative breast cancer (Robson *et al.,* 2017).

Hormone therapy is another possible treatment option for breast cancer, in HR-positive patients. Tamoxifen is a widely used hormone therapy. It functions by inhibiting the estrogen receptors and will therefore only work on ER+ breast cancers (Yang *et al.,* 2013). Tamoxifen is taken daily for at least 5 years; in some cases, the drug is taken daily for 10 years. Trials have shown that taking tamoxifen for the extended period of 10 years decreases mortality and recurrence, with mortality almost halved in comparison to 5 years. Compliance with the drug regimen can, however, significantly affect clinical outcome with patients unintentionally or intentionally not taking the medication, due to side-effects such as induction of a premature menopause and an increased risk of endometrial cancer (Yang *et al.,* 2013, Schulz *et al.,* 2018). The inhibition of ER by the drug, in premenopausal women, is highly effective at preventing cancer cell growth and division. Aromatase inhibitors are another hormone therapy that lower the levels of estrogen by inhibiting the aromatase enzyme, which produces estrogen. Therefore, reducing the ability for cancers to grow. This is particularly effective if a woman is postmenopausal, with the majority of estrogen being made via aromatase in body fat (Fabian, 2007). An example of an aromatase inhibitor is letrozole, this drug is taken in 2.5mg tablet taken once a day (NHS, 2022). The side effects of aromatase inhibitors need to be considered when using the drug, as the downregulation of estrogen will affect bone structure and health, leading to an increased risk of fractures and osteoporosis (Rachner *et al.,* 2020).

Novel treatments for breast cancer are continuously being developed, through developing entirely new methods (e.g., cancer vaccines) or refining the types of treatment already available, such as new chemotherapy drugs or altered ways of administering radiotherapy. Immunotherapy is the use of drugs to make a patient's immune system attack the cancer cells, Pembrolizumab is a monoclonal antibody that targets PD-1 a protein that is present on T cells that normally prevents them from attacking other cells. This then encourages the immune system to attack the breast cancer cells (Emens, Kok and Ojalvo, 2016). This drug has been showing promising results in treating metastatic TN breast cancer, which previously had a reduced number of options for treatment (Emens, 2018). Advances have also been made in radiotherapy and not just in the delivery of the radiation but also in the way to plan the administering of the radiation. Computed Tomography (CT) imaging allows a clinician to determine the best course of radiotherapy that is effective against the tumour as well as protecting vital organs around the breast such as the lungs. This paired with 3-D conformal radiation therapy (3D-CRT) allows for the radiation beam to match the shape of the tumour, therefore, reducing the off-target effects of the radiation (Bradley and Mendenhall, 2018). An antibody-drug conjugate is a novel hybrid drug that uses the targeting ability of a monoclonal antibody with the lethality of a chemotherapeutic agent. These drugs function by seeking out and binding to the specific antigen on a tumour, then delivering the cytotoxic agents that are attached, killing the cancer cell (Barzaman *et al.,* 2020). This new system of drugs can provide be as effective as chemotherapy while also significantly reducing the off target and side effects. Part of the tumour, in particular when the tumours are large, becomes hypoxic meaning there is an average of 1-2% oxygen present in this part of the tumour (Muz *et al.,* 2015) as opposed to 1 -13% in normal tissue, however this will vary depending on the tissue type (Carreau *et al.,* 2011). This has been shown to negatively affect chemotherapy and radiotherapy. A number of agents targeting hypoxia are currently under development, either as single agents or in combination with conventional treatments (Aiyappa, 2020). Certain naturally occurring compounds have also been found to sensitise these hypoxic areas of a tumour to radiotherapy or chemotherapy. Curcumin and naringenin in combination were found to have a radiosensitising effect in breast cancer by causing cell cycle arrest, leading to a reduction in tumour volume (Askar *et al.,* 2021). A novel treatment strategy called metronomic chemotherapy (MTC) is a potential alternative to regular chemotherapy. MTC involves administering small doses of chemotherapeutic agents but at more frequent

intervals, this is believed to have an anti-angiogenic and anti-proliferative effect on tumours, therefore preventing the growth of the tumour (Cazzaniga *et al.,* 2019). Margetuximab is a novel HER2+ targeting monoclonal antibody, clinical trials have found that it had a higher binding specificity than trastuzumab and can maintain its activity in low expression of HER2 (Bang *et al.,* 2017). This new monoclonal antibody has the potential to replace trastuzumab primary choice for targeting therapy in HER2+ cancer. Another protein that has shown promising results for targeting to improve conventional therapy, or to act as a new single modality, is calpain. Altered calpain system protein expression has been shown to be of prognostic importance across a range of cancers, including breast cancer, and is discussed further below.

1.3 The Calpain/Calpastatin System

Calpain is a calcium dependent cysteine protease that is involved in a diverse range of cellular processes. These processes also have a role in different pathologies such as neurodegenerative diseases, cardiac disease and cancer (Ono, Saido and Sorimachi, 2016). First described in 1964 by Dr Gordon Guroff (Guroff, 1964), the discovery led to further research of calpains and characterised a family of related proteases. There are currently 14 known human isoforms of calpain, the most extensively researched isoforms are micro(μ)-calpain and milli(m)-calpain, the μ- and m- referring to the levels of Ca^{2+} required for full activation. These are heterodimers made up of one large (80kDa) catalytic subunit and a regulatory subunit (30kDa). μ-calpain is encoded by CAPN1 and m-calpain is encoded by CAPN2, with the common regulatory subunit encoded by CAPNS1 (Suzuki *et al.,* 2004).

μ-calpain is also known as Calpain-1, m-calpain known as Calpain-2, and the protein encoded by CAPNS1 is known as Calpain-4. The catalytic subunit of calpain consists of 4 domains (I-IV) and the regulatory subunit consists of 2 domains (V-VI) as shown in figure 1.3.1. Domain I undergoes autolysis when activated by calcium. Domain II is split into sub domains IIa and IIb when binding with calcium ions form domain II that contains a catalytic cleft (Storr *et al.,* 2011). Domain III is involved in structural changes when the endogenous inhibitor of calpain, calpastatin, binds (Hanna *et al.,* 2008). Domains IV and VI contain 5 penta-EF hands with the last EF hand on both domains making the protein a heterodimer and domain V is described as

a hydrophobic domain (Goll *et al.,* 2003). Micro(μ)- and milli(m)- refer to the concentrations of calcium required for full activation of the respective protease isoform.

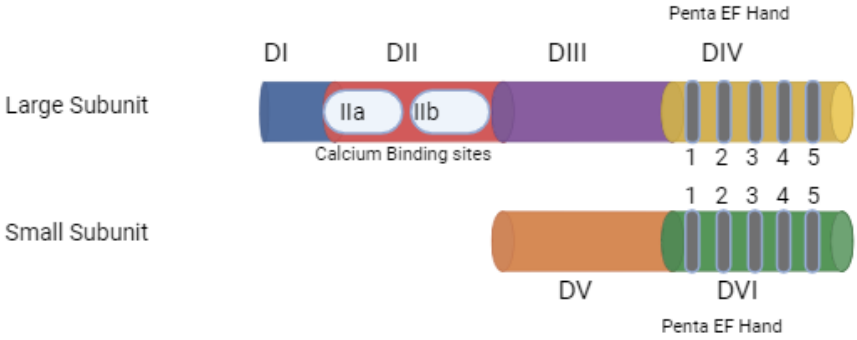

Figure 1.3.1 The structure of calpain, showing the six domains present in the structure and the penta-EF hands. Ca^{2+} binding site shown in domain II. (Adapted from Khorchid and Ikura, 2002) Created with BioRender.com

Calpains are strictly regulated and are activated by the presence of calcium ions and also through growth factors activation via ERK/MAP Kinase signalling pathways (Perrin and Huttenlocher, 2002). This tight regulation of calpains is managed through the calcium dependence, autoproteolytic cleavage, phosphorylation, and phospholipid interactions (Hanna *et al.,* 2008). Calcium binds at various locations in calpains, four locations in DIV and DVI domains, three in DIII and 2 in DIIa/b (Yoder, Wright and Borzok, 2023). Crucial to the physiological function is the binding to DIII, this forms the proteolytic site in between domain IIa and IIb (Strobl *et al.*, 2000). Proteolysis is also a route of activation of calpains, through autolysis or other calpains cleaving. Calpain-3 undergoes autolysis in its catalytic site for it to undergo its physiological processes (Taveau *et al.*, 2003). However, calpain-1 cleaves calpain-2 at both its N-terminus and protease core, therefore raising the calpain-2 activity (Hosfield *et al.*, 1999). Phosphoinositide also regulate calpains, the phospholipids bind to DIII lowering the amount of calcium required for autolysis. V_{max} of calpain-1-driven proteolytic reactions are also enhanced by the binding of phosphoinositide (Yoder, Wright and Borzok, 2023).

Regulation of calpain is also managed through its endogenous inhibitor calpastatin. Calpastatin, or CAST (Fig. 1.3.2), is made up of an L domain with an N-terminal XL region and four inhibitor domains (I-IV) (Goll *et al.,* 2003). Within each of the four inhibitory domains are 3 subdomains A, B and C. Subdomain B is believed to be the inhibitory part of the domain

while A and C improve the affinity of the interactions (Takano *et al.,* 1995). Calpastatin is encoded for by one gene rather than many like calpains and is regulated by alternative promoters or through alternative splicing leading to different isoforms, types I-IV (Parr *et al.,* 2004). Type I and II have the L domain but different N-terminal sequences, type III is from a promoter of an untranslated region of the exon 1u causing the L domain to lack an XL region and type IV is testis specific and lacks the L domain and inhibitory domain I (Storr *et al.,* 2011). When there is no requirement for calcium dependent proteolysis, calpastatin is stored in large aggregates (Averna *et al.*, 2003). With an influx of calcium, calpastatin moves into the cytosol to inhibit calpains. The subdomains bind to domain IV and VI of calpain and the B subdomain binds to domain II preventing any further catalytic activity from occurring (Kovacs and Su, 2014).

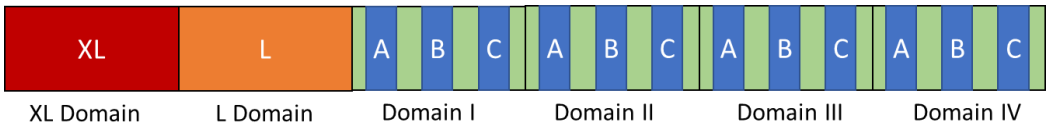

Figure 1.3.2 The structure of calpastatin. The domain structure with six domains. The four inhibitor domains (I-IV) are divided into 3 subdomains A, B and C.

There are many distinct roles of calpain within the cell one of which is cell migration, through calpains' involvement with intracellular signalling pathways it can alter cell adhesions and cytoskeletal components (Perrin and Huttenlocher, 2002). This varies depending on the cell type with the inhibition of calpains in endothelial cells and lymphocytes preventing them spreading compared to fibroblasts which stabilises focal adhesion and inhibits rear detachment. This effect is brought on through the modification of adhesive structures. Calpain can directly cleave focal adhesion protein which regulates adhesion complex disassembly leading to rear cell detachment (Franco and Huttenlocher, 2005). Calpains can also influence membrane protrusion, Franco *et al.,* (2004) showed that knocking down calpain 2 in fibroblasts resulted in abnormal cell membrane protrusions revealing dependency on calpain 2 for normal cell morphology. Calpain also plays a role in apoptosis and has been shown to regulate it in various cell types. Vindis *et al.,* (2005) showed that in microvascular endothelial cells, calpain activation leads to apoptosis. Ca2+ increased and induced calpain activation, leading to BH3-interacting domain death agonist (Bid) cleavage, cytochrome c release, and caspase 3 activation, therefore resulting in apoptosis. ATG proteins induce autophagy, however this process however is also mediated by calpains, through calpain-1 cleaving the

ATG protein thereby regulating ATG5-ATG12 conjugates and in turn preventing autophagy (Kaminskyy and Zhivotovsky, 2012).

1.3.1 The Calpain/Calpastatin System in Disease

The calpain/calpastatin system is known to be dysregulated in many different diseases including, as mentioned, neurodegenerative disease, cardiac disease, and cancer. In cardiac disease the dysregulation of calcium ion controls, within the myocardium, leads to disrupted myocardial functions and cell viability (Sandmann *et al.,* 2002). Calpains have also been shown to contribute to fibrosis in the cardiac system. The binding of angiotensin II to the AT1 receptor activates epidermal growth factor receptors (EGFR) which in turn activate calpains. Downstream of EGFR activation the calpains can cleave latent transforming growth factor-β (TGF-β) activating Suppressor of Mothers against Decapentaplegic (SMAD) through a signalling cascade, resulting in collagen synthesis and fibrosis (Letavernier *et al.,* 2012). The calpain system is also linked to myocarditis with calpain-1 translocation to the mitochondria causing decreased ATP synthesis, overproduction of ROS and activating an inflammasome leading to pyroptosis (Liu *et al.*, 2022).

Calpains also play a role in the pathogenesis of Parkinson's disease. Calpains are widely expressed within the brain, calpains cleave and aggregate the protein α-synuclein (α-syn). α-syn is a toxic substance that leads to the formation of Lewy's bodies that contribute to neuronal death (Gao *et al.,* 2022). Therefore, increased level of calcium ions results in the downstream progression of Parkinson's disease. The upregulation of calpains is also found to be present in Alzheimer's disease, this causes various effect on the pathology of the disease such as increasing the number of amyloid beta aggregates on the neurons (Mahaman *et al.*, 2019).

1.3.2 The Calpain/Calpastatin System in Cancer

The calpain/calpastatin system is widely expressed by cancer cells and is involved in a variety of processes (Storr *et al*., 2011). Expression has been linked to tumour progression including,

as mentioned above, in breast cancer. A study conducted by Storr *et al.,* (2012) showed that in triple-negative or basal-like breast cancers a high expression level of calpain 2 was linked with a decreased breast cancer survival compared to low expression, which showed a comparable survival rate to non-basal or receptor positive breast cancers. The calpain system has also been linked to lymphovascular invasion (LVI) in breast cancer (the earliest stage of metastasis), a study analysing gene expression via gene expression microarray analysis of 91 breast cancer patients for association with LVI, identified 89 transcripts to be significantly associated with LVI – one of these, significantly downregulated, was calpastatin. Calpastatin was selected for further investigation, as it had the lowest selection error, and samples underwent real-time PCR and immunohistochemistry verification. This revealed that calpastatin has a significant association with LVI (Storr *et al.,* 2011) and has been verified using additional independent patient cohorts. Low calpain-9 has also been shown to be associated with an adverse effect on breast cancer survival after endocrine therapy (Davis *et al.,* 2014). The inflammatory breast cancer subtype is also affected by calpains, a study conducted by Storr *et al.,* (2016) found that low calpain-1 and calpastatin expression is associated with a negative effect on survival following neoadjuvant chemotherapy. The studies described above describe some of the studies linking the expression of calpain with breast cancer prognosis, additional studies in other cancer types show such associations i.e., including Ovarian, Prostate, and Lung cancers (Zhang *et al*., 2019), (Xu *et al*., 2019) (Mamoune *et al*., 2003). Such studies indicate the potential for the calpain/calpastatin system as a therapeutic target, by developing in vitro models and assessing changes in calpains and the effect that this has on conventional or novel treatments of breast cancer.

Recent unpublished data from the current group suggest that inhibition of the calpain system can sensitise hypoxic breast cancer cells to radiotherapy - this needs further investigation. It is also unclear how the different CAST isoforms function to regulate the various signalling pathways and processes in breast cancer cells. Having cloned and overexpressed the different CAST isoforms their function needs to be more fully explored.

1.4 Aims and Objectives

1.4.1 Hypotheses and Aims.

Hypothesis 1: Inhibiting calpain activity will improve breast cancer treatment response to conventional radiotherapy.

Aim 1: To assess the ability of calpain inhibitors in sensitising breast cancer cell lines to radiotherapy.

Hypothesis 2: Overexpressing the CAST II isoform will alter gene expression having downstream effects and in turn influence disease specific survival in TNBC (MDA-MB-231) and Luminal (T47D) breast cancer cell line models and provide a comparison between two subtypes of breast cancer.

Aim 2: To assess the differentially expressed genes (DEG) data obtained from RNAseq of CAST overexpression cell lines (MDA-MB-231 and T47D) for clinically significant changes in gene expression when calpastatin is overexpressed and validate these findings by Q-RT-PCR and Western blotting..

1.4.2 Objectives:

1. To assess the ability of calpain inhibitors to sensitise breast cancer cell lines the following objectives will be carried out:
    - Assess conventional calpain inhibitors effect on clonogenic survival with and without calcium ionophore activation.
    - Assess the combination of the calpain inhibitors and ionising radiation on clonogenic survival of the breast cancer cells with and without calcium ionophore activation.

2. To assess the RNAseq data of the CAST overexpression cell lines the following objectives will be carried out:

- Identify DEGs of interest from the RNAseq data of the CAST overexpression cell lines versus respective wildtype controls.
- Assess DEGs using bioinformatic programs including cBioPortal and Ingenuity Pathway Analysis (IPA)
- Validate the genes of interest in breast cancer cell lines via Q-RT-PCR and Western blotting.

Chapter 2: Materials & Methods

2.1 Methods for Objective 1:

2.1.1 Cell Culture:

The breast cancer cell lines MDA-MB-231 and MDA-MB-468 were used to assess the effect of calpain inhibitors to increase killing when exposed to ionising radiation. MDA-MB-231 and MDA-MB-468 were cultured in Minimal Essential Medium (MEM) (Sigma, UK) and supplemented with 1% non-essential amino acids (Sigma, UK) , 2-mM of L-glutamine (Sigma, UK), 1% penicillin/streptomycin (Sigma, UK), and 10% iron-supplemented donor bovine serum (Gibco). The cell cultures were maintained in an incubator at 37°C and 5% CO2 and used over a passage window of 12. Monthly mycoplasma tests were conducted to ensure cells were infection free and STR cell line authentication and verification conducted approximately every 6 months.

Cells were passaged upon reaching 70-80% confluency into a T-25cm^2, T-75cm^2, or T-175cm^2 flask depending on experimental requirements. The passage involved removing the media from the flask, washing with phosphate-buffered saline (PBS) (Sigma, UK), then detaching cells by covering with trypsin (0.05%) (Sigma, UK) for 4 minutes. Following this, trypsin was inactivated using complete media and then split accordingly (1:2, 1:3, 1:5, or 1:10). For long-term storage, cells were grown to 70-80% confluency, trypsinised (Sigma, UK), inactivated with media, then counted on a haemocytometer. The suspension was then centrifuged at 1000rpm for 5 minutes. A 2x10^6 cells/ml suspension was prepared in 10% dimethyl sulfoxide (DMSO), and 500µl was aliquoted into cryovials. The cryovials were placed into a -80°C freezer

overnight in a Mr Frosty container and then transferred to liquid nitrogen for long-term storage. The retrieval of the cells from liquid nitrogen was conducted by thawing the cryovial and pipetting cells into a Falcon tube containing 5ml of complete media, and this was centrifuged to remove DMSO. The supernatant was aspirated, and the pellet was resuspended in 1ml complete media then added to 4ml of complete media in a T-25cm^2 flask and incubated.

2.1.2 Cell Growth Curves for Cell Proliferation Assay

Growth Curves were used to calculate the doubling times for each cell line to confirm the cells were growing correctly. A 6-well plate was seeded with 1x10^5 cells/ml and placed in an incubator at 37°C and 5% CO_2, and this was done in triplicate. Over a period of 96 hours, at every 24 hours, selected wells were aspirated of the media and washed in 1ml PBS, then trypsinised (500µl) for 4 minutes and inactivated with new complete media. The cells were counted on a haemocytometer, and following this, the average cell count was plotted on a graph, with time on the x-axis and cell number on the y-axis. This allowed for the doubling time to be calculated from the exponential portion of the growth curve.

2.1.3 Plating Efficiency for Clonogenic Assay

The cells collected from the proliferation assay at the 24-hour point were serially diluted to make concentrations of 100 and 200 cells/ml. Three flasks of 100 and 200 cells were prepared in T-25cm^2 flasks and incubated at 37°C and 5% CO_2 for 14 days (MDA-MB-231) or 21 days (MDA-MB-436). After the incubation period, flasks were aspirated, washed in PBS, fixed with 50% methanol for 15 minutes, and then 100% methanol for another 15 minutes. Finally, the colonies were stained with 0.5% crystal violet. The flasks were washed with distilled water and left to dry before counting the colonies. The colonies were counted, and the plating efficiency was calculated by the number of colonies x100 divided by the number of cells plated. A colony with more than 50 cells was counted as a survivor. Plating efficiency (PE) was calculated as:

$$PE(\%) = \frac{Number\ of\ Colonies\ Formed\ x\ 100}{Number\ of\ Cells\ Plated}$$

2.1.4 Preparation of Calpain Inhibitors

The calpain inhibitors PD150606 (Sigma-Aldrich) and Calpeptin (Merck) were made into stock solutions 5mg of Calpeptin and PD150606 was dissolved with DMSO and a stock solution of 10mM of Calpeptin and 10mM of PD150606 was made. These were then aliquoted to avoid the need for repeated thawing and freezing of the drugs were then stored at -20°C. 1mg of Calcium Ionophore (Sigma-Aldrich) was prepared with DMSO to a stock solution of 10mM and stored at 4°C. 2.5mg of Doxorubicin (Sigma-Aldrich) was measured and then prepared in DMSO to a stock solution of 50mM and stored at -20°C.

2.1.5 Clonogenic Assays for Calpain Inhibitors

Once cells were confirmed as growing appropriately and with expected PE's clonogenic survival experiments were conducted to assess calpain inhibitor single agent cytotoxic effects and determine potential IC50 concentrations. MDA-MB-231 and MDA-MB-468 were seeded at $1x10^6$ cells per well in a 6 well plate in triplicate for each dose and left for 24 hours in an incubator at 37° and 5% CO_2. After 24 hours the cells were treated at 50µM, 75µM and 100µM for Calpeptin and 50µM, 100µM and 150µM for PD150606 with and without 10µM of calcium ionophore activation. With calcium ionophore, cells were treated for 30 minutes after which the calpain inhibitors were added to the cells and treated for 24 hours. After 24 hours cells were counted and serially diluted and plated at different cell densities in T25cm^2 flasks. MDA-MB-468 were plated at various densities to account for the small colony size and the potential cytotoxicity of the calpain inhibitors. At the highest concentration 3 T25cm^2 flasks of 300 and 600 cells were seeded, the next concentration below was seeded for 200 and 400 cells and the lowest concentration with the controls were seeded with 100 and 200 cells. For the MDA-MB-231 cell line, all concentrations of drugs and the controls were plated at 100 and 200 cells due to the large colony size of MDA-MB-231 otherwise the colonies would overlap and cannot be counted. The flasks for both cell lines were left to incubate at 37°C and 5% CO_2 for 14 days. Colonies were then fixed, stained and counted as in the method above. The surviving fraction was calculated using the equation below. A minimum of three independent experiments were conducted, each in triplicate.

$$S.F. = \frac{\text{Number of Colonies Counted}}{(\text{Cell Seeded Density x PE\%})}$$

2.1.6 Radiation Response in Cell Lines

To initially assess if cells were responding as expected from historical data cells were exposed to a single dose of radiation and surviving fraction determined. MDA-MB-231/468 were seeded in a T-25cm^2 Flask with 5x10^{5}cells/ml. The cells were left for 24 hours in an incubator at 37°C and 5% After the 24-hour period both sets of cells were irradiated in an Xstrahl CIX2 X-ray cabinet irradiation to a single dose of 4 Gray (Gy) at a dose rate of 0.998Gy/min. Sham irradiation were given to controls. The cells were then incubated for a suitable number of days 14 for MDA-MB-231 and MDA-MB-468. Flasks were washed, fixed, stained and counted to calculate the surviving fraction using the equation mentioned above. This was then compared to the historical data obtained by previous students to verify the cells have a similar radiation response.

2.1.7 Combination Therapy of Radiation and Calpain Inhibitors

Once cells were showing to be growing appropriately and responding to radiation as expected drug-radiation combination experiments were conducted. MDA-MB-468 cells were seeded at 5x10^{5}cells/ml in a T25cm^2 flask for each radiation dose, 2, 4, 6, or 8 Gy and treated with an estimated IC50 dose for PD150606 with and without calcium ionophore activation. Prior to the treatment of PD150606 for 30 minutes, all the cells with and without the calcium ionophore treatment had PD150606 added to them, with DMSO as the control, for 24 hours. After incubation cells were irradiated at doses of 2, 4, 6 or 8Gy at a dose rate of 0.9984Gy/min using the Xstrahl CIX2 X-ray cabinet irradiation system, control cells were sham irradiated. After the cells were trypsinised, resuspended and serially diluted to an appropriate number of cells and seeded in T-25cm^2 flasks and incubated for 14 days for respective cell lines to calculate the surviving fraction and dose-response, following the clonogenic assay method above. The number of cells seeded for colony formation was increased, per flask, at high drug and radiation doses to account for cell killing and potential synergistic effects. The equation to calculate surviving fraction was amended slightly to account for effects of drug i.e.:

$$S.F. = \frac{Number\ of\ Colonies\ Formed\ after\ Irradiation}{(Number\ of\ Cells\ Plated\ x\ PE\ x\ S.F\ of\ Inhibitor}$$

Radiation response curves were fitted using the well characterised linear-quadratic (LQ) model by the German Cancer Research Centre and available at - http://angiogenesis.dkfz.de/oncoexpress/software/cs-cal/index.htm. This allowed various radiation-response parameters to be calculated (SF2, α, β and α/β ratio etc)

2.1.9 Statistical Analysis of In vitro data

Graphs were produced using GraphPad Prism 9 Software and Microsoft Excel. The mean values of experiments completed in triplicate were used and error bars calculated using standard deviation (SD) combined from each experiment using the following formula:

$$\text{SD Combined} = \sqrt{\frac{\{(n_1 - 1)\ \text{x}\ SD_1^2\ +\ (n_2 - 1)\ \text{x}\ SD_2^2}{n_1 + n_2 - y}}$$

In the SD combined formula, SD_1 and SD_2 are the SDs for each experiment. n is the number of replicates in each experiment. y is the number of experiments. (Mukherjee, 2004). Student's t-test was used to assess for significance between two groups with a critical value of $p<0.05$.

2.2 Methods for Objective 2:

2.2.1 Differentially Expressed Genes of RNAseq Data of CAST II Overexpression Cell Lines

The RNAseq data of MDA-MB-231 and T47D CAST Overexpression cell lines was previously obtained by Dr. R.Vasan by treating MDA-MB-231 and T47D CASTI-III Overexpression cell lines and controls, grown to confluency in 3 independent passages and treated with 10µM of calcium ionophore for 2 hours to activate the calpain system, after which the cells were immediately washed and counted to a $5x10^6$ cell suspension and frozen as cell pellets in 1.5ml Eppendorf tubes. 24 samples were then packed and sent on dry ice to Novogene (UK) Company Ltd, Cambridge for RNA sequencing. This produced a list of DEGs for each isoform of CAST in each cell line compared to the controls sent for RNA sequencing which was then used for bioinformatic analysis. Due to the limited time available one of the three CAST isoforms was chosen for analysis. The differentially expressed genes (DEGs) from the CAST II overexpression data for both cell lines was selected by only selecting DEGs that showed a significant fold change. CAST II was chosen as it showed a distinctly

different subcellular localisation pattern to CAST I and III i.e., perinuclear location as opposed to diffuse cytoplasmic. Others in the group are assessing CAST I and III.

2.2.2 Ingenuity Pathway Analysis of DEGs

Qiagen's Ingenuity Pathway Analysis (IPA) is a program that allows for analysis of datasets such as DEGs lists obtained from RNA sequencing, downstream effects and biomarkers can be identified using IPA and placed in the context of biological systems. IPA was utilised to easily identify DEGs through different filters and perform upstream analysis which identified transcription regulators. The program also allows for the easy identification of any potential relationships between 2 different gene using a path explorer tool to develop a pathway that links the genes determined through published literature.

DEGs were identified from the DEG list of CAST II overexpression of both MDA-MB-231 and T47D. The list of DEGs were filtered differently to shortlist DEGs to take forward for further analysis. By filtering to sort the lists by smallest p-value the top 10 most significant DEGs were shortlisted for both cell lines. In both cell lines the list of DEGs were sorted to show the significant DEGs with the highest fold changes and the 10 topmost upregulated DEGs were shortlisted. The same was done but the list of DEGs sorted to show the lowest fold changes and the 10 topmost downregulated significant DEGs were identified and taken forward for further analysis. The common and unique DEGs to both CASTII overexpression MDA-MB-231 and T47D were identified by exporting the list of DEGs to Microsoft Excel and colour coding the unique and common genes between the lists. From this spreadsheet the 10 topmost significant common DEGs between the 2 cell lines were shortlisted and also the 10 topmost significant unique DEGs were shortlisted for each cell line. Upstream analysis for both cell lines to obtain predicted to be activated and inhibited transcription regulators was also performed by using the upstream analysis tool on the IPA program. This tool produced a list of genes that were known to be affected upstream of the CASTII overexpression. The list produced from this analysis was filtered to only show significant transcription regulators. Each transcription regulators were given a z-score. A z-score of higher than 2 was considered to be predicted to be activated and a z-score lower than -2 was considered to be predicted to be inhibited.

2.2.3 Survival Analysis of DEGs

The METABRIC cohort is a collection of breast tumour samples that underwent genomic and transcriptomic analysis 997 validation sets of tumours and 995 primary breast tumours(Curtis *et al*., 2012). Using the METABRIC dataset accessed through cBioPortal, selected DEGs were queried and compared with the survival of the patients. The DEG were queried in the search bar and then the mRNA expression for each gene was obtained. This data was entered in SPSS and categorized into 'high' or 'low' expression based on the median mRNA expression. This was then plotted against the overall disease specific survival obtained from the clinical data from the METABRIC cohort. Kaplan-Meiers were then plotted and DEGs with a significant association with breast cancer specific survival were shortlisted for correlation analysis.

2.2.4 Correlation Analysis using Calpastatin Probes

DEGs with significant (p-value = <0.05) Kaplan-Meiers were then used in correlation analysis with 6 calpastatin probes in SPSS. This determined if there is an association between the shortlisted DEGs and the calpastatin. The calpastatin probes were available from the METABRIC cohort and bind to specific sites on the gene. The probes were correlated with the DEGs shortlisted from the survival analysis using Spearman's Rank Coefficient to determine if there is any significant correlation between the probes and the identified DEGs. DEG's that showed a significant correlation (p-value= <0.05) were then shortlisted.

2.2.5 Selection of DEGs for Verification

DEG's that correlated with calpastatin probes and had a significant association with survival were shortlisted. This yielded a list of DEGs that was too high in number to perform validation on. This group was then reduced by only including DEGs that showed a p-value of <0.01 in the survival analysis. This left 6 possible DEGs then the top 3 most significant DEGs were selected for verification, CACNA2D4, CEBPB and NONO. Primers were designed using NCBI primer design tool and then ordered from Eurofins Scientific for each of these genes. Only an antibody for CACNA2D4 (Novus Biological, NPB1-85920) was ordered due to the gap in the literature on this gene in breast cancer, this was a polyclonal antibody for western blot and IHC application.

Chapter 3: Results

3.1 Phenotypic Results

3.1.1 Doubling Times and Plating Efficiencies of Cell Lines

The cell lines selected for experiments, MDA-MB-231 and MDA-MB-468, underwent characterization to ensure they were growing as expected, according to published literature and prior experience withing the research group, before any further experiments were conducted using them. Proliferation assays were carried out over 96 hours with cells being counted at 24 hour time intervals following the method described in section 2.1.2. Growth curves are shown in Figure 3.1.1. MDA-MB-468 showed a doubling time of 33±1.5 hours which agreed with previous research groups data of 31±1.24 hours (Aiyappa, 2020) and the literature (Watanabe *et al*., 2001) . MDA-MB-231 showed a doubling time of 26±1.3 hours which also agreed with previous data of our research group and literature (Vasan, 2022) (Watanabe *et al*., 2001).

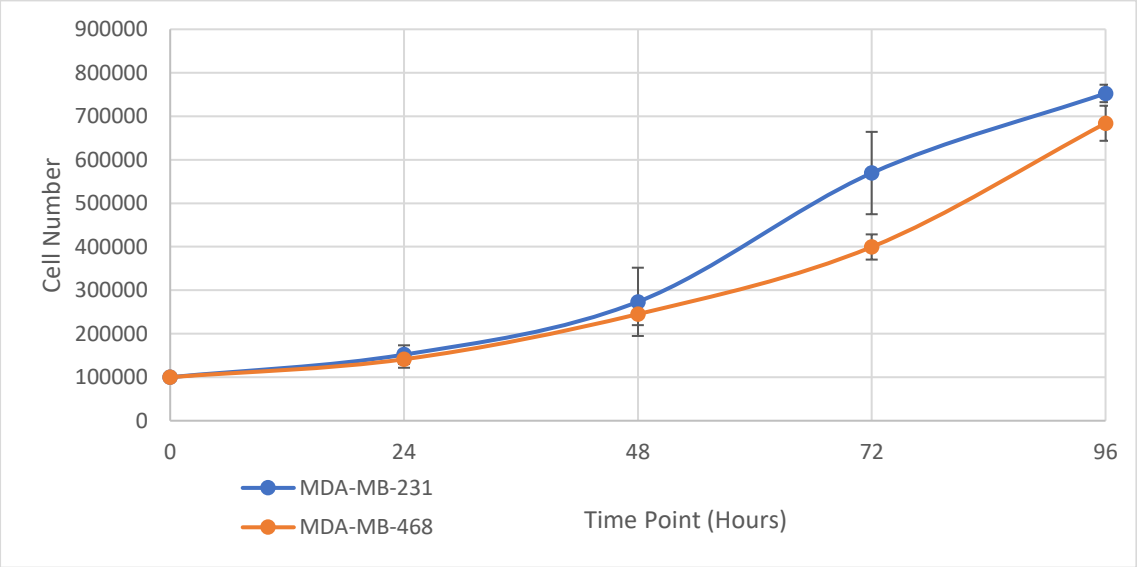

Figure 3.1.1 Cumulative Growth Curve for the cell lines MDA-MB-231 (blue line) and MDA-MB-468 (orange line). The average cell number was calculated and plotted at each timepoint. The error bars represent the standard deviation of the 3 experiments. and were obtained from three independent experiments, each conducted in triplicate. Doubling times were calculated from the exponential portion of the growth curve.

Plating Efficiencies were obtained through a clonogenic assay seeded from cells that had been growing for 48 hours following the method described in section 2.1.3. The cells were seeded at low density and their colony forming ability assessed following a 2-week incubation. The plating efficiency of MDA-MB-231 was determined as 51%±2.8 and MDA-MB-468 plating efficiency was calculated as 41%±1.2. This concurs with previous data obtained within our group and the literature and shown in Table 3.1.1 (Vasan, 2022, Aiyappa, 2020, Zhang *et al*., 2014) The similar results obtained with the previous data from both the literature and the previous work within our group indicated that the cell lines were behaving as expected.

Cell Line	Plating Efficiency (%)	Plating Efficiency (%) from previous data
MDA-MB-231	51.4±2.8	51.2±1.2
MDA-MB-468	41.1±1.2	44±1.52

Table 3.1.1. Plating efficiencies of MDA-MB-231 and MDA-MB-468.

3.1.2 Cytotoxicity of Calpain Inhibitors by Clonogenic Survival

Conventional calpain inhibitors, calpeptin and PD150606, were used to assess the effect of inhibiting calpains on clonogenic survival. Other students in the group have shown that calpeptin at 100µM inhibited calpain activity by 42.56±2.07% (Vasan, 2022, data not shown). As mentioned previously calpains are calcium dependent proteases (Potz, Abid and Sellke, 2016), and so experiments were conducted with and without calcium stimulation. Cells were treated for 30 minutes with 10µM of calcium ionophore before being treated with a range of concentrations of calpain inhibitors. Each drug was dosed in MDA-MB-231 and MDA-MB-468 and treated for 24 hours with and without calcium activation and was repeated in triplicate. An IC50 dose of doxorubicin (taken from previous student work, Vasan, 2020) was used to ensure cells were responding as expected. The calcium ionophore 10µM was also used as a single agent to assess the independent effect of calcium stimulation. Data are shown in Figure 3.1.2

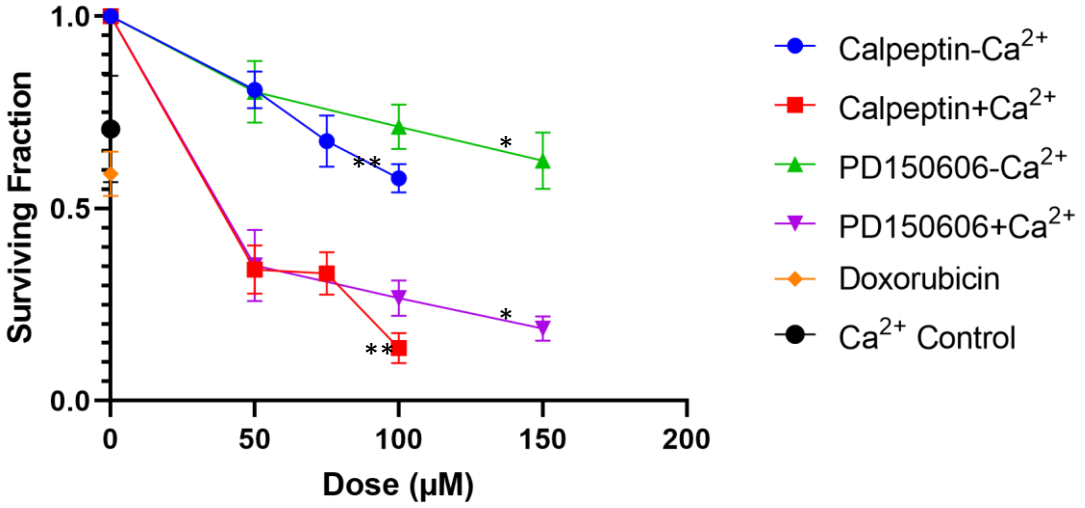

Figure 3.1.2. Dose response curves for PD150606 and Calpeptin in MDA-MB-468. The Plating efficiency of MDA-MB-468 was 41%±1.2%. Cells with calcium activation were treated with 10µM of calcium ionophore for 30 minutes. Doxorubicin at 5nM was used a control. The error bars represent the standard deviation of the 3 experiments. and were obtained from three independent experiments, each conducted in triplicate. * (p=<0.05) Student's t-test between PD150606+Ca2+/-Ca2+.**(p=<0.05) Student's t-test between Calpeptin+Ca2+/-Ca2+.

The doxorubicin control showed that cells were responding as expected as the IC50 dose taken from previous work showed 41% cell killing. The calcium ionophore alone data shows that independently using calcium ionophore does resulting in cytotoxic activity, with a surviving fraction of 0.7. As can be seen in Figure 3.1.2 both calpain inhibitors demonstrated a dose response relationship in unstimulated conditions, with increasing dose of drug increasing cell killing. The calpain inhibitors showed a synergistic relationship with calcium ionophore activation. Without the calcium ionophore activation the killing at the highest dose of calpeptin at 100µM is 43% in contrast at the same dose with calcium ionophore activation showed 87% cell killing. Calcium ionophore alone showed 30% killing therefore calpeptin with the treatment of calcium ionophore shows 57% killing alone which is more than calpeptin without calcium ionophore activation, therefore indicating the relationship between calpeptin and calcium ionophore is synergistic and increases the cytotoxicity. This relationship was also exhibited in the lower concentrations with calpeptin with the level of cell killing being higher with each concentration when combined with calcium ionophore treatment. At 50µM, not including the cell killing from calcium ionophore treatment, 36%

cell killing was displayed compared to 20% for calpeptin alone, at 75µM this was 37% in combination compared to 33% cell killing with the drug alone. PD150606 also showed a synergistic relationship with calcium ionophore. At the highest dose of 150µM without calcium ionophore 38% cell killing was shown compared to the 82% cell killing for the same dose with calcium ionophore. This cell killing of calcium ionophore alone showed 30% therefore the combination with PD150606 killed a further 52% of cells. This also was displayed in the lower concentrations of PD150606 with 100µM showing 44% killing not including calcium ionophore killing compared to 29% killing with 100µM of PD150606 alone. This was also displayed at 50µM of PD150606 with 35% cell killing excluding the cell killing of calcium ionophore, compared to only 20% cell killing with PD150606 alone. The level of cell killing shows an increase when combined with calcium ionophore indicating a synergistic relationship. Both agents seemed to induce similar level of killing under both stimulated and unstimulated conditions. Student's t-tests showed a significant difference between each drug with and without calcium ionophore activation indicating a synergistic relationship between the calpain inhibitors and calcium ionophore treatment, PD150606+Ca^{2+} v PD150606-Ca^{2+} (*p-value = 4.54006E-05) and Calpeptin+Ca^{2+} v Calpeptin-Ca^{2+} (**p-value = 0.004015909). Therefore, showing that the activation of the calpain system through treating the cells with calcium ionophore significantly increases the cytotoxicity compared to the calpain inhibitors alone. Student's t-tests were also performed to compare the calpain inhibitor cytotoxicity with and without calcium ionophore activation. PD150606-Ca^{2+} v Calpeptin-Ca^{2+} and PD150606+Ca^{2+} v Calpeptin+Ca^{2+}. This dose response showed no significant differences, therefore highlighting that the calpain inhibitors show similar levels of cytotoxicity.

The same experiment was also conducted using the MDA-MB-231 cell line, with data shown in Figure 3.1.3.

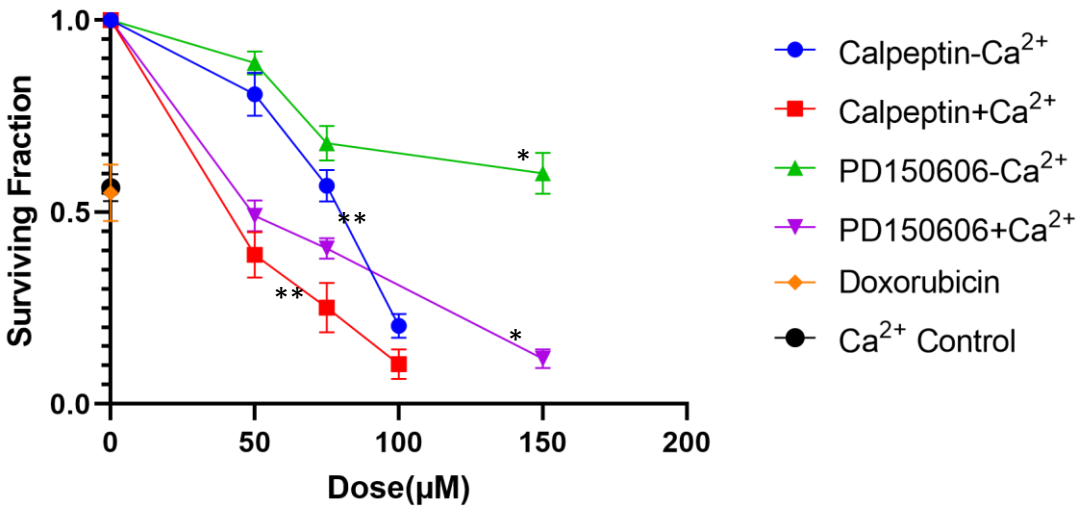

Figure 3.1.3 Dose response curves for PD150606 and Calpeptin in MDA-MB-231. The Plating efficiency of MDA-MB-231 were 51%±.2.8%. Cells with calcium activation were treated with 10µM of calcium ionophore for 30 minutes. Doxorubicin at 5nM was used a control. The error bars represent the standard deviation of the 3 experiments. and were obtained from three independent experiments, each conducted in triplicate. * ($p=<0.05$) Student's t-test between PD150606+Ca^{2+}/-Ca^{2+}.**($p=<0.05$) Student's t-test between Calpeptin+Ca^{2+}/-Ca^{2+}.

The doxorubicin control showed a that the cells were behaving correctly with 45% cell killing which was expected. Cells treated with calcium ionophore independently displayed 44% cell killing, indicating that for MDA-MB-231 calcium ionophore is cytotoxic when used alone. Cell killing was higher, from both calpain inhibitors, in MDA-MB-231 compared to MDA-MB-468. Calpeptin at 100µM without calcium ionophore had a surviving fraction of 20% - this is only slightly higher than the 10% surviving fraction for the same concentration of calpeptin with calcium ionophore. PD150606 showed a similar effect of toxicity to that seen with MDA-MB-468's. However, the relationship between the calcium ionophore and PD150606 displayed, differs to the relationship in MDA-MB-231.

MDA-MB-231 only showed a synergistic relationship in one concentration of PD150606, with 40% cell killing at the highest dose of 150µM with PD150606 alone but with PD150606 in combination with calcium ionophore but discounting the cell killing of the calcium ionophore, 45% cell killing is displayed therefore indicating the synergistic relationship between PD150606 and calcium ionophore at 150µM. In contrast this relationship between the lower

concentrations of 50µM and 100µM show an antagonistic relationship between PD150606 and calcium ionophore. Taking away the cell killing of calcium ionophore from the combination of 50µM and 100µM, there is only 7% and 16% cell killing respectively. Compared to the PD150606 alone at the 50µM and 100µM showing 12% and 33% cell killing. Calpeptin also showed an antagonistic relationship between all the concentrations and calcium ionophore. The cell killing at 50µM, 75µM and 100µM with calcium ionophore treatment but not including the cell killing exhibited by treatment was 18%, 31% and 46% respectively, this is lower than Calpeptin alone in this cell line at the same concentrations with 50µM showing 20% killing, 75µM killing 44% and 100µM displaying 80% killing. This relationship is a stark contrast to the relationship between the calpain inhibitors and calcium ionophore in MDA-MB-468. The relationship between the calpain inhibitors and the calcium ionophore was not tested for due to the calcium ionophore only being used as an agent to activate the calpain system not to induce any cytotoxicity.

A Student's t-test was performed to assess for any statistical significance between the calpain inhibitors. For calpeptin-Ca2+ v calpeptin+Ca2+ it showed a significant difference (*p-value =0.048474). PD150606-Ca2+ v PD150606+Ca2+ also was significant (**p-value= 0.006675), which indicates that there is a stronger difference between the different drugs with and without calcium ionophore and the effect on MDA-MB-231. This significant difference is only assessing the cytotoxicity of the combination of the inhibitors and calcium ionophore treatment which exhibited much higher cell killing but displayed an antagonistic relationship. There was no statistical significance seen between the two drugs for both without calcium ionophore Calpeptin-Ca2+ v PD150606-Ca2+, and with calcium ionophore Calpeptin+Ca2+ v PD150606-Ca2+. In summary the effect of calpeptin and PD150606 is significantly stronger when the cells are pretreated with calcium ionophore which in tur activates the calpain system. However, MDA-MB-231 at 100µM showed high levels of cytotoxicity even without calcium ionophore treatment.

Calpain Inhibitors	MDA-MB-468 (µM)	MDA-MB-231 (µM)
PD150606-Ca^{2+}	198	185
PD150606+Ca^{2+}	37	47
Calpeptin-Ca^{2+}	135	80
Calpeptin+Ca^{2}	36	35

Table 3.1.2 The estimated IC50 Values calculated from the dose response curves for Calpeptin and PD150606 for cell lines MDA-MB-468 and MDA-MB-231

The above data was used to obtain estimated IC50 values, to use in a combination experiment of radiation and calpain inhibitors. The estimated IC50's are shown in table 3.1.2

3.1.3 Radiation Clonogenic Survival

To initially verify that both cell lines, MDA-MB-468 and MDA-MB-231, were responding correctly to radiation (according to radiation survival curves calculated by previous members of the research group) they were each exposed to a single dose of 4Gy and immediately plated for colony formation. Surviving fractions of 9% (PE 41.1%) for MDA-MB-468's and 2% (PE 51.4) for MDA-MB-231's were obtained, agreeing with previous data (Aiyappa, 2020) indicating that the cells were responding the same way as previously used.

3.2 Bioinformatics Results

3.2.1 Differentially Expressed Genes Identified from RNAseq of CASTII overexpression cell lines

DEGs were identified from the RNAseq dataset for MDA-MB-231 and T47D CAST II overexpression cell lines as described in section 2.2.2. The top 10 most significant DEGs were identified for both MDA-MB-231 and T47D and shown in table 3.2.1 and 3.2.2 respectively. The top 10 most upregulated and downregulated DEGs identified for MDA-MB-231 are shown in table 3.2.3 and 3.2.4 respectively. The top 10 most upregulated and downregulated DEGs identified from T47D are shown in table 3.2.5 and 3.2.6 respectively. Table 3.2.7 displays the most significant common DEGs between the CAST II overexpression cell lines. The unique DEGs for both MDA-MB-231 and T47D CAST II overexpression cell lines are displayed in table

3.2.8 and 3.2.9 respectively. The selected DEG's were then further assessed through survival analysis with the METABRIC cohort.

Gene Symbol	Expr Log Ratio	Expr p-value
LINC02582	-5.945	4.87E-84
CACNA2D4	-4.837	4.1E-79
DCAF12L1	-5.246	3.41E-75
PGM5	6.991	1.43E-66
MAGEC1	-4.42	1.23E-63
CD33	-7.486	2.87E-59
TIE1	-3.597	3.04E-59
TNFSF18	4.723	3.43E-57
AADAC	5.604	1.12E-54
AADACP1	3.931	2.44E-53

Table 3.2.1. The top 10 most significant DEGs from MDA-MB-231 CAST II RNAseq data.

The gene CD33 is the DEG with the lowest expr log ratio in the MDA-MB-231 CASTII overexpression cell line as shown in table 3.2.1. The DEG showed an expr log ratio of -7.486 which indicates a downregulation of CD33 with a fold change of -7.486 compared to the expression of CD33 in wildtype MDA-MB-231. PGM5 showed the highest fold change with 6.991 representing an upregulation of this gene.

Gene Symbol	Expr Log Ratio	Expr p-value
TAGLN	5.947	<000E-000*
FHL1	5.762	<000E-000*
FLRT2	5.607	<000E-000*
SPARC	5.482	<000E-000*
FN1	5.003	<000E-000*
ALCAM	3.775	<000E-000*
AREG	2.941	<000E-000*
WNT5A	-4.975	<000E-000*
FAM133A	5.283	1.08E-302
EPHA3	4.657	8.15E-285

Table 3.2.2 The top 10 most significant DEGs from T47D CAST II RNAseq data. '*' denotes a p-value of less than 2.225074e-308 due to limitations in the R software

The most downregulated DEG shown in table 3.2.2 is WNT5A with an expr log ratio of -4.975 indicating that the expression of WNT5A is downregulated by -4.975 in the CASTII overexpression cell line. TAGLN is the highest upregulated DEG in table 3.2.2 with an expr log

ratio of 5.947 indicating an upregulation of 5.947 in MDA-MB-231 CASTII overexpression cell line. Table 3.2.1 showed 10 DEGs, with 6 of these being downregulated and 5 being upregulated in the MDA-MB-231 CASTII overexpression cell line in contrast in table 3.2.2 9 of the DEGs are upregulated and 1 DEG is downregulated in the T47D CASTII overexpression cell line. This may potentially indicate that within the luminal subtype in T47D that there is a higher number of genes being upregulated because of the CASTII overexpression compared to MDA-MB-231 cell line that displayed an even presentation of downregulated and upregulated DEGs in the 10 topmost significant DEGs.

Symbol	Expr Log Ratio	Expr p-value
LRRC61	10.08	1.29E-16
PWWP3B	8.183	1.17E-10
CARD18	7.923	1.51E-10
ITM2A	7.481	1.71E-08
ZBED10P	7.388	4.31E-08
CCL4	7.337	2.94E-08
PPP1R14C	7.133	5.31E-15
PGM5	6.991	1.43E-66
LHFPL4	6.542	4.4E-30
BEND4	6.483	0.0000193

Table 3.2.3 The top 10 most upregulated DEGs from MDA-MB-231 CAST II RNAseq data.

As shown in table 3.2.3 LRRC61 is the most upregulated DEG in MDA-MB-231 CASTII overexpression cell line. There is a much higher expr log ratio of 10.08 when compared to the next highest upregulated DEG with an expr log ratio of 8.183. The expr log ratio of 10.08 represents the fold change of the DEG in MDA-MB-231 CASTII compared to MDA-MB-231 wildtype.

Symbol	Expr Log Ratio	Expr p-value
MAGEB2	14.197	2.66E-33
LINC00200	12.631	1.32E-26
PAGE5	11.073	1.19E-20
SELENOOLP	8.301	1.86E-11
CHMP1B2P	8.244	2.82E-11
FABP4	7.309	1E-11
SLCO4C1	7.107	1.12E-08
LINC01611	6.721	0.000000499
EREG	6.474	9.14E-277
MYH13	6.468	1.1E-28

Table 3.2.4 The top 10 most downregulated DEGs from MDA-MB-231 CAST II RNAseq data.

DDX53 is the most downregulated DEG in CASTII overexpression MDA-MB-231 with an expr log ratio of -8.835 as shown in table 3.2.4, this is showing that DDX53 is downregulated by a fold change of -8.835 when compared to the expression of the gene in wildtype MDA-MB-231

Symbol	Expr Log Ratio	Expr p-value
DDX53	-8.835	2.2E-12
MKRN9P	-8.439	3.82E-10
CD33	-7.486	2.87E-59
NLRP5	-7.239	4.33E-08
SNX20	-7.215	1.03E-15
ZNF727	-7.134	0.0000148
LINC00317	-7.112	9.57E-08
EPHB1	-6.868	1.99E-37
CDH7	-6.538	0.00000558
FGF14-AS2	-6.531	0.00000279

Table 3.2.5 The top 10 most upregulated DEGs from T47D CAST II RNAseq data.

As can be seen in table 3.2.5 the highest upregulated DEG in T47D CASTII overexpression cell line is MAGEB2 with an expr log ratio of 14.197. This expr log ratio represents a fold change of 14.197 compared to wildtype T47D. This fold change is much higher compared to the highest fold change in CASTII MDA-MB-231 in table 3.2.3 with a fold change of 10.08, LRRC61. The next topmost upregulated DEGs in CASTII T47D, LINC00200 and PAGE5 have a fold change of 12.631 and 11.073 respectively. These DEGs are upregulated more than LRRC61 potentially

highlight the overexpression of CASTII have an increased effect in T47D compared to MDA-MB-231.

Symbol	Expr Log Ratio	Expr p-value
TFDP3	-12.472	6.4E-26
GRIK3	-10.97	2.73E-20
HOXB13	-8.436	8.69E-12
GABRP	-8.073	1E-59
ANKRD20A4P (includes others)	-7.68	1.24E-09
CYP4F22	-7.553	5.39E-09
DRD5	-7.523	4.78E-09
CX3CL1	-7.492	7.63E-09
MXRA5	-7.487	4.52E-09
PIP	-7.114	8.14E-178

Table 3.2.6 The top 10 most downregulated DEGs from T47D CAST II RNAseq data.

As can be seen in table 3.2.6 TFDP3 is the most downregulated DEG in the T47D CASTII overexpression cell line with an expr log ratio of -12.472. This represents the change in expression of TFDP3 in T47D CASTII overexpression cell line. TFDP3 shows a much higher fold change than the most downregulated DEG in MDA-MB-231 shown in table 3.2.4, DDX53, with a fold change of -8.835. This is similar to the upregulated DEGs shown in tables 3.2.3 and 3.2.5, indicating that T47D exhibited a stronger effect as a result of the CASTII overexpression.

Symbol	MDA-MB-231 Expr Log Ratio	MDA-MB-231 Expr p-value	T47D Expr Log Ratio	T47D Expr p-value
TAGLN	1.128	0.00000486	5.947	<000E-000*
FLRT2	-2.025	7.06E-23	5.607	<000E-000*
WNT5A	-1.031	0.0000703	-4.975	<000E-000*
FAM133A	-0.949	0.000292	5.283	1.08E-302
EREG	2.036	2.49E-10	6.474	9.14E-277
ALDH1A3	0.862	0.00084	-3.393	4.84E-275
MAGEC1	-4.42	1.23E-63	2.051	7.69E-33
TNFSF18	4.723	3.43E-57	2.252	5.57E-106
LINC00839	4.916	9.06E-52	0.44	0.00404
LINC03014	-3.739	1.43E-45	-1.184	0.00684

Table 3.2.7. The top 10 most significant common DEGs from T47D and MDA-MB-231 CAST II RNAseq data.

‘*’ denotes a p-value of less than 2.225074e-308 due to limitations in the R software

The DEGs that were common between the two cell lines, MDA-MB-231 and T47D, showed different expr log ratios. For some DEGs there was an upregulation in one cell line and a downregulation in the other cell line. FLRT2 displayed this with -2.025 expr log ratio in MDA-MB-231 and 5.607 expr log ratio in T47D. These differences between the cell lines highlight the difference in the effect of CASTII overexpression between the 2 cell lines, which both represent different molecular subtypes of breast cancer, T47D for luminal and MDA-MB-231 for triple negative.

Gene	Expr Log Ratio	Expr p-value
LINC02582	-5.945	4.87E-84
CACNA2D4	-4.837	4.1E-79
DCAF12L1	-5.246	3.41E-75
PGM5	6.991	1.43E-66
CD33	-7.486	2.87E-59
TIE1	-3.597	3.04E-59
AADAC	5.604	1.12E-54
AADACP1	3.931	2.44E-53
TREML2	-4.796	4.54E-51
C5orf46	5.643	7E-45

Table 3.2.8. The top 10 most significant unique DEGs from MDA-MB-231 CAST II RNAseq data.

As shown in table 3.2.8 the DEGs overlap with DEGs shown in table 3.2.1 with the addition of TREML2 and C5orf46. TREML2 and C5orf46 showed an expr log ratio of -4.796 and 5.643 respectively. This shows that TREML2 was downregulated in MDA-MB-231 and C5orf46 was upregulated in the cell line.

Symbol	Expr Log Ratio	Expr p-value
FHL1	5.762	<000E-000*
SPARC	5.482	<000E-000*
FN1	5.003	<000E-000*
ALCAM	3.775	<000E-000*
AREG	2.941	<000E-000*
EPHA3	4.657	8.15E-285
SH3BGRL	5.399	9.67E-281
C3	-2.532	5.27E-262
LAMB4	3.217	7.22E-259
FKBP10	4.255	8.55E-243

Table 3.2.9. The top 10 most significant unique DEGs from T47D CAST II RNAseq data. '*' denotes a p-value of less than 2.225074e-308 due to limitations in the R software

FHL1 as shown in table 3.2.9 showed an expr log ratio of 5.762 it is also the most significant DEG unique to T47D CASTII. The expr log ratio represents the fold change of the DEGs in the overexpression cell line. Table 3.2.9 also has overlap with table 3.2.2. The unique DEGs to each cell line have a varying distribution of downregulated and upregulated DEGs with there being a more even amount in MDA-MB-231, in contrast in T47D there is only 1 down regulated DEG to 9 upregulated DEGs.

3.2.2 Ingenuity Pathway Analysis – Upstream Analysis of Transcription regulators

Using IPA to perform upstream analysis to identify the transcription regulators associated with the DEGs in both CAST II overexpression cell lines following the method described in 2.2.2. Transcription regulators were predicted to be activated or inhibited; this was determined by IPA using a z-score. The z-score is given to each transcription regulator, a score of >2 is considered to be predicted to be activated and a score of <-2 is considered to be predicted to be inhibited. The DEGs displayed in tables 3.2.10 and 3.2.11 were taken forward for further assessment with survival analysis with the METABRIC Cohort.

As shown in table 3.2.10 there are 19 transcription regulators that were predicted to be activated and 4 transcription regulators that were predicted to be inhibited in MDA-MB-231 CAST II overexpression cell line. There was a significant difference in the number of transcription regulators that were predicted to be activated compared to the those predicted to be inhibited.

Predicted Activation		Predicted Inhibition
MYC	BHLHE40	GATA1
SRF	PYCARD	RBL1
CREB1	NFE2L2	ZFP36
JUN	SMAD1	BCL3
CEBPB	STAT5B	
KLF6	NFKBIA	
POU5F1	FOS	
NFKB1	YAP1	
E2F1	MYOCD	
E2F3		

Table 3.2.10. The predicted activation and inhibition of transcription regulators from the MDA-MB-231 CAST II overexpression cell line

23 transcription regulators were predicted to be activated in T47D CASTII overexpression as shown in table 3.2.11. 27 transcription regulators were predicted to be inhibited in the cell line using the IPA upstream analysis. Both cell lines exhibited a large number of transcription regulators that would be either activated or inhibited as a result of the CASTII overexpression.

Predicted Activation		Predicted Inhibition	
MYCL	RUNX2	IRF7	SPI1
KAT5	KLF4	FOXC1	FOXA1
ATF4	CREB1	HNF4A	IRF1
MYC	EED	CIITA	PML
TFEB	NKX2-3	STAT1	SMAD7
MRTFA	IRF2BP2	NONO	HOXA4
SREBF2	PRRX1	SMARCA4	IRF5
FOSL1	SMAD2	PTF1A	CEBPA
YAP1	MYCBP	IRF3	SMARCB1
MRTFB		FOXO3	STAT2
SMAD3		STAT5B	HIF3A
KDM3A		SIX2	RAD21
SP1		IRF9	VAV2
SREBF1		CERS5	

Table 3.2.11. The predicted activation and inhibition of transcription regulators from the T47D CAST II overexpression cell line

3.2.3 Survival Analysis of DEGs

The DEGs identified from the CAST II Overexpression RNAseq Data (section 3.2.1) were taken forward for survival analysis using the METABRIC Cohort dataset described in 2.2.3. The expression of the identified DEGs was taken from the METABRIC cohort and categorised into high and low expression by using the median and grouping into high or low of that median and plotted against breast cancer specific survival. 1979 of the 2509 patient samples had mRNA expression data available. The number of patients in each categorised group of high or low varied for each gene used for survival analysis. As discussed with my supervisors hazard ratios were chosen not to be shown as they were not appropriate for the data used.

As shown in tables 3.2.12 and 3.2.13 various DEGs showed a significant association (p-value<0.05) with breast cancer survival. To narrow down genes to investigate further the DEGs unique to both MDA-MB-231 and T47D CASTII overexpression cell lines were assessed for significant association with survival in the METABRIC cohort. Significant results are shown in table 3.2.12 and 3.2.13 with their Kaplan-Meier plots shown below (Figures 3.2.1-3.2.7). Further Kaplan-Meier plots are displayed in appendix A. The Kaplan-Meier plots highlight the effect of high and low expression of the gene and its association with breast cancer specific survival. CACNA2D4, PGM5 and C5ORF46 all unique to MDA-MB-231 CASTII, showed a significant association with survival.

Gene	No. of High Expression	No. of Low Expression	p-value
CACNA2D4	995	984	5.228E-7
PGM5	993	986	0.000326
C5orf46	992	987	0.000440

Table 3.2.12. The number of patients in each category for each DEGs that is unique to MDA-MB-231 CASTII overexpression and the p-value of the survival analysis.

Figure 3.2.1, for CACNA2D4, shows that high expression correlates with a better survival outcome, with the green line remaining higher than the blue low expression line throughout the recorded period.

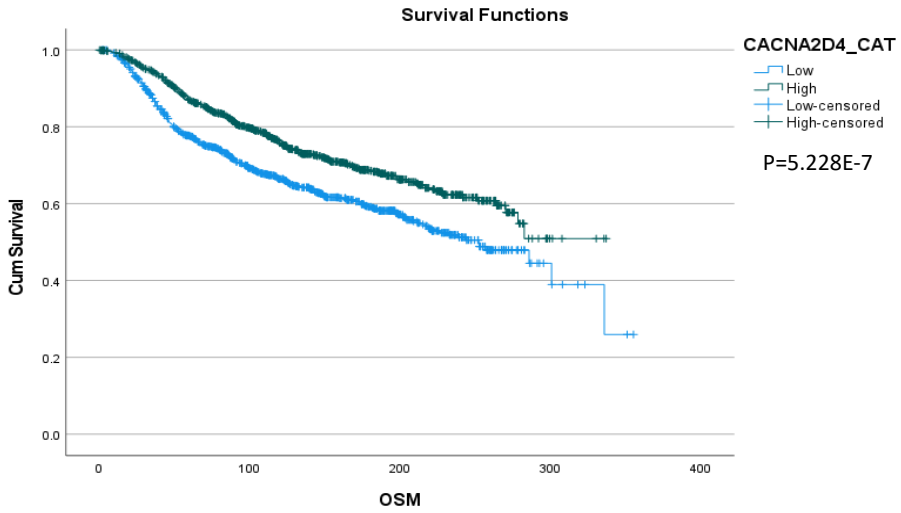

Figure 3.2.1. Kaplan-Meier plot of CACNA2D4, unique to MDA-MB-231 CASTII overexpression. Showed a significant association with survival (P=5.228E-7).

PGM5 showed that low expression is linked with worse overall survival until approximately 260 months which high expression is then linked with worse overall survival (Figure 3.2.2), this is displayed on the plot by the green line crossing over the blue line sloping below indicating a worse association with survival.

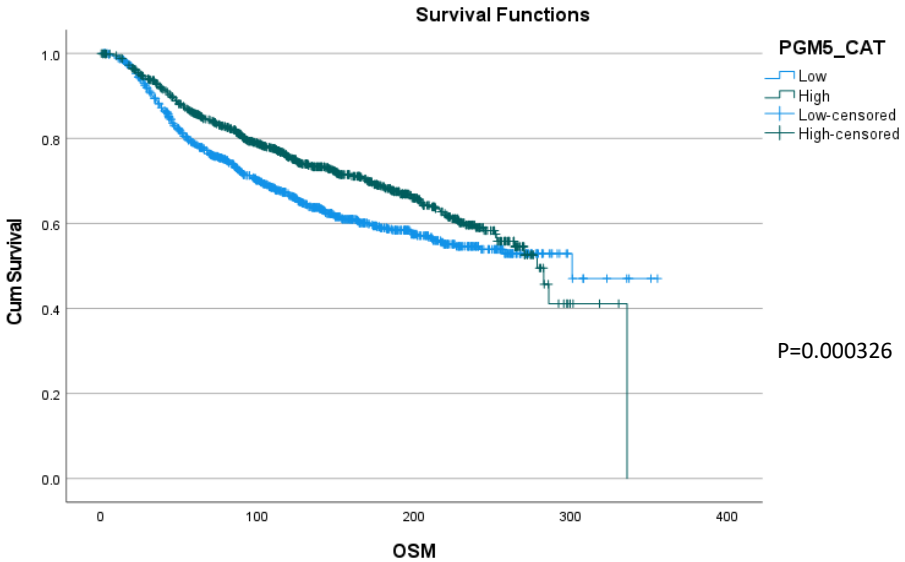

Figure 3.2.2. Kaplan-Meier plot of PGM5, unique to MDA-MB-231 CASTII overexpression. Showed a significant association with survival (P=0.000326).

High expression of C5ORF46, shown by the survival analysis, is related with poor overall survival. At approximately 275 months, low expression becomes worse for overall survival followed by at 330 months high expression being linked to worse overall survival (Figure 3.2.3). This is seen by the blue line sloping below the green line but then plateaus and the high expression line drops sharply indicating how at different time points expression for C5ORF46 may potentially affect survival.

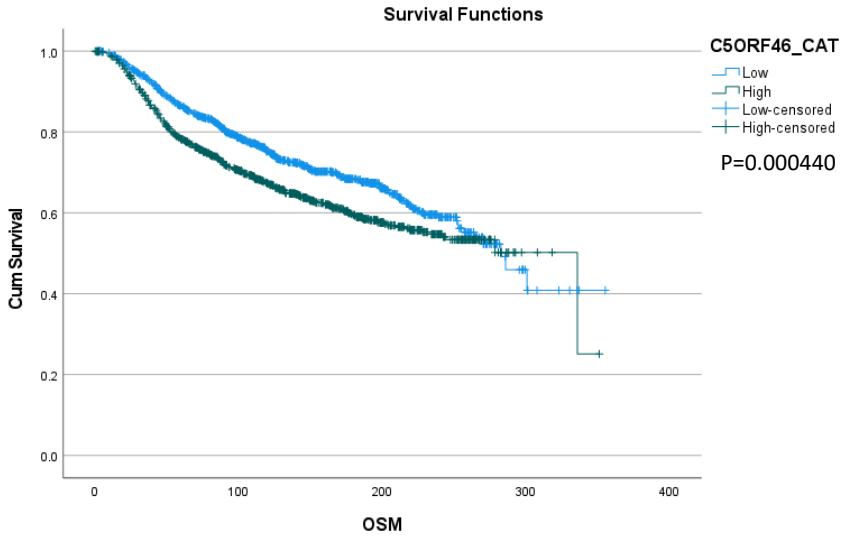

Figure 3.2.3. Kaplan-Meier plot of C5ORF46, unique to MDA-MB-231 CASTII overexpression. Showed a significant association with survival (P=0.000440).

DEGs unique to T47D CAST II overexpression cell showed significant association with survival in the DEGs, FN1, ALCAM, EPHA3 and SH3BGRL (Figures 3.2.4-3.2.7). With FN1 a low expression is associated with a better overall survival, however by approximately 330 months this becomes associated with worse survival as the blue low expression line drops to lower than the green high expression line as shown in figure 3.2.4.

Gene	No. of High Expression	No. of Low Expression	p-value
FN1	994	985	0.000082
ALCAM	986	993	0.041130
EPHA3	982	997	0.009744
SH3BGRL	990	989	0.004249

Table 3.2.13. The number of patients in each category for each DEGs that is unique T47D CASTII overexpression and the p-value of the survival analysis.

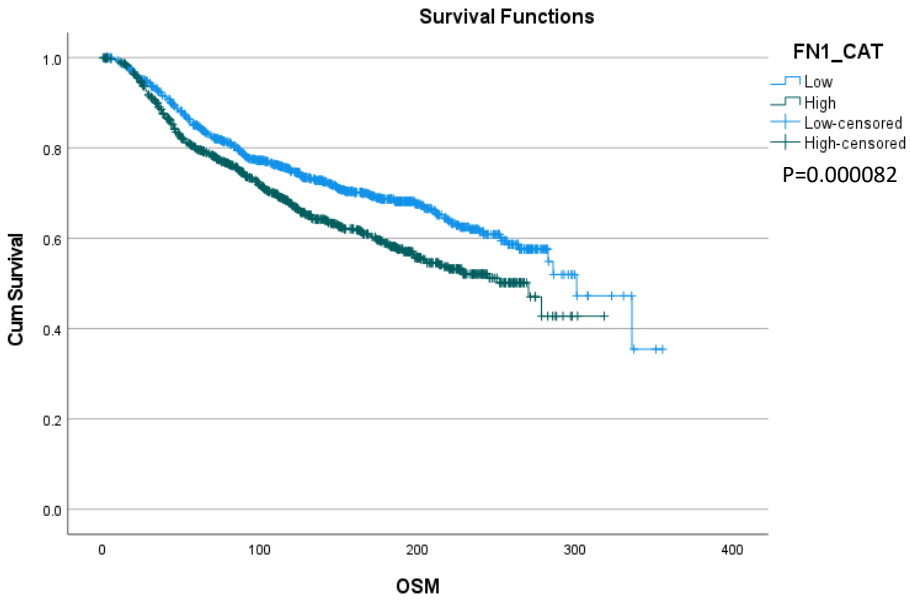

Figure 3.2.4. Kaplan-Meier plot of FN1, unique to T47D CASTII overexpression.

Showed a significant association with survival (P=0.000082).

The Kaplan-Meier plot (Figure 3.2.5) for ALCAM indicated that high expression is associated with better overall survival in breast cancer. There is a significant drop is survival at around 340 months with low expression with all patients not surviving past this time point.

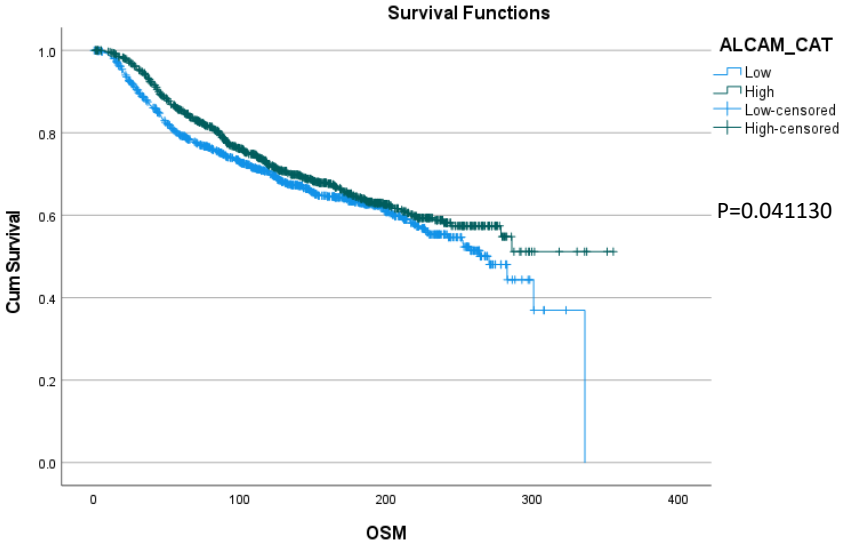

Figure 3.2.5. Kaplan-Meier plot of ALCAM, unique to T47D CASTII overexpression.

Showed a significant association with survival (P=0.041).

EPHA3 is associated with better overall survival with high expression of the gene. The high expression line consistently shows better overall survival without much change as shown in figure 3.2.6. However, with low expression there is a consistent decline with survival.

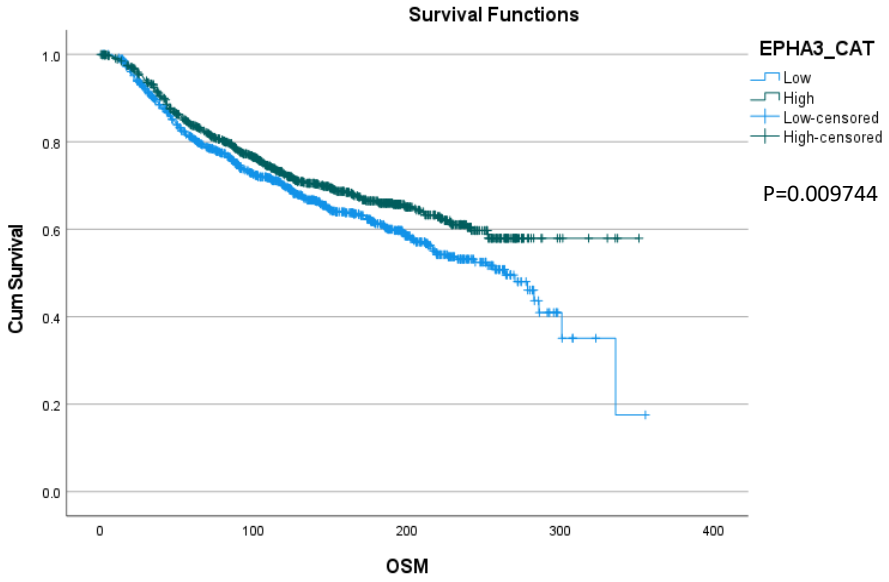

Figure 3.2.6. Kaplan-Meier plot of EPHA3, unique to T47D CASTII overexpression. Showed a significant association with survival (P=0.009744).

High expression of SH3BGRL is associated with a better overall survival until approximately 250 months then becomes associated with worse survival, followed by 330 months with low expression becoming more associated with worse overall survival as shown in figure 3.2.7.

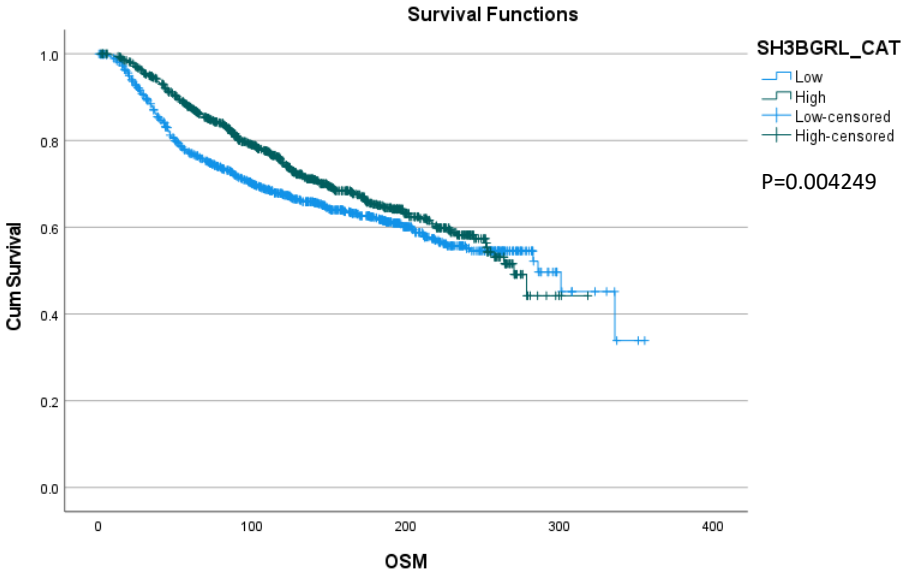

Figure 3.2.7. Kaplan-Meier plot of SH3BGRL, unique to T47D CASTII overexpression. Showed a significant association with survival (P=0.004249).

The DEGs that showed a significant association with breast cancer specific survival were taken forward and used for correlation analysis with CAST probes using Spearman's Rank Coefficient. The mRNA expression taken from the METABRIC cohort will be correlated with the mRNA expression of 6 CAST probes also taken from the METABRIC cohort, this will indicate any association between the CAST and the genes identified.

3.2.4 Correlation Analysis of DEGs with CAST Probes

The DEGs found to be significantly associated with survival in the METABRIC cohort were taken for further analysis by assessing for any correlation with 6 CAST probes, taken from the METABRIC cohort. The CAST probes are designed for the normal expression of CAST not the increased expression found in the overexpression cell lines potentially being a reason for the small number of DEGs that are significantly correlated. Spearman's Rank Coefficient was used to assess for correlation with the CAST probes with significance being $p=<0.05$. The correlation analysis of unique DEGs to MDA-MB-231 and T47D CASTII overexpression cell lines are displayed in figures 3.2.8 and 3.2.9. The remaining correlation heatmaps are displayed in appendix A. The darker the colour of the squares in the grid indicates a stronger correlation. The correlations are displayed using Morpheus software by the Broad Institute.

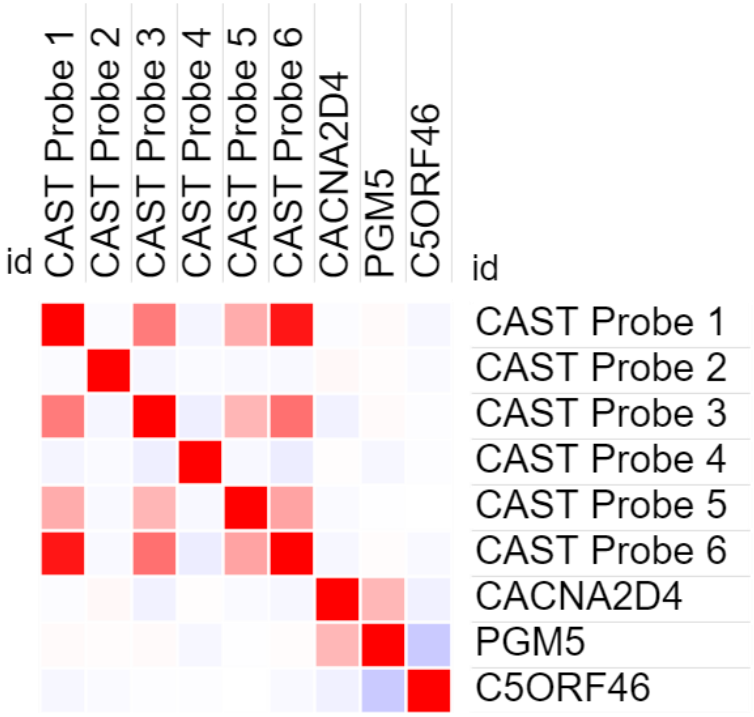

Figure 3.2.8. Heatmap of Spearman's Rank Coefficient of DEGs unique to CAST II overexpression MDA-MB-231 with data from the METABRIC cohort

Figure 3.2.8 displays a heatmap showing the correlation of unique DEGs to the MDA-MB-231 cell line. The only significant correlation found between the DEGs from both the CAST II overexpression cell lines and the CAST probes was between CACNA2D4 and CAST Probe 3 ($p=0.030$ and $r^2= -0.049$). This correlation is displayed by the faint blue colouring in figure 3.2.8. None of PGM5 or C5ORF46 showed a significant correlation.

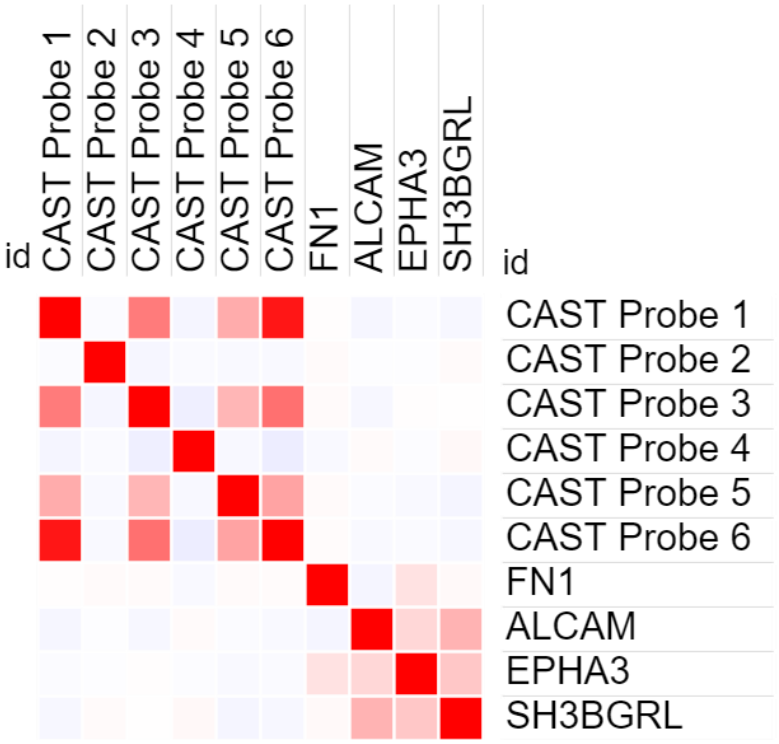

Figure 3.2.9. Heatmap of Spearman's Rank Coefficient of DEGs unique to CAST II overexpression T47D with data from the METABRIC cohort.

The heatmap displayed in figure 3.2.9 shows the correlation between the CAST probes and unique DEGS to T47D CASTII Overexpression cell line. None of the DEGs showed any correlation with the CAST probes.

The DEGs with significant correlation and a significant association with survival were taken forward for verification using western blot and q-RT-PCR techniques. To identify a smaller group of DEGs for verification, a critical value of $p<0.001$ for the survival analysis was used and correlates with the CAST probes. Then the top 3 most significant DEGs were selected for verification, CACNA2D4, NONO and CEBPB.

3.2.5 Pathway Analysis of DEGs selected for verification.

The DEGs taken forward from the correlation analysis for verification in the cell lines, were also analysed with IPA to assess for potential relationships with the calpain system. CACNA2D4, NONO and CEBPB underwent analysis to assess for any relationships with the CAST, CAPN1 and CAPN2 genes using the RNAseq DEG data. The pathway to connect the genes

was selected as the pathway with the strongest literature supporting the relationship. Figure 3.2.10 shows the pathway that links CACNA2D4 with the selected calpain genes and CAST and suggests that there is an indirect relationship between CACNA2D4 and CAPN1/2 and CAST, interestingly the link described in IPA all are through the common gene of EGR1.

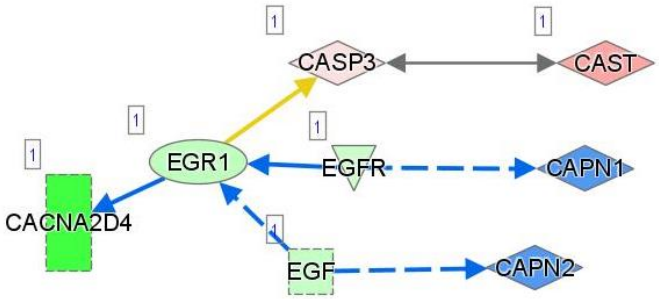

Figure 3.2.10. The pathway analysis establishing the connection between CACNA2D4 and CAST, CAPN1 and CAPN2. A blue line indicates that it is predicted to be inhibited. Yellow line indicates that the effect is inconsistent with the literature. A Grey line indicates that is no predicted effect. A solid line indicates a direct relationship, and a dotted line shows an indirect effect. Taken from Qiagen IPA.

Figure 3.2.11 shows the relationship between CEBPB and CAPN1/2 and CAST. This suggests that CEBPB has a direct relationship with CAPN2 taken from published literature but has no predicted effect from the RNAseq dataset. CAST and CAPN1 however show an indirect relationship with a different gene linking CEBPB with CAST and CAPN1 each. This suggests a close relationship with the calpain system and CEBPB but would need further verification.

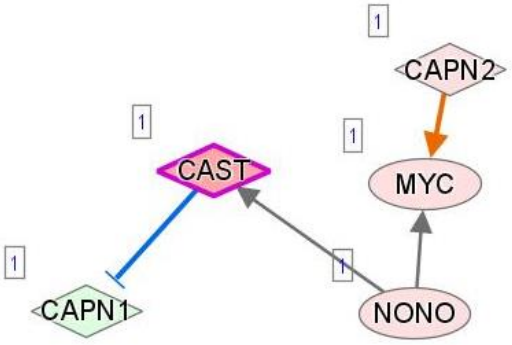

Figure 3.2.11. The pathway analysis establishing the connection between CEBPB and CAST, CAPN1 and CAPN2. A blue line indicates that it is predicted to be inhibited. A grey line indicates that is no predicted effect. A solid line indicates a direct relationship, and a dotted line shows an indirect effect. Taken from Qiagen IPA.

Figure 3.2.12 shows the relationships of CAPN1/2 and CAST with NONO. There is a direct relationship between NONO and CAST however there was no predicted effect. NONO linked with CAPN1 through CAST the endogenous inhibitor of calpain, suggesting that the strongest link between the NONO and CAPN1 is through CAST. CAPN2 is linked with NONO through MYC a known oncogene.

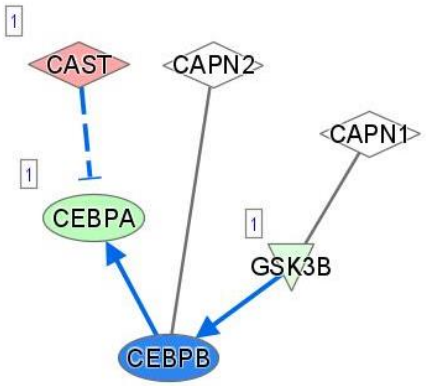

Figure 3.2.12. The pathway analysis establishing the connection between NONO and CAST, CAPN1 and CAPN2. A blue line indicates that it is predicted to be inhibited. A grey line indicates that is no predicted effect. A orange line indicates that there is predicted activation. A solid line indicates a direct relationship. Taken from Qiagen IPA.

Chapter 4: Discussion

4.1 Phenotypic Discussion

To assess the cytotoxicity of calpain inhibition, 2 commercially available calpain inhibitors were selected for clonogenic survival assays in 2 breast cancer cell lines MDA-MB-231 and MDA-MB-468. Both of these cell lines are of the triple negative molecular subtype of breast cancer, presenting a more aggressive phenotype, and have limited treatment options clinically. The 2 selected calpain inhibitor drugs were Calpeptin and PD150606. Calpeptin functions by penetrating the cell membrane and binding to the active site of calpain, stopping activation. However, it has also been reported to inhibit other families of proteases such as cathepsins (Barnoy *et al*., 1997). Despite the level of inhibition of these off target proteases being low, potential differences in the effect of calpeptin compared to other calpain inhibitors may be a result of such off target effects. PD150606 is a more specific calpain inhibitor and is

not reported to affect any other protease. It functions by binding to the penta-EF hand of calpain, rather than the active site (Lin *et al.,* 1997). No previous work had been carried out using these calpain inhibitors in breast cancer cell lines to assess clonogenic survival, therefore an initial range of doses needed to be selected, for both inhibitors, to obtain estimated IC_{50} values. The effect on proliferation from the calpain inhibitors was not assessed as radioresponse is normally assessed by clonogenic survival – there were also time restrictions that limited what could be achieved in the available time. Antiproliferative responses could, perhaps, be examined in future, e.g., if chemoresponse rather than radioresponse is of interest – clonogenic survival would, however, also still be required.

It is known that micro- and milli-calpains are ubiquitously expressed but have low endogenous levels of activity, requiring calcium for increased activity. Previous work within our group showed that there is a significant increase in calpain activity after treatment with calcium ionophore, specifically a dose of 10µM (Vasan, 2022). Furthermore, hypoxia is associated with increased intracellular Ca^{2+} (Girault *et al*., 2020), therefore it would be expected that within cancer cells in a hypoxic environment there would be an increase in calpain activity. Whilst hypoxia was not, due to time constraints, assessed in the current project the effect of calcium activation was assessed. The treatment of calcium ionophore alone did, as expected (due to activation of multiple signalling pathways), cause some cell killing but this was accounted for when calculating the surviving fraction following calpain inhibitor treatment.

Both calpeptin and PD150606 showed cytotoxic effects on MDA-MB-231 and MDA-MB-468. Overall MDA-MB-231 showed a greater sensitivity to the calpain inhibitors displaying a lower surviving fraction for both drugs with and without the calcium ionophore treatment. Calpeptin demonstrated that it is more potent than PD150606. At the chosen highest dose of calpeptin, 100µM, the lowest surviving fraction was recorded whereas the highest dose of PD150606 at 150µM, displayed a high number of cytotoxicity but was lower than Calpeptin with a lower dose. The higher potency of calpeptin may be a result of the off target effects of the drug such as cathepsin. A major significant difference between the cytotoxic effects of calpain inhibition is the treatment of calcium ionophore. In both cell lines there was a statistically significant difference between the calpain inhibitors with and without the activation of calpains. In MDA-MB-468 there was a significant difference between PD150606 treated with calcium ionophore and treated without ($p=<0.05$), this was the same for calpeptin ($p=<0.05$) between cells with

and without calcium ionophore treatment. MDA-MB-231 displayed the same outcome with a significant difference (p=<0.05) between the surviving fraction of calpeptin and PD150606 with and without the calcium ionophore treatment. The effectiveness of calpeptin and PD150606 without the prior activation of calpains showed significantly less cell killing compared to cells with calpain activation. As mentioned, calpains are ubiquitously expressed at low levels (Goll *et al.,* 2003) and there is low endogenous activity, therefore a minimal effect of calpain inhibition would be expected, this is reflected in the results of the experiment.

With MDA-MB-468, calpeptin showed the lowest surviving fraction of approximately 0.58 and PD150606 showed a surviving fraction of 0.62, this is a major contrast to calpeptin and PD150606 with calcium ionophore treatment with the lowest surviving fraction being 0.13 and 0.18 respectively. In MDA-MB-231 a similar trend was observed, with the lowest surviving fraction for PD150606 being 0.55. However, calpeptin without calcium ionophore showed a high level of cell killing at 100µM with a surviving fraction of 0.2 compared to 75µM showing a surviving fraction of 0.56. The drastic decrease in surviving fraction was only observed in calpeptin without calcium ionophore in MDA-MB-231 cells and there is no definitive explanation for why this was observed. The characteristics of the cell might potentially cause the cell line to have an increased sensitivity to calpeptin at that concentration. It would be of interest to conduct Western blotting and a calpain activity assay in both cell lines to examine relative levels of protein expression and calpain activity in each line e.g., using a tBOC assay. Further experiments with doses of calpeptin between 75µM and 100µM could identify at which dose this response is observed. In contrast, emulating the increase intracellular Ca^{2+} that is observed in hypoxia using calcium ionophore showed a higher level of cytotoxicity compared to no increase in Ca^{2+}. The inhibition of calpain causes cell killing and could be attributed to many different functions of the calpain system. One of these functions is cellular survival, calpains are known to cleave *p53* therefore preventing the *p53* dependent apoptosis (Atencio *et al*., 2000), which may explain the cell killing observed from the clonogenic assays. Another survival pathway involving calpain is the calpain mediated cleavage of IκBα, and in turn allows for the transcription factor NF-κβ to activate (Han *et al*., 1999). These survival pathways that play a functional role with calpain may explain the increase level of cell killing in the cells treated with calcium ionophore – it would be interesting to monitor levels of such proteins pre- and post-calpain inhibitor treatment. With the increase in calpain activity from

calcium ionophore pathways such as the cleavage of p53 would be activated however with the inhibition of calpain through the drug treatments, p53 can function correctly and causes apoptosis.

To establish an IC_{50} dose for each drug in each cell line an estimated IC_{50} was taken due to the time constraints - a dose response curve with enough datapoints could not be completed. A linear regression model was used to estimate the IC_{50} dose to take forward for the combination experiments with radiation and the calpain inhibitors. If more time was available, a new range of doses would have been selected to establish an accurate IC_{50} dose. The cell line chosen for initial combination experiments was MDA-MB-468 with PD150606. The response in this cell line to PD150606 showed a clear difference between prior calcium ionophore treatment or no prior treatment. The estimated IC_{50} doses were calculated for PD150606 in MDA-MB-468. The combination experiments of radiation and the calpain inhibitors in MDA-MB-468 were completed in triplicate, but unfortunately the experiments did not produce any reliable data. Due to time limitations the experiments were carried out concurrently rather than, ideally, sequentially so any error that had occurred could not have been observed until all 3 experiments were completed. The reason for the errors cannot be determined. Drug-radiation combination experiments should be prioritised and hopefully current single agent toxicity data, with and without calcium activation, will be of assistance in such efforts.

4.1.1 Suggested Future Work

Firstly, the combination of radiation and the selected calpain inhibitors can be completed in both cell lines chosen to assess for radiosensitising properties of the calpain inhibitors. A repeat of the experiments but using hypoxic conditions, including assessing the effect of the drugs alone and in combination with radiation to assess for radiosensitivity with calpain inhibitors in hypoxia, will be of interest. This set of experiments can also be repeated on different cell lines representing other breast cancer molecular subtypes. As indicated above, additional Western blotting and activity assays would also be of use, to compare response between cell lines, and in terms of the different agents. Calpeptin and PD150606 can also be used to assess for chemo sensitisation in breast cancer cell lines in hypoxic and normoxic conditions.

4.2 Bioinformatics

Calpastatin, the endogenous inhibitor of calpain, has been linked with breast cancer progression through regulation of lymphovascular invasion (Storr *et al*., 2011). Our group had RNA Sequencing performed on 6 CAST overexpression cell lines, CAST I-III MDA-MB-231 and CAST I-III T47D. Overexpressing and parental control cell lines were treated by Ca-ionophore to activate the calpain system then washed and counted then frozen in cell pellets and sent to Novogene (UK) Company Ltd for RNA sequencing, as described in section 2.2.1.From cellular fluorescence studies CAST II showed a distinctly different subcellular localisation pattern i.e. perinuclear punctate v diffuse cytoplasmic for CAST I and III. As this was an MRes project, with limited time available, CAST II overexpression in both cell lines was used for bioinformatic analysis (CAST I and III being investigate by another student in the group). The two cell lines represent two molecular subtypes of breast cancer, MDA-MB-231 for triple-negative and T47D for luminal phenotype.

The RNAseq data obtained from MDA-MB-231 and T47D CAST II overexpression cell lines showed a variety of DEGs that were up- or downregulated at different levels. The lists of DEGs could be filtered through different parameter, such as by the fold change of the DEG, either through upregulation or downregulation or by the p-value to filter through significance of the DEG and with DEGs unique or common to both cell lines. This revealed potential DEGs of interest. The 10 topmost, out of 3684 DEGs for MDA-MB-231 and 8857 DEGs for T47D, most upregulated and downregulated, most statistically significant, unique to the cell line and common between the two cell lines were identified. Unique DEGs to MDA-MB-231 CAST II overexpression, shown in table 3.2.8, LINC02582, CACNA2D4 and several more. A recent study by Wang *et al.,* (2019) showed that LINC02582 is associated with radioresistance in breast cancer. The overexpression of LINC02582 promoted radioresistance while the inhibition of LINC02582 showed radiosensitivity. The mechanism of this radioresistance is reported to be via the interaction between LINC02582 and ubiquitin specific peptidase 7 (USP7), this deubiquitinates and stabilises checkpoint kinase 1, this being an effector for kinase DNA damage repair resulting in the increase in radioresistance. The inhibition of LINC02582 also shown by Wang *et al.,* (2019) displayed radiosensitivity in breast cancer cell lines. The RNAseq

data showed a fold change of -5.945 in LINC02582, the decrease in the gene because of the CASTII overexpression could indicate that the inhibition of the calpain system could have a downstream effect of decreasing expression of LINC02582 thus increasing the radiosensitivity of breast cancer cells. This needs further work to check the validity and test the hypothesis. CACNA2D4, showed a decrease in expression in the CASTII overexpression cell lines and is unique to the MDA-MB-231 cell line. Research into this gene is very minimal, mutated CACNA2D4 is known for causing retinal dysfunctions (Ba-Abbad *et al.,* 2016), however a recent study by Pidsley *et al.,* (2022) found that inclusion of CACNA2D4 methylation was a more effective predictor of prostate cancer specific-survival compared to just grade alone. CACNA2D4 showed a significant association with breast cancer specific-survival and a significant correlation between the gene and a CAST probe, highlighting the potential avenue of research in breast cancer. If time had allowed it would have been interesting to verify via qRT-PCR and Western blotting, and to assesses expression in breast cancer TMA sections by IHC.

DEGs unique to T47D CASTII overexpression cell lines were shortlisted in table 3.2.9. The top two most significant DEGs from this list includes FHL1 and SPARC. Four and a half LIM protein 1 (FHL1) is involved in skeletal and cardiac muscle growth (Chu *et al*., 2000). FHL1 has been shown to interact with estrogen receptors (ER), including ERα and ERβ, and can regulate breast cancer cell growth, through binding to the AF-1 domain therefore reduce the transcriptional activity of ERα, however the interaction between FHL1 and ERβ is not fully understood (Ding *et al*., 2011). FHL1 showed a 5.762 fold change, the increase in expression of FHL1 due to the overexpression of CASTII may potentially have a negative effect on breast cancer cell growth due to the interaction with ERs, however the relationship between CASTII and FHL1 is yet to be established. Secreted protein, acidic and rich in cysteine or SPARC is a glycoprotein, involved in the physiological functions of embryonic development, tissue repair and cell regeneration. SPARC has been demonstrated to be associated with many different cancers including breast cancer (Shi *et al*., 2022). One of the key associations of SPARC is the relationship with the tumour suppressor p53. Evidence suggests that when SPARC is suppressed p53 can be regulated, in turn causing apoptosis through the mitochondrial intrinsic pathway; when SPARC is overexpressed, it acts as an oncogene pathway inhibiting p53 function (Camacho *et al*., 2020). Table 3.2.9 displays a 5.482 fold change for SPARC in the

CASTII overexpression T47D cell line. Calpains may potentially have a downstream effect of suppressing SPARC but due to the inhibition of calpain from the calpastatin overexpression an increase of SPARC is observed, which may result in the p53 gene being suppressed resulting in survival of malignant cells.

Using the IPA software upstream analysis was performed to identify potential transcription regulators that were predicted to be inhibited or activated because of the CASTII overexpression. It is known that transcription factors that are dysregulated can contribute to the progression of disease including cancer (Lee and Young, 2013). Therefore, transcription regulators were chosen for upstream analysis. Only transcription regulators that were predicted to be activated or inhibited were identified and used for further assessment. Transcription regulators for CASTII overexpression MDA-MB-231 predicted to be activated included MYC and several more shown in table 3.2.10. MYC is a well know driver of many different cancers being involved in the formation and progression of cancer (Duffy *et al*., 2021). Calpain has also been linked with MYC, it has been observed that calpain cleaves MYC to form a transcriptionally inactive protein, MYC-nick. This process is known to occur under stress conditions such as hypoxia (Conacci-Sorrell *et al.*, 2014). Transcription regulators that were predicted to be inhibited in CAST II overexpression MDA-MB-231 included GATA1 and others, shown in table 3.2.10. GATA1 plays a role in the haemopoietic system, specifically the switching of foetal haemoglobin to adult haemoglobin, it has also been studied to be involved in solid tumours (Gao *et al*., 2022). The transcription regulator has been observed in the epithelial-mesenchymal transition in breast cancer leading to tumour progression and metastasis in breast cancer (Li *et al*., 2015). For transcription regulators in CASTII overexpression T47D cell line the predicted to be activated regulators included MYCL and several more shown in table 3.2.11. Part of the same family of MYC, MYCL is also a driver of cancer. MYCL has been linked to several different cancers including triple negative breast cancer (Jiang *et al.,* 2022). There are no know relationships between MYCL and the calpain system but as previously mentioned calpains are known to cleave MYC, so there is reason that calpain may potentially play a role in the physiological function of MYCL. Finally, the transcription regulators that were predicted to be inhibited in CASTII overexpression T47D included IRF7 and several more shown in table 3.2.11. IRF7 has been described as having anti-tumour properties, by inducing apoptosis downstream that leads to caspase-8 being induced

and causes apoptosis in cancer cells and not normal cells (Ning *et al*., 2011). The transcription regulators identified from the upstream analysis yield results that showed a stronger association with cancer than DEGs identified through the RNAseq dataset. However, with IPA the software only indicates that there is an alteration as a result of the CASTII overexpression but does not show how this transcription regulator is affected. Following this with survival analysis to assess for importance in breast cancer survival provides a direction as to which transcription factors to consider investigating further. The transcription regulators shortlisted were taken for further assessment using survival analysis with the METABRIC cohort.

The calpain system has many different physiological functions and is known to have downstream effects on many different pathways. It is reasonable to believe that genes indirectly effected by the calpain/calpastatin system are also significantly associated with breast cancer survival. METABRIC is a cohort of breast cancer patient samples that includes annotation such as clinical data and expression data, making it a useful dataset to identify genes that are potentially associated significantly with breast cancer specific survival. Survival analysis was performed for each of the shortlisted DEGs, and transcription regulators identified and shortlisted. Using data from the METABRIC cohort 54 genes were identified as being significant associated with survival ($p=<0.05$). The mRNA expression data obtained from METABRIC was stratified into low and high expression by using the median value. The expression level was then plotted against breast cancer specific survival to plot a Kaplan-Meier. Approximately 150 DEGs were shortlisted and taken for survival analysis, interestingly 54 of these showed a significant association with breast cancer specific survival. This indicates that the genes altered by the CASTII overexpression may be relevant to breast cancer survival. To further refine DEGs to use for verification, correlation analysis was performed using 6 calpastatin probes obtained from the METABRIC dataset. Spearman's Rank coefficient was used for the correlation with the DEGs significantly associated with survival and the CAST probes. It should be noted however that the probes used were designed for normal expression levels of CAST and not the overexpressed levels that would be present in the cell lines used for analysis. The correlation analysis revealed 17 DEGs that had a significant correlation with a CAST probe and a significant association with breast cancer specific survival. This number was still too high to be taken for verification using Western blot and Q-RT-PCR techniques, so therefore the critical value for a significant association with survival was reduced to $p<0.01$.

This reduced the number to 6 DEGs, ITM2A (p=0.000514), CACNA2D4 (p=5.228E-7), CEBPB (p=4.7904E-7), FOS (p=0.000697), NONO (p=0.000038) and SIX2 (p=0.000472). The top 3 most significant were selected for verification, CACNA2D4, CEBPB and NONO.

CCAAT Enhancer Binding Protein Beta or CEBPB is a transcription factor involved with regulating genes that play a role in immune and inflammatory responses (Kinoshita, Akira and Kishimoto, 1992). CEBPB was identified from the upstream analysis using IPA from the MDA-MB-231 CASTII overexpression cell line. The transcription factor has been heavily linked with cancer, including in this breast cancer. The function by which CEBPB effects breast cancer varies, an elevation of CEBPB mRNA expression has been linked to metastatic breast cancer, a higher tumour grade and an overall worse prognosis compared to normal expression of CEBPB mRNA (Zahnow *et al.,* 2009). The survival analysis using the METABRIC cohort revealed that high expression of CEBPB is associated with a worse overall survival in patients. CEBPB mRNA is coded for 3 different isoforms, LAP1, LAP2 and LIP each with unique functions. LIP is considered an inhibitor for LAP1/2, high expression of LIP is linked with a worse prognosis in breast cancer. The high LIP/LAP ratios being reduced to a low LIP/LAP ratio showed reduced migration and matrix invasion of triple negative breast cancer (Sterken *et al*., 2022). These studies highlight that high expression of CEBPB and some of its isoforms translate to a worse breast cancer specific survival. Interestingly some studies have observed a different effect of high and low expression. Li *et al*., (2018) observed that repressed expression of a CEBPB isoform, *LAP*, resulted in the maintaining of tumour immunosuppression. The effect of the repressed expression would contribute to tumour survival and does not agree with the survival analysis indicating that low expression is associated with better survival. High expression was shown to be associated with a worse survival. However, a study by Qi *et al*., (2023) found CEBPB regulates migration, invasion and EMT in breast cancer through the inhibition of THBS2 and O-fucosylation, this indicate that a high expression of CEBPB can have a positive effect on breast cancer specific survival. Using IPA path explorer tool, any relationships between CEBPB and CAPN1*/2* and CAST was searched for using the RNAseq data. A path was linked to CEBPB from to GSK3B (Lee *et al*., 2010) and then an interaction is reported between CAPN1 and GSK3B*,* however the evidence supporting any relationship between CAPN1 and GSK3B is very minimal and would need further validation (Li *et al*., 2019). A direct relationship between CEBPB and CAPN2 was indicated however only a protein-protein

interaction was described with *IL13* leading to the binding of CEBPB and CAPN2 however again there is minimal evidence for this (Pan *et al*., 2013). CEBPB showed a pathway to CAST first through CEBPA through transcriptional activity (Wiper-Bergeron *et al.,* 2003), then CAST is linked to CEBPA through CAST decreasing the activation of a luciferase reporter gene for a promoter from CEBPA (Patel and Lane, 1999).

Non-POU Domain Containing Octamer Binding also known as NONO is an RNA binding protein that is involved in many different cellular processes including transcriptional regulation and RNA splicing (Mircsof *et al*., 2015). In the CASTII overexpression T47D RNAseq data NONO was a transcription regulator that was predicted to be inhibited. The survival analysis of NONO using the METABRIC cohort data indicated that high expression of NONO is associated with worse breast cancer specific survival. Iino *et al*., (2020) observed that NONO promotes proliferation in breast cancer, it was found that a NONO knockdown significantly reduced the cell proliferation in two different breast cancer cell lines. This concurs with the survival analysis with a low expression showing better survival. Another study by Zhu *et al.,* (2016) indicated that NONO regulates SREBP-1. Both of these genes were positively correlated therefore an increase in NONO resulted in an increase in SREBP-1 which in turn increases the transcription of lipogenic genes and lipid production in breast cancer cells. This also supports that overall high expression has worse overall survival. The path explorer tool was used to establish any relationships between NONO and CAPN1*/2* and CAST. NONO displayed a direct relationship with CAST with CAST mRNA binds with NONO (Hu *et al*., 2020). The path explorer also determined that the closest relationship between NONO and CAPN1 was through CAST, the endogenous inhibitor of CAPN1. The final path determined between NONO and CAPN2 was connected via MYC, a known oncogene and is also known to be linked with the calpain system.

Calcium Voltage-Gated Channel Auxiliary Subunit Alpha2delta 4 or CACNA2D4 encodes for a protein in the voltage dependent calcium channel complex, these channels regulate calcium influx into a cell. There is very minimal research into CACNA2D4 in breast cancer. However, CACNA2D4 was a unique DEG is to CASTII overexpression MDA-MB-231 and in the top 10 most statistically significant DEGs, postulating that CACNA2D4 may have a significant relationship with the overexpression of CASTII and potential the calpain system. Furthermore, CACNA2D4 also showed a significant association with survival and a significant correlation with a CAST probe. The analysis of this gene highlights the potential for a target in breast cancer. The path

explorer tool was used to identify any relationships between CACNA2D4 and CAPN1/2 and CAST. CACNA2D4 showed a relationship with EGR1 this gene then connected with CASP3 to then connect to CAST, and with EGFR to connect CAPN1 and finally EGR to connect to CAPN2. The relationships established with the calpain system however are not closely related with at least two genes being needed to establish a relationship between CACNA2D4 and the calpain system. This analysis combined with the minimal information about CACNA2D4 in breast cancer shows an interesting gene to follow up on.

4.2.1 Suggestions for Future Work

The verification of CACNA2D4, NONO and CEBPB could not be completed due to the time limitations and primers being delivered too late. Future work to follow on would be to complete the verification of the identified genes using Q-rt-PCR and Western blots. Immunohistochemistry can also be performed to confirm the presence of these genes in breast cancer tissue.

4.3 Conclusions

The inhibition of the calpain system poses an interesting avenue for research. The effect of calpain inhibition using commercially available calpain inhibitors in triple-negative breast cancer cell lines shows cytotoxic effects as a single agent with similar results between the calpeptin and PD150606. The activation of the calpain system before the inhibition of calpains showed increased cell killing, highlighting the importance of the calpain activity to breast cancer survival. DEGs affected by calpastatin overexpression showing significant association with survival in breast cancer within a cohort of patients and being linked with the calpain system indicate the potential importance of calpain system in breast cancer.

References

- Ahn, H.J., Jung, S.J., Kim, T.H., Oh, M.K. and Yoon, H.-K. (2015) 'Differences in Clinical Outcomes between Luminal A and B Type Breast Cancers according to the St. Gallen Consensus 2013', *Journal of Breast Cancer*, 18(2), pp. 149–159. Available at: https://doi.org/10.4048/jbc.2015.18.2.149.
- Aiyappa, R (2020) *TARGETING DNA REPAIR AND HYPOXIA TO IMPROVE RADIORESPONSE IN BREAST CANCER*, Thesis (PhD), University of Nottingham
- Andreassen, P.R., Seo, J., Wiek, C. and Hanenberg, H. (2021) 'Understanding BRCA2 Function as a Tumor Suppressor Based on Domain-Specific Activities in DNA Damage Responses', *Genes*, 12(7), p. 1034. Available at: https://doi.org/10.3390/genes12071034.
- Askar, M.A., El Shawi, O.E., Abou zaid, O.A.R., Mansour, N.A. and Hanafy, A.M. (2021) 'Breast cancer suppression by curcumin-naringenin-magnetic-nano-particles: In vitro and in vivo studies', *Tumor Biology*, 43(1), pp. 225–247. Available at: https://doi.org/10.3233/TUB-211506.
- Atencio, I.A., Ramachandra, M., Shabram, P. and Demers, G.W. (2000) 'Calpain inhibitor 1 activates p53-dependent apoptosis in tumor cell lines', *Cell Growth & Differentiation: The Molecular Biology Journal of the American Association for Cancer Research*, 11(5), pp. 247–253.
- Averna, M., De Tullio, R., Capini, P., Salamino, F., Pontremoli, S. and Melloni, E. (2003) 'Changes in calpastatin localization and expression during calpain activation: a new mechanism for the regulation of intracellular Ca2+-dependent proteolysis', *Cellular and Molecular Life Sciences CMLS*, 60(12), pp. 2669–2678. Available at: https://doi.org/10.1007/s00018-003-3288-0.
- Ba-Abbad, R., Arno, G., Carss, K., Stirrups, K., Penkett, C.J., Moore, A.T., Michaelides, M., Raymond, F.L., Webster, A.R. and Holder, G.E. (2016) 'Mutations in CACNA2D4 Cause Distinctive Retinal Dysfunction in Humans', *Ophthalmology*, 123(3), pp. 668-671.e2. Available at: https://doi.org/10.1016/j.ophtha.2015.09.045.
- Bang, Y.J., Giaccone, G., Im, S.A., Oh, D.Y., Bauer, T.M., Nordstrom, J.L., Li, H., Chichili, G.R., Moore, P.A., Hong, S., Stewart, S.J., Baughman, J.E., Lechleider, R.J. and Burris, H.A. (2017) 'First-in-human phase 1 study of margetuximab (MGAH22), an Fc-modified chimeric monoclonal antibody, in patients with HER2-positive advanced solid tumors', *Annals of Oncology*, 28(4), pp. 855–861. Available at: https://doi.org/10.1093/annonc/mdx002.
- Barnoy, S., Glaser, T. and Kosower, N.S. (1997) 'Calpain and calpastatin in myoblast differentiation and fusion: Effects of inhibitors', *Biochimica et Biophysica Acta (BBA) - Molecular Cell Research*, 1358(2), pp. 181–188. Available at: https://doi.org/10.1016/S0167-4889(97)00068-2.
- Barzaman, K., Karami, J., Zarei, Z., Hosseinzadeh, A., Kazemi, M.H., Moradi-Kalbolandi, S., Safari, E. and Farahmand, L. (2020) 'Breast cancer: Biology, biomarkers, and treatments', *International Immunopharmacology*, 84, p. 106535. Available at: https://doi.org/10.1016/j.intimp.2020.106535.
- Bentzen, S.M. (2006) 'Preventing or reducing late side effects of radiation therapy: radiobiology meets molecular pathology', *Nature Reviews Cancer*, 6(9), pp. 702–713. Available at: https://doi.org/10.1038/nrc1950.
- Bonadonna, G., Brusamolino, E., Valagussa, P., Rossi, A., Brugnatelli, L., Brambilla, C., De Lena, M., Tancini, G., Bajetta, E., Musumeci, R. and Veronesi, U. (1976) 'Combination chemotherapy as an adjuvant treatment in operable breast cancer', *The New England Journal of Medicine*, 294(8), pp. 405–410. Available at: https://doi.org/10.1056/NEJM197602192940801.
- Bradley, J.A. and Mendenhall, N.P. (2018) 'Novel Radiotherapy Techniques for Breast Cancer', *Annual Review of Medicine*, 69(1), pp. 277–288. Available at: https://doi.org/10.1146/annurev-med-042716-103422.
- *Breast cancer incidence (invasive) statistics* (2015) *Cancer Research UKb*. Available at: https://www.cancerresearchuk.org/health-professional/cancer-statistics/statistics-by-cancer-type/breast-cancer/incidence-invasive
- Brunt, A.M., Haviland, J.S., Wheatley, D.A., Sydenham, M.A., Alhasso, A., Bloomfield, D.J., Chan, C., Churn, M., Cleator, S., Coles, C.E., Goodman, Andrew, Harnett, A., Hopwood, Penelope, Kirby, A.M., Kirwan, C.C., Morris, C., Nabi, Z., Sawyer, E., Somaiah, N., Stones, L., Syndikus, I., Bliss, J.M., Yarnold, J.R., Alhasso, A., Armstrong, A., Bliss, J., Bloomfield, D., Bowen, J., Brunt, M., Chan, C., Chantler, H.,

Churn, M., Cleator, S., Coles, C., Donovan, E., Goodman, Andy, Griffin, S., Haviland, J., Hopwood, Penny, Kirby, A., Kirk, J., Kirwan, C., MacLennan, M., Morris, C., Nabi, Z., Sawyer, E., Sculphur, M., Sinclair, J., Somaiah, N., Stones, L., Sydenham, M., Syndikus, I., Tremlett, J., Venables, K., Wheatley, D. and Yarnold, J. (2020) 'Hypofractionated breast radiotherapy for 1 week versus 3 weeks (FAST-Forward): 5-year efficacy and late normal tissue effects results from a multicentre, non-inferiority, randomised, phase 3 trial', *The Lancet*, 395(10237), pp. 1613–1626. Available at: https://doi.org/10.1016/S0140-6736(20)30932-6.

- Buckley, N.E. and Mullan, P.B. (2012) 'BRCA1 – Conductor of the Breast Stem Cell Orchestra: The Role of BRCA1 in Mammary Gland Development and Identification of Cell of Origin of BRCA1 Mutant Breast Cancer', *Stem Cell Reviews and Reports*, 8(3), pp. 982–993. Available at: https://doi.org/10.1007/s12015-012-9354-y.
- Camacho, D., Jesus, J.P., Palma, A.M., Martins, S.A., Afonso, A., Peixoto, M.L., Pelham, C.J., Moreno, E. and Gogna, R. (2020) 'Chapter Five - SPARC-p53: The double agents of cancer', in K.D. Tew and P.B. Fisher (eds) *Advances in Cancer Research*. Academic Press, pp. 171–199. Available at: https://doi.org/10.1016/bs.acr.2020.05.004.
- Cameron, D., Piccart-Gebhart, M.J., Gelber, R.D., Procter, M., Goldhirsch, A., de Azambuja, E., Castro, G., Untch, M., Smith, I., Gianni, L., Baselga, J., Al-Sakaff, N., Lauer, S., McFadden, E., Leyland-Jones, B., Bell, R., Dowsett, M. and Jackisch, C. (2017) '11 years' follow-up of trastuzumab after adjuvant chemotherapy in HER2-positive early breast cancer: final analysis of the HERceptin Adjuvant (HERA) trial', *Lancet (London, England)*, 389(10075), pp. 1195–1205. Available at: https://doi.org/10.1016/S0140-6736(16)32616-2.
- Cancer Research (2022). *Invasive Breast Cancer Statistics* UK Available at https://www.cancerresearchuk.org/health-professional/cancer-statistics/statistics-by-cancer-type/breast-cancer/incidence-invasive#heading-Zero [Accessed 30/01/2023]
- Cancer Research UK (2022) *Breast cancer mortality statistics*. Available at: https://www.cancerresearchuk.org/health-professional/cancer-statistics/statistics-by-cancer-type/breast-cancer/mortality#heading-Zero (Accessed: November 4, 2022).
- Cancer Research UK, *Risk factors for breast cancer* (2023). Available at: https://www.cancerresearchuk.org/about-cancer/breast-cancer/risks-causes/risk-factors (Accessed: 7 August 2023).
- Carreau, A., Hafny-Rahbi, B.E., Matejuk, A., Grillon, C. and Kieda, C. (2011) 'Why is the partial oxygen pressure of human tissues a crucial parameter? Small molecules and hypoxia', *Journal of Cellular and Molecular Medicine*, 15(6), pp. 1239–1253. Available at: https://doi.org/10.1111/j.1582-4934.2011.01258.x.
- Casaubon, J.T., Kashyap, S. and Regan, J.-P. (2023) 'BRCA1 and BRCA2 Mutations', in *StatPearls*. Treasure Island (FL): StatPearls Publishing. Available at: http://www.ncbi.nlm.nih.gov/books/NBK470239/ (Accessed: 21 September 2023).
- Cazzaniga, M.E., Biganzoli, L., Cortesi, L., De Placido, S., Donadio, M., Fabi, A., Ferro, A., Generali, D., Lorusso, V., Milani, A., Montagna, E., Munzone, E., Orlando, L., Pizzuti, L., Simoncini, E., Zamagni, C. and Pappagallo, G.L. (2019) 'Treating advanced breast cancer with metronomic chemotherapy: what is known, what is new and what is the future?', *OncoTargets and therapy*, 12, pp. 2989–2997. Available at: https://doi.org/10.2147/OTT.S189163.
- Chen, K., Liu, J., Zhu, L., Su, F., Song, E. and Jacobs, L.K. (2015) 'Comparative effectiveness study of breast-conserving surgery and mastectomy in the general population: A NCDB analysis', *Oncotarget*, 6(37), pp. 40127–40140.
- Chu, P.-H., Ruiz-Lozano, P., Zhou, Q., Cai, C. and Chen, J. (2000) 'Expression patterns of FHL/SLIM family members suggest important functional roles in skeletal muscle and cardiovascular system', *Mechanisms of Development*, 95(1), pp. 259–265. Available at: https://doi.org/10.1016/S0925-4773(00)00341-5.
- Collaborative Group on Hormonal Factors in Breast Cancer (2019) 'Type and timing of menopausal hormone therapy and breast cancer risk: individual participant meta-analysis of the worldwide

epidemiological evidence', *Lancet (London, England)*, 394(10204), pp. 1159–1168. Available at: https://doi.org/10.1016/S0140-6736(19)31709-X.

- Conacci-Sorrell, M., Ngouenet, C., Anderson, S., Brabletz, T. and Eisenman, R.N. (2014) 'Stress-induced cleavage of Myc promotes cancer cell survival', *Genes & Development*, 28(7), pp. 689–707. Available at: https://doi.org/10.1101/gad.231894.113.
- Cortesi, L., Rugo, H.S. and Jackisch, C. (2021) 'An Overview of PARP Inhibitors for the Treatment of Breast Cancer', *Targeted Oncology*, 16(3), pp. 255–282. Available at: https://doi.org/10.1007/s11523-021-00796-4.
- Curtis, C., Shah, S.P., Chin, S.-F., Turashvili, G., Rueda, O.M., Dunning, M.J., Speed, D., Lynch, A.G., Samarajiwa, S., Yuan, Y., Gräf, S., Ha, G., Haffari, G., Bashashati, A., Russell, R., McKinney, S., Langerød, A., Green, A., Provenzano, E., Wishart, G., Pinder, S., Watson, P., Markowetz, F., Murphy, L., Ellis, I., Purushotham, A., Børresen-Dale, A.-L., Brenton, J.D., Tavaré, S., Caldas, C. and Aparicio, S. (2012) 'The genomic and transcriptomic architecture of 2,000 breast tumours reveals novel subgroups', *Nature*, 486(7403), pp. 346–352. Available at: https://doi.org/10.1038/nature10983.
- Davis, J., Martin, S.G., Patel, P.M., Green, A.R., Rakha, E.A., Ellis, I.O. and Storr, S.J. (2014) 'Low calpain-9 is associated with adverse disease-specific survival following endocrine therapy in breast cancer', *BMC Cancer*, 14, p. 995. Available at: https://doi.org/10.1186/1471-2407-14-995.
- Ding, L., Niu, C., Zheng, Y., Xiong, Z., Liu, Y., Lin, J., Sun, H., Huang, K., Yang, W., Li, X. and Ye, Q. (2011) 'FHL1 interacts with oestrogen receptors and regulates breast cancer cell growth', *Journal of Cellular and Molecular Medicine*, 15(1), pp. 72–85. Available at: https://doi.org/10.1111/j.1582-4934.2009.00938.x.
- Duffy, M.J., O'Grady, S., Tang, M. and Crown, J. (2021) 'MYC as a target for cancer treatment', *Cancer Treatment Reviews*, 94. Available at: https://doi.org/10.1016/j.ctrv.2021.102154.
- *Early and locally advanced breast cancer: diagnosis and management* (2018). London: National Institute for Health and Care Excellence (NICE) (National Institute for Health and Care Excellence: Guidelines). Available at: http://www.ncbi.nlm.nih.gov/books/NBK519155/ (Accessed: 31 January 2023).
- Eiger, D., Agostinetto, E., Saúde-Conde, R. and de Azambuja, E. (2021) 'The Exciting New Field of HER2-Low Breast Cancer Treatment', *Cancers*, 13(5), p. 1015. Available at: https://doi.org/10.3390/cancers13051015.
- Ellis, M.J., Tao, Y., Luo, J., A'Hern, R., Evans, D.B., Bhatnagar, A.S., Chaudri Ross, H.A., von Kameke, A., Miller, W.R., Smith, I., Eiermann, W. and Dowsett, M. (2008) 'Outcome Prediction for Estrogen Receptor–Positive Breast Cancer Based on Postneoadjuvant Endocrine Therapy Tumor Characteristics', *JNCI Journal of the National Cancer Institute*, 100(19), pp. 1380–1388. Available at: https://doi.org/10.1093/jnci/djn309.
- Emens, L.A. (2018) 'Breast Cancer Immunotherapy: Facts and Hopes', *Clinical cancer research : an official journal of the American Association for Cancer Research*, 24(3), pp. 511–520. Available at: https://doi.org/10.1158/1078-0432.CCR-16-3001.
- Emens, L.A., Kok, M. and Ojalvo, L.S. (2016) 'Targeting the programmed cell death-1 pathway in breast and ovarian cancer', *Current Opinion in Obstetrics and Gynecology*, 28(2), pp. 142–147. Available at: https://doi.org/10.1097/GCO.0000000000000257.
- Fabian, C.J. (2007) 'The what, why and how of aromatase inhibitors: hormonal agents for treatment and prevention of breast cancer', *International Journal of Clinical Practice*, 61(12), pp. 2051–2063. Available at: https://doi.org/10.1111/j.1742-1241.2007.01587.x.
- Franco, S.J. and Huttenlocher, A. (2005) 'Regulating cell migration: calpains make the cut', *Journal of Cell Science*, 118(17), pp. 3829–3838. Available at: https://doi.org/10.1242/jcs.02562.
- Freudenberg, J.A., Wang, Q., Katsumata, M., Drebin, J., Nagatomo, I. and Greene, M.I. (2009) 'The role of HER2 in early breast cancer metastasis and the origins of resistance to HER2-targeted therapies', *Experimental and molecular pathology*, 87(1), pp. 1–11. Available at: https://doi.org/10.1016/j.yexmp.2009.05.001.

- Gao, A., McCoy, H.M., Zaman, V., Shields, D.C., Banik, N.L. and Haque, A. (2022) 'Calpain activation and progression of inflammatory cycles in Parkinson's disease', *Frontiers in bioscience (Landmark edition)*, 27(1), p. 20. Available at: https://doi.org/10.31083/j.fbl2701020.
- Gao, Y., Wang, R., Liu, J., Zhao, K., Qian, X., He, X. and Liu, H. (2022) 'SENP1 promotes triple-negative breast cancer invasion and metastasis via enhancing CSN5 transcription mediated by GATA1 deSUMOylation', *International Journal of Biological Sciences*, 18(5), pp. 2186–2201. Available at: https://doi.org/10.7150/ijbs.60594.
- Gaudet, M.M., Gapstur, S.M., Sun, J., Diver, W.R., Hannan, L.M. and Thun, M.J. (2013) 'Active smoking and breast cancer risk: original cohort data and meta-analysis', *Journal of the National Cancer Institute*, 105(8), pp. 515–525. Available at: https://doi.org/10.1093/jnci/djt023.
- Girault, A., Ahidouch, A. and Ouadid-Ahidouch, H. (2020) 'Roles for Ca2+ and K+ channels in cancer cells exposed to the hypoxic tumour microenvironment', *Biochimica et Biophysica Acta (BBA) - Molecular Cell Research*, 1867(4), p. 118644. Available at: https://doi.org/10.1016/j.bbamcr.2020.118644.
- Goll, D.E., Thompson, V.F., Li, H., Wei, W. and Cong, J. (2003) 'The Calpain System', *Physiological Reviews*, 83(3), pp. 731–801. Available at: https://doi.org/10.1152/physrev.00029.2002.
- Guarneri, V. and Conte, P. (2009) 'Metastatic Breast Cancer: Therapeutic Options According to Molecular Subtypes and Prior Adjuvant Therapy', *The Oncologist*, 14(7), pp. 645–656. Available at: https://doi.org/10.1634/theoncologist.2009-0078.
- Han, Y., Weinman, S., Boldogh, I., Walker, R.K. and Brasier, A.R. (1999) 'Tumor necrosis factor-alpha-inducible IkappaBalpha proteolysis mediated by cytosolic m-calpain. A mechanism parallel to the ubiquitin-proteasome pathway for nuclear factor-kappab activation', *The Journal of Biological Chemistry*, 274(2), pp. 787–794. Available at: https://doi.org/10.1074/jbc.274.2.787.
- Hanna, R.A., Campbell, R.L. and Davies, P.L. (2008) 'Calcium-bound structure of calpain and its mechanism of inhibition by calpastatin', *Nature*, 456(7220), pp. 409–412. Available at: https://doi.org/10.1038/nature07451.
- Hennigs, A., Riedel, F., Gondos, A., Sinn, P., Schirmacher, P., Marmé, F., Jäger, D., Kauczor, H.-U., Stieber, A., Lindel, K., Debus, J., Golatta, M., Schütz, F., Sohn, C., Heil, J. and Schneeweiss, A. (2016) 'Prognosis of breast cancer molecular subtypes in routine clinical care: A large prospective cohort study', *BMC Cancer*, 16(1), p. 734. Available at: https://doi.org/10.1186/s12885-016-2766-3.
- Heys, S.D., Hutcheon, A.W., Sarkar, T.K., Ogston, K.N., Miller, I.D., Payne, S., Smith, I., Walker, L.G., Eremin, O., and Aberdeen Breast Group (2002) 'Neoadjuvant docetaxel in breast cancer: 3-year survival results from the Aberdeen trial', *Clinical Breast Cancer*, 3 Suppl 2, pp. S69-74. Available at: https://doi.org/10.3816/cbc.2002.s.015.
- Hosfield, C.M., Elce, J.S., Davies, P.L. and Jia, Z. (1999) 'Crystal structure of calpain reveals the structural basis for Ca(2+)-dependent protease activity and a novel mode of enzyme activation.', *The EMBO Journal*, 18(24), pp. 6880–6889. Available at: https://doi.org/10.1093/emboj/18.24.6880.
- Hu, Z., Dong, L., Li, S., Li, Z., Qiao, Y., Li, Y., Ding, J., Chen, Z., Wu, Y., Wang, Z., Huang, S., Gao, Q., Zhao, Y. and He, X. (2020) 'Splicing Regulator p54nrb /Non-POU Domain-Containing Octamer-Binding Protein Enhances Carcinogenesis Through Oncogenic Isoform Switch of MYC Box-Dependent Interacting Protein 1 in Hepatocellular Carcinoma', *Hepatology (Baltimore, Md.)*, 72(2), pp. 548–568. Available at: https://doi.org/10.1002/hep.31062.
- Iino, K., Mitobe, Y., Ikeda, K., Takayama, K., Suzuki, T., Kawabata, H., Suzuki, Y., Horie-Inoue, K. and Inoue, S. (2020) 'RNA-binding protein NONO promotes breast cancer proliferation by post-transcriptional regulation of SKP2 and E2F8', *Cancer Science*, 111(1), pp. 148–159. Available at: https://doi.org/10.1111/cas.14240.
- Jiang, H., Li, X., Wang, W., Hu, Y. and Ren, D. (2022) 'MYCL promotes the progression of triple-negative breast cancer by activating the JAK/STAT3 pathway', *Oncology Reports*, 48(5), p. 203. Available at: https://doi.org/10.3892/or.2022.8418.
- Kaminskyy, V. and Zhivotovsky, B. (2012) 'Proteases in autophagy', *Biochimica et Biophysica Acta (BBA) - Proteins and Proteomics*, 1824(1), pp. 44–50. Available at: https://doi.org/10.1016/j.bbapap.2011.05.013.

- Katsura, C., Ogunmwonyi, I., Kankam, H.K. and Saha, S. (2022) 'Breast cancer: presentation, investigation and management', *British Journal of Hospital Medicine*, 83(2), pp. 1–7. Available at: https://doi.org/10.12968/hmed.2021.0459.
- Kauer-Dorner, D. and Berger, D. (2018) 'The Role of Brachytherapy in the Treatment of Breast Cancer', *Breast Care*, 13(3), pp. 157–161. Available at: https://doi.org/10.1159/000489638.
- Kennecke, H., Yerushalmi, R., Woods, R., Cheang, M.C.U., Voduc, D., Speers, C.H., Nielsen, T.O. and Gelmon, K. (2010) 'Metastatic Behavior of Breast Cancer Subtypes', *Journal of Clinical Oncology*, 28(20), pp. 3271–3277. Available at: https://doi.org/10.1200/JCO.2009.25.9820.
- Kent W. Mouw, M.D. and Jay R. Harris, M.D. (2012) 'Irradiation in Early-Stage Breast Cancer: Conventional Whole-Breast, Accelerated Partial-Breast, and Accelerated Whole-Breast Strategies Compared', *Oncology*, 26(9). Available at: https://www.cancernetwork.com/view/irradiation-early-stage-breast-cancer-conventional-whole-breast-accelerated-partial-breast-and (Accessed: 6 November 2022).
- Khorchid, A. and Ikura, M. (2002) 'How calpain is activated by calcium', *Nature Structural Biology*, 9(4), pp. 239–241. Available at: https://doi.org/10.1038/nsb0402-239.
- Kinoshita, S., Akira, S. and Kishimoto, T. (1992) 'A member of the C/EBP family, NF-IL6 beta, forms a heterodimer and transcriptionally synergizes with NF-IL6', *Proceedings of the National Academy of Sciences of the United States of America*, 89(4), pp. 1473–1476. Available at: https://doi.org/10.1073/pnas.89.4.1473.
- Kovacs, L. and Su, Y. (2014) 'The Critical Role of Calpain in Cell Proliferation', *Journal of biomolecular research & therapeutics*, 3(3), p. 1000112. Available at: https://doi.org/10.4172/2167-7956.1000112.
- Kyrgiou, M., Kalliala, I., Markozannes, G., Gunter, M.J., Paraskevaidis, E., Gabra, H., Martin-Hirsch, P. and Tsilidis, K.K. (2017) 'Adiposity and cancer at major anatomical sites: umbrella review of the literature', *The BMJ*, 356, p. j477. Available at: https://doi.org/10.1136/bmj.j477.
- Lee, S.-H., Krisanapun, C. and Baek, S.J. (2010) 'NSAID-activated gene-1 as a molecular target for capsaicin-induced apoptosis through a novel molecular mechanism involving GSK3beta, C/EBPbeta and ATF3', *Carcinogenesis*, 31(4), pp. 719–728. Available at: https://doi.org/10.1093/carcin/bgq016.
- Lee, T.I. and Young, R.A. (2013) 'Transcriptional Regulation and its Misregulation in Disease', *Cell*, 152(6), pp. 1237–1251. Available at: https://doi.org/10.1016/j.cell.2013.02.014.
- Letavernier, E., Zafrani, L., Perez, J., Letavernier, B., Haymann, J.-P. and Baud, L. (2012) 'The role of calpains in myocardial remodelling and heart failure', *Cardiovascular Research*, 96(1), pp. 38–45. Available at: https://doi.org/10.1093/cvr/cvs099.
- Letrozole (2022) *NHS* Available at https://www.nhs.uk/medicines/letrozole/#:~:text=Letrozole%20comes%20as%202.5mg,that%20suits%20your%20everyday%20routine. [Accessed 11/01/23]
- Li, H., Li, C.-W., Li, X., Ding, Q., Guo, L., Liu, S., Liu, C., Lai, C.-C., Hsu, J.-M., Dong, Q., Xia, W., Hsu, J.L., Yamaguchi, H., Du, Y., Lai, Y.-J., Sun, X., Koller, P.B., Ye, Q. and Hung, M.-C. (2019) 'MET Inhibitors Promote Liver Tumor Evasion of the Immune Response by Stabilizing PDL1', *Gastroenterology*, 156(6), pp. 1849-1861.e13. Available at: https://doi.org/10.1053/j.gastro.2019.01.252.
- Li, W., Tanikawa, T., Kryczek, I., Xia, H., Li, G., Wu, K., Wei, S., Zhao, L., Vatan, L., Wen, B., Shu, P., Sun, D., Kleer, C., Wicha, M., Sabel, M., Tao, K., Wang, G. and Zou, W. (2018) 'Aerobic Glycolysis Controls Myeloid-Derived Suppressor Cells and Tumor Immunity via a Specific CEBPB Isoform in Triple-Negative Breast Cancer', *Cell metabolism*, 28(1), pp. 87-103.e6. Available at: https://doi.org/10.1016/j.cmet.2018.04.022.
- Li, Yang, Ke, Q., Shao, Y., Zhu, G., Li, Yanshu, Geng, N., Jin, F. and Li, F. (2015) 'GATA1 induces epithelial-mesenchymal transition in breast cancer cells through PAK5 oncogenic signaling', *Oncotarget*, 6(6), pp. 4345–4356.
- Lin, G., Chattopadhyay, D., Maki, M., Wang, K.K.W., Carson, M., Jin, L., Yuen, P., Takano, E., Hatanaka, M., DeLucas, L.J. and Narayana, S.V.L. (1997) 'Crystal structure of calcium bound domain VI of calpain at 1.9 Å resolution and its role in enzyme assembly, regulation, and inhibitor binding', *Nature Structural Biology*, 4(7), pp. 539–547. Available at: https://doi.org/10.1038/nsb0797-539.

- Liu, X., Li, M., Chen, Z., Yu, Yong, Shi, H., Yu, Ying, Wang, Y., Chen, R. and Ge, J. (2022) 'Mitochondrial calpain-1 activates NLRP3 inflammasome by cleaving ATP5A1 and inducing mitochondrial ROS in CVB3-induced myocarditis', *Basic Research in Cardiology*, 117(1), p. 40. Available at: https://doi.org/10.1007/s00395-022-00948-1.
- Lyu, X. and Luo, B. (2021) 'Prognostic factors and survival prediction in HER2-positive breast cancer with bone metastases: A retrospective cohort study', *Cancer Medicine*, 10(22), pp. 8114–8126. Available at: https://doi.org/10.1002/cam4.4326.
- Mahaman, Y.A.R., Huang, F., Kessete Afewerky, H., Maibouge, T.M.S., Ghose, B. and Wang, X. (2019) 'Involvement of calpain in the neuropathogenesis of Alzheimer's disease', *Medicinal Research Reviews*, 39(2), pp. 608–630. Available at: https://doi.org/10.1002/med.21534.
- Makki, J. (2015) 'Diversity of Breast Carcinoma: Histological Subtypes and Clinical Relevance', *Clinical Medicine Insights. Pathology*, 8, pp. 23–31. Available at: https://doi.org/10.4137/CPath.S31563.
- Mamoune, A., Luo, J.-H., Lauffenburger, D.A. and Wells, A. (2003) 'Calpain-2 as a Target for Limiting Prostate Cancer Invasion1', *Cancer Research*, 63(15), pp. 4632–4640.
- McCart Reed, A.E., Kalinowski, L., Simpson, P.T. and Lakhani, S.R. (2021) 'Invasive lobular carcinoma of the breast: the increasing importance of this special subtype', *Breast Cancer Research : BCR*, 23, p. 6. Available at: https://doi.org/10.1186/s13058-020-01384-6.
- McDonald, J.A., Goyal, A. and Terry, M.B. (2013) 'Alcohol Intake and Breast Cancer Risk: Weighing the Overall Evidence', *Current breast cancer reports*, 5(3), p. 10.1007/s12609-013-0114-z. Available at: https://doi.org/10.1007/s12609-013-0114-z.
- Mezni, E., Vizier, C., Guerin, M., Sabatier, R., Bertucci, F. and Gonçalves, A. (2020) 'New Therapeutics in HER2-Positive Advanced Breast Cancer: Towards a Change in Clinical Practices?', *Cancers*, 12(6), p. 1573. Available at: https://doi.org/10.3390/cancers12061573.
- Mircsof, D., Langouët, M., Rio, M., Moutton, S., Siquier-Pernet, K., Bole-Feysot, C., Cagnard, N., Nitschke, P., Gaspar, L., Žnidarič, M., Alibeu, O., Fritz, A.-K., Wolfer, D.P., Schröter, A., Bosshard, G., Rudin, M., Koester, C., Crestani, F., Seebeck, P., Boddaert, N., Prescott, K., Hines, R., Moss, S.J., Fritschy, J.-M., Munnich, A., Amiel, J., Brown, S.A., Tyagarajan, S.K. and Colleaux, L. (2015) 'Mutations in NONO lead to syndromic intellectual disability and inhibitory synaptic defects', *Nature neuroscience*, 18(12), pp. 1731–1736. Available at: https://doi.org/10.1038/nn.4169.
- Momeni, H.R. (2011) 'Role of Calpain in Apoptosis', *Cell Journal (Yakhteh)*, 13(2), pp. 65–72.
- Moo, T.-A., Sanford, R., Dang, C. and Morrow, M. (2018) 'Overview of Breast Cancer Therapy', *PET clinics*, 13(3), pp. 339–354. Available at: https://doi.org/10.1016/j.cpet.2018.02.006.
- MUKHERJEE, A. (2004). AW64 a novel thioredoxin inhibitor. (PhD), University of Nottingham, Nottingham
- Muz, B., de la Puente, P., Azab, F. and Azab, A.K. (2015) 'The role of hypoxia in cancer progression, angiogenesis, metastasis, and resistance to therapy', *Hypoxia*, 3, pp. 83–92. Available at: https://doi.org/10.2147/HP.S93413.
- Nava, M.B., Catanuto, G., Pennati, A., Garganese, G. and Spano, A. (2009) 'Conservative Mastectomies', *Aesthetic Plastic Surgery*, 33(5), pp. 681–686. Available at: https://doi.org/10.1007/s00266-009-9382-4.
- NHS, (2017) *Breast cancer in women - Causes*, *nhs.uk*. Available at: https://www.nhs.uk/conditions/breast-cancer/causes/
- Ning, S., Pagano, J. and Barber, G. (2011) 'IRF7: activation, regulation, modification and function', *Genes and immunity*, 12(6), pp. 399–414. Available at: https://doi.org/10.1038/gene.2011.21.
- Onitilo, A.A., Engel, J.M. and Stankowski, R.V. (2014) 'Cardiovascular toxicity associated with adjuvant trastuzumab therapy: prevalence, patient characteristics, and risk factors', *Therapeutic Advances in Drug Safety*, 5(4), pp. 154–166. Available at: https://doi.org/10.1177/2042098614529603.
- Ono, Y., Saido, T.C. and Sorimachi, H. (2016) 'Calpain research for drug discovery: challenges and potential', *Nature Reviews Drug Discovery*, 15(12), pp. 854–876. Available at: https://doi.org/10.1038/nrd.2016.212.

- Palmieri, C., Owide, J. and Fryer, K. (2022) 'Estimated Prevalence of Metastatic Breast Cancer in England, 2016-2021', *JAMA Network Open*, 5(12), p. e2248069. Available at: https://doi.org/10.1001/jamanetworkopen.2022.48069.
- Pan, H.C., Yang, C.N., Hung, Y.W., Lee, W.J., Tien, H.R., Shen, C.C., Sheehan, J., Chou, C.T. and Sheu, M.L. (2013) 'Reciprocal modulation of C/EBP-α and C/EBP-β by IL-13 in activated microglia prevents neuronal death', *European Journal of Immunology*, 43(11), pp. 2854–2865. Available at: https://doi.org/10.1002/eji.201343301.
- Pandit, P., Patil, Roshankumar, Palwe, V., Gandhe, S., Patil, Rahul and Nagarkar, R. (2019) 'Prevalence of Molecular Subtypes of Breast Cancer: A Single Institutional Experience of 2062 Patients', *European Journal of Breast Health*, 16(1), pp. 39–43. Available at: https://doi.org/10.5152/ejbh.2019.4997.
- Parr, T., Jewell, K.K., Sensky, P.L., Brameld, J.M., Bardsley, R.G. and Buttery, P.J. (2004) 'Expression of calpastatin isoforms in muscle and functionality of multiple calpastatin promoters', *Archives of Biochemistry and Biophysics*, 427(1), pp. 8–15. Available at: https://doi.org/10.1016/j.abb.2004.04.001.
- Patel, Y.M. and Lane, M.D. (1999) 'Role of calpain in adipocyte differentiation', *Proceedings of the National Academy of Sciences of the United States of America*, 96(4), pp. 1279–1284. Available at: https://doi.org/10.1073/pnas.96.4.1279.
- Perou, C.M., Sørlie, T., Eisen, M.B., van de Rijn, M., Jeffrey, S.S., Rees, C.A., Pollack, J.R., Ross, D.T., Johnsen, H., Akslen, L.A., Fluge, Ø., Pergamenschikov, A., Williams, C., Zhu, S.X., Lønning, P.E., Børresen-Dale, A.-L., Brown, P.O. and Botstein, D. (2000) 'Molecular portraits of human breast tumours', *Nature*, 406(6797), pp. 747–752. Available at: https://doi.org/10.1038/35021093.
- Perrin, B.J. and Huttenlocher, A. (2002) 'Calpain', *The International Journal of Biochemistry & Cell Biology*, 34(7), pp. 722–725. Available at: https://doi.org/10.1016/S1357-2725(02)00009-2.
- Pidsley, R., Lam, D., Qu, W., Peters, T.J., Luu, P., Korbie, D., Stirzaker, C., Daly, R.J., Stricker, P., Kench, J.G., Horvath, L.G. and Clark, S.J. (2022) 'Comprehensive methylome sequencing reveals prognostic epigenetic biomarkers for prostate cancer mortality', *Clinical and Translational Medicine*, 12(10), p. e1030. Available at: https://doi.org/10.1002/ctm2.1030.
- Potz, B.A., Abid, M.R. and Sellke, F.W. (2016) 'Role of Calpain in Pathogenesis of Human Disease Processes', *Journal of nature and science*, 2(9), p. e218.
- Qi, L., Sun, B., Yang, B. and Lu, S. (2023) 'CEBPB regulates the migration, invasion and EMT of breast cancer cells by inhibiting THBS2 expression and O-fucosylation', *Human Molecular Genetics*, 32(11), pp. 1850–1863. Available at: https://doi.org/10.1093/hmg/ddad022.
- Rachner, T.D., Göbel, A., Jaschke, N.P. and Hofbauer, L.C. (2020) 'Challenges in Preventing Bone Loss Induced by Aromatase Inhibitors', *The Journal of Clinical Endocrinology & Metabolism*, 105(10), pp. 3122–3133. Available at: https://doi.org/10.1210/clinem/dgaa463.
- Robson, M., Im, S.-A., Senkus, E., Xu, B., Domchek, S.M., Masuda, N., Delaloge, S., Li, W., Tung, N., Armstrong, A., Wu, W., Goessl, C., Runswick, S. and Conte, P. (2017) 'Olaparib for Metastatic Breast Cancer in Patients with a Germline BRCA Mutation', *The New England Journal of Medicine*, 377(6), pp. 523–533. Available at: https://doi.org/10.1056/NEJMoa1706450.
- Sachdev, J.C. and Jahanzeb, M. (2016) 'Use of Cytotoxic Chemotherapy in Metastatic Breast Cancer: Putting Taxanes in Perspective', *Clinical Breast Cancer*, 16(2), pp. 73–81. Available at: https://doi.org/10.1016/j.clbc.2015.09.007.
- Sandmann, S., Prenzel, F., Shaw, L., Schauer, R. and Unger, T. (2002) 'Activity profile of calpains I and II in chronically infarcted rat myocardium – influence of the calpain inhibitor CAL 9961', *British Journal of Pharmacology*, 135(8), pp. 1951–1958. Available at: https://doi.org/10.1038/sj.bjp.0704661.
- Schirrmacher, V. (2018) 'From chemotherapy to biological therapy: A review of novel concepts to reduce the side effects of systemic cancer treatment (Review)', *International Journal of Oncology*, 54(2), pp. 407–419. Available at: https://doi.org/10.3892/ijo.2018.4661.
- Schoch, K.M., Evans, H.N., Brelsfoard, J.M., Madathil, S.K., Takano, J., Saido, T.C. and Saatman, K.E. (2012) 'Calpastatin overexpression limits calpain-mediated proteolysis and behavioral deficits following traumatic brain injury', *Experimental Neurology*, 236(2), pp. 371–382. Available at: https://doi.org/10.1016/j.expneurol.2012.04.022.

- Schulz, M., Klopp-Schulze, L., Keilhack, S., Meyer, S., Botermann, L. and Kloft, C. (2018) 'Adherence to tamoxifen in breast cancer patients: What role does the pharmacist play in German primary care?', *Canadian Pharmacists Journal : CPJ*, 152(1), pp. 28–34. Available at: https://doi.org/10.1177/1715163518815720.
- Shi, S., Ma, H.-Y., Han, X.-Y., Sang, Y.-Z., Yang, M.-Y. and Zhang, Z.-G. (2022) 'Prognostic Significance of SPARC Expression in Breast Cancer: A Meta-Analysis and Bioinformatics Analysis', *BioMed Research International*, 2022, p. 8600419. Available at: https://doi.org/10.1155/2022/8600419.
- Stapelkamp, C., Holmberg, L., Tataru, D., Møller, H. and Robinson, D. (2011) 'Predictors of early death in female patients with breast cancer in the UK: a cohort study', *BMJ Open*, 1(2), p. e000247. Available at: https://doi.org/10.1136/bmjopen-2011-000247.
- Sterken, B.A., Ackermann, T., Müller, C., Zuidhof, H.R., Kortman, G., Hernandez-Segura, A., Broekhuis, M., Spierings, D., Guryev, V. and Calkhoven, C.F. (2022) 'C/EBPβ isoform-specific regulation of migration and invasion in triple-negative breast cancer cells', *npj Breast Cancer*, 8(1), pp. 1–13. Available at: https://doi.org/10.1038/s41523-021-00372-z.
- Storr, S.J., Carragher, N.O., Frame, M.C., Parr, T. and Martin, S.G. (2011a) 'The calpain system and cancer', *Nature Reviews Cancer*, 11(5), pp. 364–374. Available at: https://doi.org/10.1038/nrc3050.
- Storr, S.J., Lee, K.W., Woolston, C.M., Safuan, S., Green, A.R., Macmillan, R.D., Benhasouna, A., Parr, T., Ellis, I.O. and Martin, S.G. (2012) 'Calpain system protein expression in basal-like and triple-negative invasive breast cancer', *Annals of Oncology*, 23(9), pp. 2289–2296. Available at: https://doi.org/10.1093/annonc/mds176.
- Storr, S.J., Mohammed, R.A.A., Woolston, C.M., Green, A.R., Parr, T., Spiteri, I., Caldas, C., Ball, G.R., Ellis, I.O. and Martin, S.G. (2011b) 'Calpastatin is associated with lymphovascular invasion in breast cancer', *The Breast*, 20(5), pp. 413–418. Available at: https://doi.org/10.1016/j.breast.2011.04.002.
- Storr, S.J., Mohammed, R.A.A., Woolston, C.M., Green, A.R., Parr, T., Spiteri, I., Caldas, C., Ball, G.R., Ellis, I.O. and Martin, S.G. (2011) 'Calpastatin is associated with lymphovascular invasion in breast cancer', *The Breast*, 20(5), pp. 413–418. Available at: https://doi.org/10.1016/j.breast.2011.04.002.
- Storr, S.J., Zhang, S., Perren, T., Lansdown, M., Fatayer, H., Sharma, N., Gahlaut, R., Shaaban, A. and Martin, S.G. (2016) 'The calpain system is associated with survival of breast cancer patients with large but operable inflammatory and non-inflammatory tumours treated with neoadjuvant chemotherapy', *Oncotarget*, 7(30), pp. 47927–47937. Available at: https://doi.org/10.18632/oncotarget.10066.
- Strobl, S., Fernandez-Catalan, C., Braun, M., Huber, R., Masumoto, H., Nakagawa, K., Irie, A., Sorimachi, H., Bourenkow, G., Bartunik, H., Suzuki, K. and Bode, W. (2000) 'The crystal structure of calcium-free human m-calpain suggests an electrostatic switch mechanism for activation by calcium', *Proceedings of the National Academy of Sciences of the United States of America*, 97(2), pp. 588–592.
- Suzuki, K., Hata, S., Kawabata, Y. and Sorimachi, H. (2004) 'Structure, Activation, and Biology of Calpain', *Diabetes*, 53(suppl_1), pp. S12–S18. Available at: https://doi.org/10.2337/diabetes.53.2007.S12.
- Takano, E., Ma, H., Yang, H.Q., Maki, M. and Hatanaka, M. (1995) 'Preference of calcium-dependent interactions between calmodulin-like domains of calpain and calpastatin subdomains', *FEBS Letters*, 362(1), pp. 93–97. Available at: https://doi.org/10.1016/0014-5793(95)00219-Y.
- Taveau, M., Bourg, N., Sillon, G., Roudaut, C., Bartoli, M. and Richard, I. (2003) 'Calpain 3 Is Activated through Autolysis within the Active Site and Lyses Sarcomeric and Sarcolemmal Components', *Molecular and Cellular Biology*, 23(24), pp. 9127–9135. Available at: https://doi.org/10.1128/MCB.23.24.9127-9135.2003.
- Vasan, R (2022) *THE ROLE OF THE CALPAIN SYSTEM IN BREAST CANCER PROGRESSION AND TREATMENT RESPONSE*. Thesis (PhD), University of Nottingham
- Vindis, C., Elbaz, M., Escargueil-Blanc, I., Augé, N., Heniquez, A., Thiers, J.-C., Nègre-Salvayre, A. and Salvayre, R. (2005) 'Two Distinct Calcium-Dependent Mitochondrial Pathways Are Involved in Oxidized LDL-Induced Apoptosis', *Arteriosclerosis, Thrombosis, and Vascular Biology*, 25(3), pp. 639–645. Available at: https://doi.org/10.1161/01.ATV.0000154359.60886.33.

- Vondeling, G.T., Menezes, G.L., Dvortsin, E.P., Jansman, F.G.A., Konings, I.R., Postma, M.J. and Rozenbaum, M.H. (2018) 'Burden of early, advanced and metastatic breast cancer in The Netherlands', *BMC Cancer*, 18(1), p. 262. Available at: https://doi.org/10.1186/s12885-018-4158-3.
- Waks, A.G. and Winer, E.P. (2019) 'Breast Cancer Treatment: A Review', *JAMA*, 321(3), pp. 288–300. Available at: https://doi.org/10.1001/jama.2018.19323.
- Wang, B., Zheng, J., Li, R., Tian, Y., Lin, J., Liang, Y., Sun, Q., Xu, A., Zheng, R., Liu, M., Ji, A., Bu, J. and Yuan, Y. (2019) 'Long noncoding RNA LINC02582 acts downstream of miR-200c to promote radioresistance through CHK1 in breast cancer cells', *Cell Death & Disease*, 10(10), pp. 1–15. Available at: https://doi.org/10.1038/s41419-019-1996-0.
- Watanabe, N., Okochi, E., Mochizuki, M., Sugimura, T. and Ushijima, T. (2001) 'The Presence of Single Nucleotide Instability in Human Breast Cancer Cell Lines1', *Cancer Research*, 61(21), pp. 7739–7742.
- Wei, N.-N., Li, F., Cai, P., Yin, H.-M., Zhu, C.-M., Zhang, Q. and Li, D.-J. (2020) 'Progress of clinical study on hypofractionated radiotherapy after breast-conserving surgery', *Annals of Palliative Medicine*, 9(2), pp. 46371–46471. Available at: https://doi.org/10.21037/apm.2020.02.18.
- Wen, H.Y. and Brogi, E. (2018) 'Lobular Carcinoma in Situ', *Surgical pathology clinics*, 11(1), pp. 123–145. Available at: https://doi.org/10.1016/j.path.2017.09.009.
- Wiper-Bergeron, N., Wu, D., Pope, L., Schild-Poulter, C. and Haché, R.J.G. (2003) 'Stimulation of preadipocyte differentiation by steroid through targeting of an HDAC1 complex', *The EMBO journal*, 22(9), pp. 2135–2145. Available at: https://doi.org/10.1093/emboj/cdg218.
- Wu, L. and Zhu, J. (2015) 'Linear reduction in thyroid cancer risk by oral contraceptive use: a dose-response meta-analysis of prospective cohort studies', *Human Reproduction (Oxford, England)*, 30(9), pp. 2234–2240. Available at: https://doi.org/10.1093/humrep/dev160.
- Xu, F., Gu, J., Lu, C., Mao, W., Wang, L., Zhu, Q., Liu, Z., Chu, Y., Liu, R. and Ge, D. (2019) 'Calpain-2 Enhances Non-Small Cell Lung Cancer Progression and Chemoresistance to Paclitaxel via EGFR-pAKT Pathway', *International Journal of Biological Sciences*, 15(1), pp. 127–137. Available at: https://doi.org/10.7150/ijbs.28834.
- Yadav, D., Shukla, N.K. and Mishra, M.C. (2022) 'Management of Locally Advanced Breast Cancer', in S.C. Sharma, A. Mazumdar, and R. Kaushik (eds) *Breast Cancer: Comprehensive Management*. Singapore: Springer Nature, pp. 305–337. Available at: https://doi.org/10.1007/978-981-16-4546-4_16.
- Yang, G., Nowsheen, S., Aziz, K. and Georgakilas, A.G. (2013) 'Toxicity and adverse effects of Tamoxifen and other anti-estrogen drugs', *Pharmacology & Therapeutics*, 139(3), pp. 392–404. Available at: https://doi.org/10.1016/j.pharmthera.2013.05.005.
- Yersal, O. and Barutca, S. (2014) 'Biological subtypes of breast cancer: Prognostic and therapeutic implications', *World Journal of Clinical Oncology*, 5(3), pp. 412–424. Available at: https://doi.org/10.5306/wjco.v5.i3.412.
- Yoder, M.W., Wright, N.T. and Borzok, M.A. (2023) 'Calpain Regulation and Dysregulation—Its Effects on the Intercalated Disk', *International Journal of Molecular Sciences*, 24(14), p. 11726. Available at: https://doi.org/10.3390/ijms241411726.
- Zahnow, C.A. (2009) 'CCAAT/enhancer-binding protein β: its role in breast cancer and associations with receptor tyrosine kinases', *Expert reviews in molecular medicine*, 11, p. e12. Available at: https://doi.org/10.1017/S1357.
- Zhang, S., Deen, S., Storr, S.J., Chondrou, P.S., Nicholls, H., Yao, A., Rungsakaolert, P. and Martin, S.G. (2019) 'Calpain system protein expression and activity in ovarian cancer', *Journal of Cancer Research and Clinical Oncology*, 145(2), pp. 345–361. Available at: https://doi.org/10.1007/s00432-018-2794-2.
- Zhang, Y., Storr, S.J., Johnson, K., Green, A.R., Rakha, E.A., Ellis, I.O., Morgan, D.A.L. and Martin, S.G. (2014) 'Involvement of metformin and AMPK in the radioresponse and prognosis of luminal versus basal-like breast cancer treated with radiotherapy', *Oncotarget*, 5(24), pp. 12936–12949.
- Zhu, Z., Zhao, X., Zhao, L., Yang, H., Liu, L., Li, J., Wu, J., Yang, F., Huang, G. and Liu, J. (2016) 'p54nrb/NONO regulates lipid metabolism and breast cancer growth through SREBP-1A', *Oncogene*, 35(11), pp. 1399–1410. Available at: https://doi.org/10.1038/onc.2015.197.

Appendix A: Supplementary Information for Chapter 3

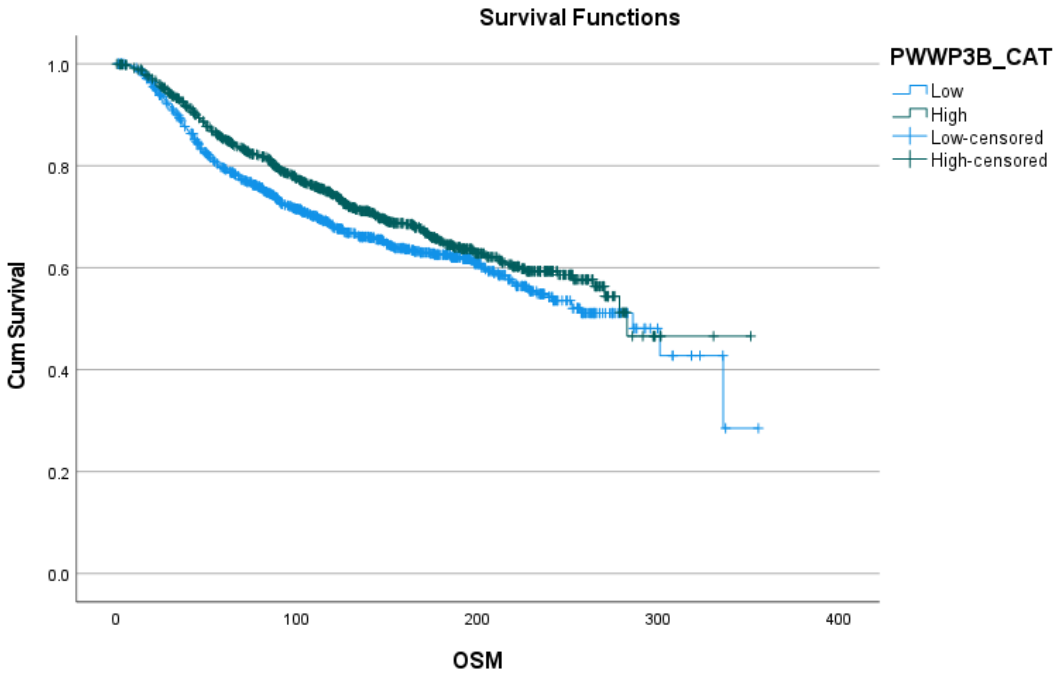

Figure A1. Kaplan-Meier plot of PWWP3B, in the top 10 upregulated MDA-MB-231 CASTII overexpression. Showed a significant association with survival (P=0.017).

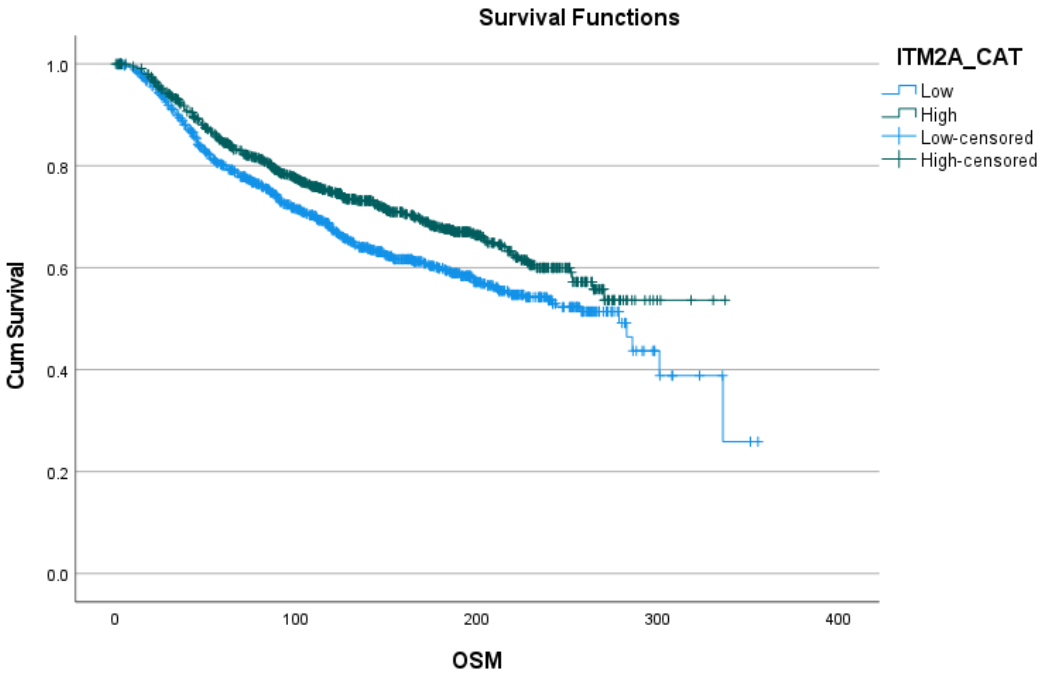

Figure A2. Kaplan-Meier plot of ITM2A, in the top 10 upregulated MDA-MB-231 CASTII overexpression. Showed a significant association with survival (P<0.001).

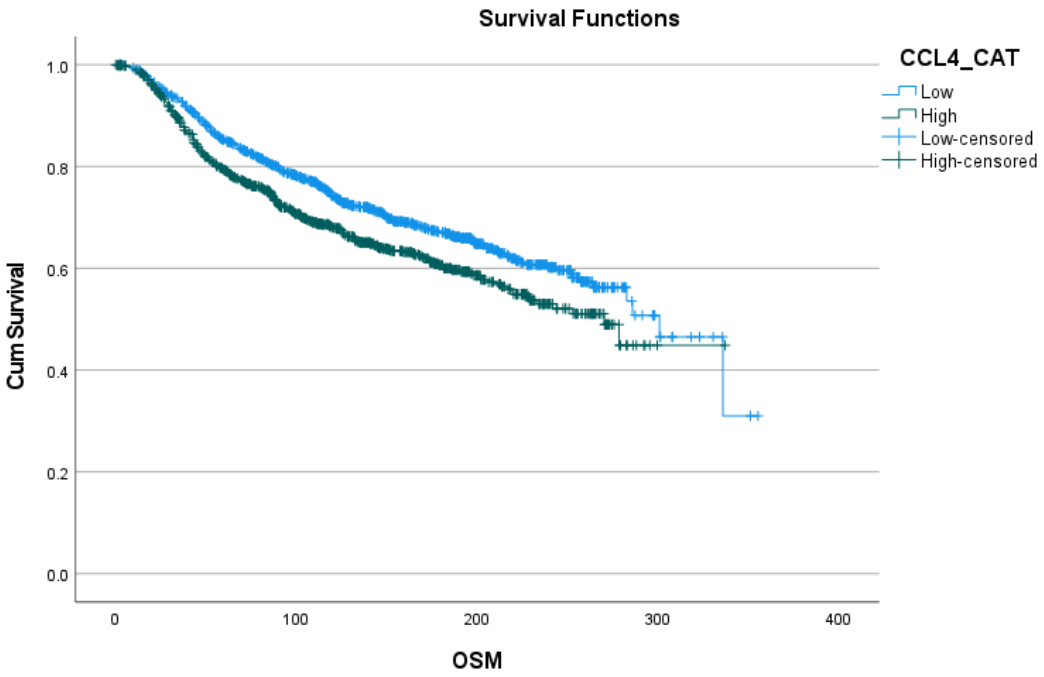

Figure A3. Kaplan-Meier plot of CCL4, in the top 10 upregulated MDA-MB-231 CASTII overexpression. Showed a significant association with survival (P=0.001).

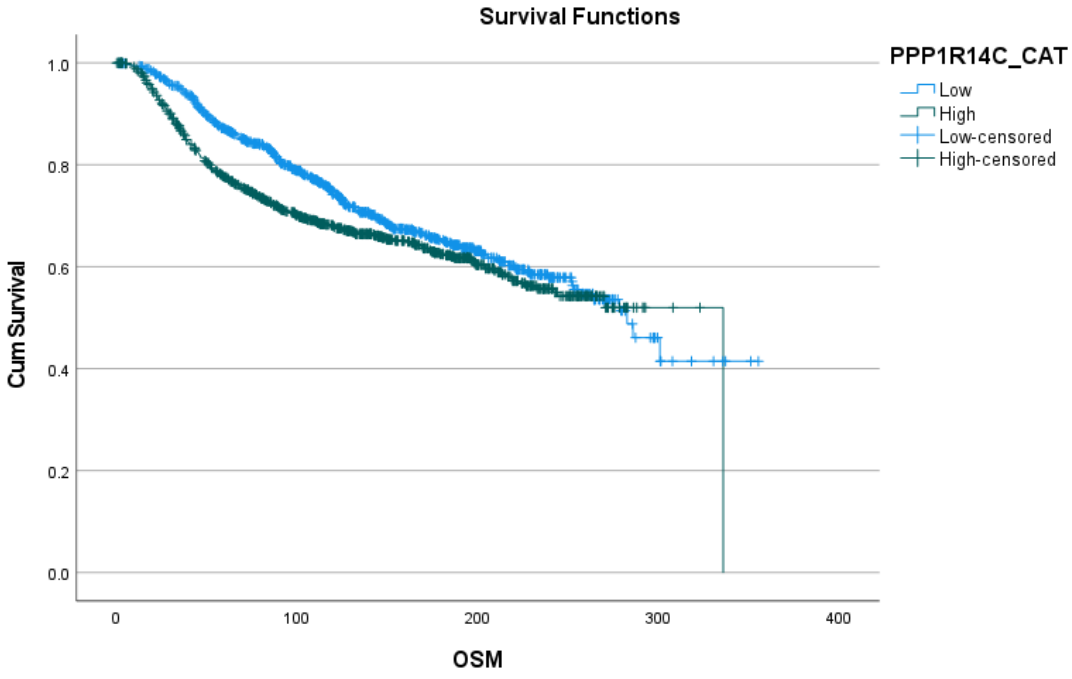

Figure A4. Kaplan-Meier plot of PPP1R14C, in the top 10 upregulated MDA-MB-231 CASTII overexpression. Showed a significant association with survival (P=0.006).

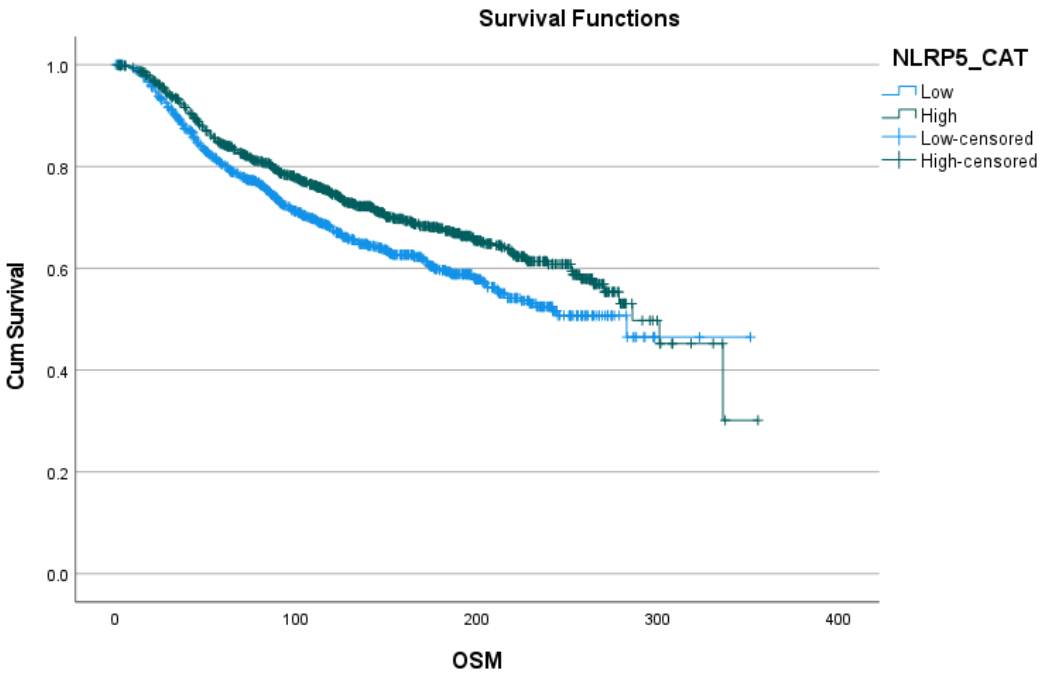

Figure A5. Kaplan-Meier plot of NLRP5, in the top 10 upregulated MDA-MB-231 CASTII overexpression. Showed a significant association with survival (P<0.001).

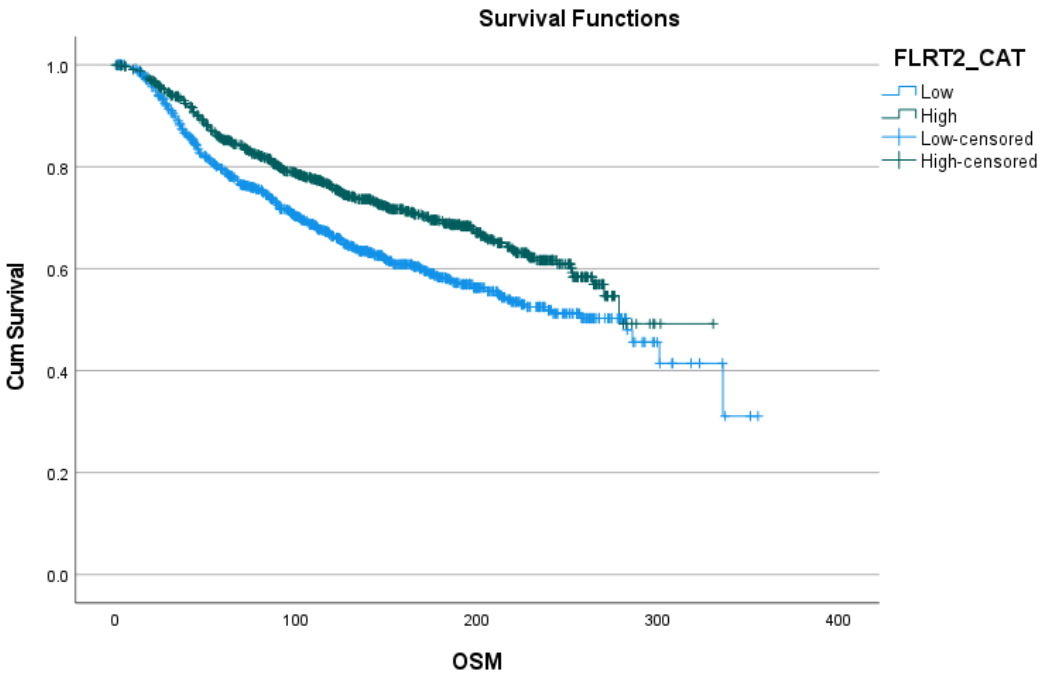

Figure A6. Kaplan-Meier plot of FLRT2, in the top 10 most significant DEGs T47D CASTII overexpression. Showed a significant association with survival (P<0.001).

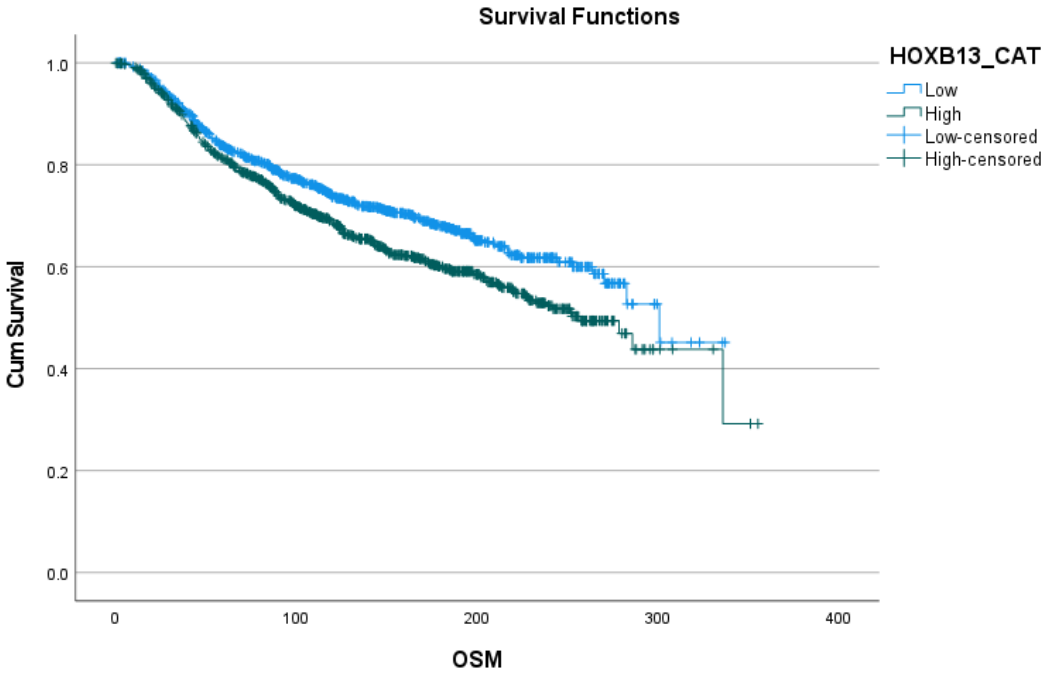

Figure A7. Kaplan-Meier plot of HOXB13, in the top 10 downregulated DEGs T47D CASTII overexpression. Showed a significant association with survival (P=0.002).

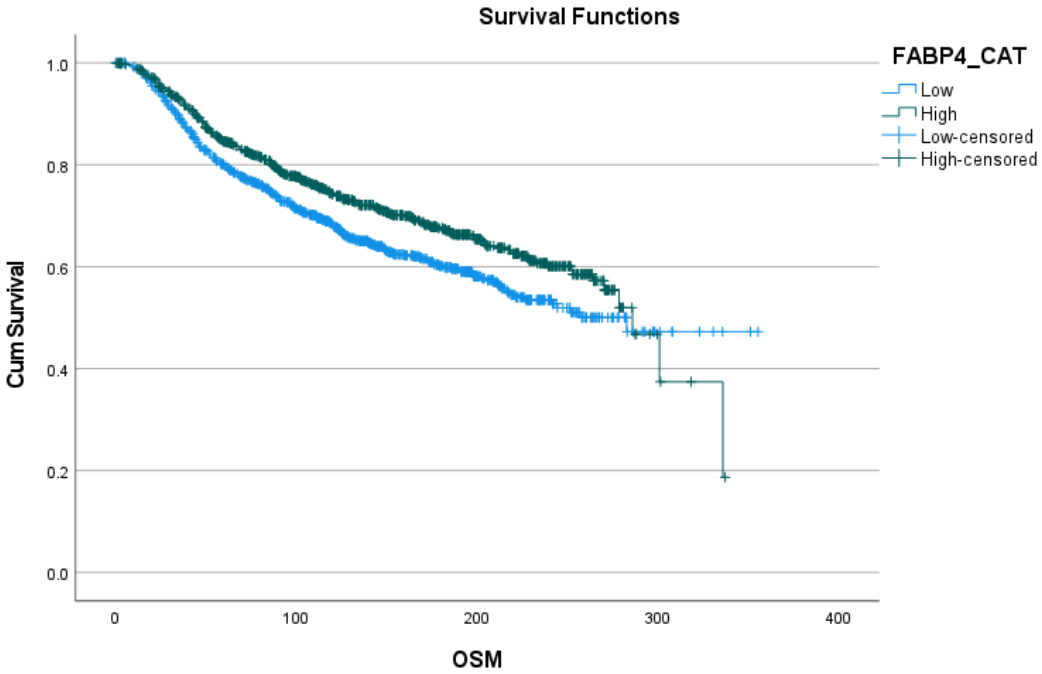

Figure A8. Kaplan-Meier plot of FABP4, in the top 10 upregulated DEGs T47D CASTII overexpression.. Showed a significant association with survival (P=0.002).

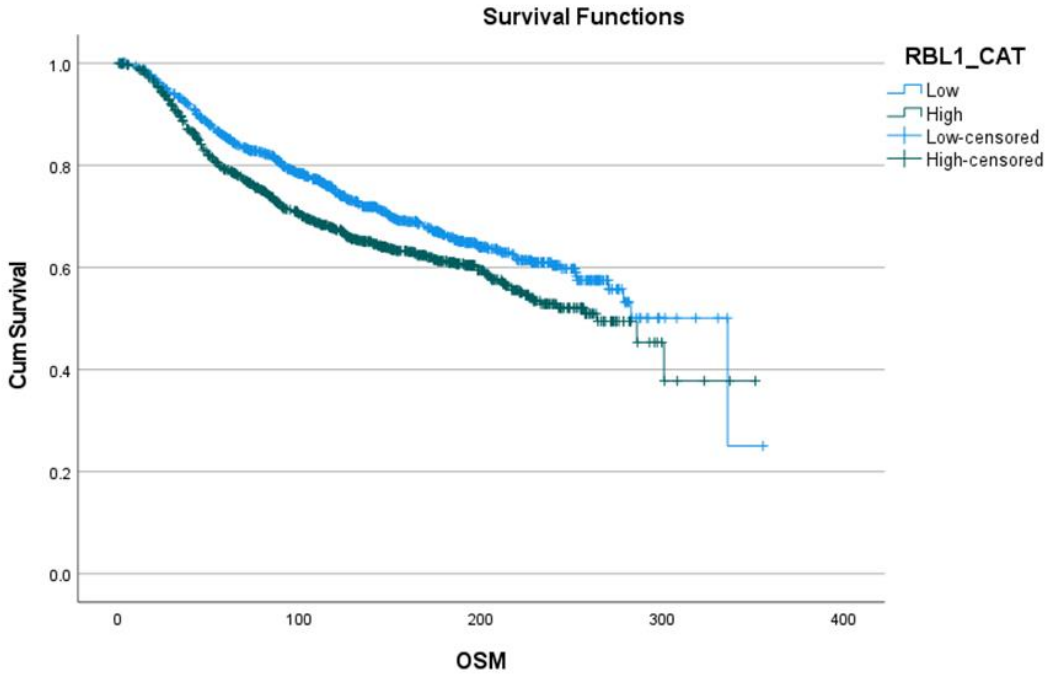

Figure A9. Kaplan-Meier plot of RBL1, in the predicted to be inhibited transcription regulators in MDA-MB-231 CASTII overexpression. Showed a significant association with survival (P<0.001).

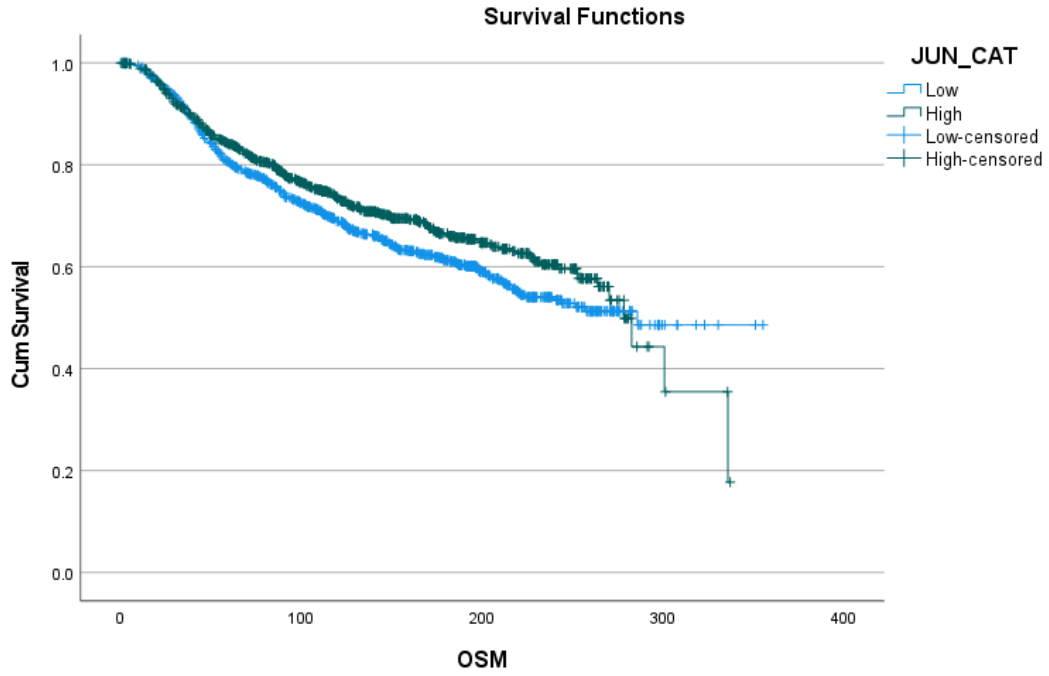

Figure A10. Kaplan-Meier plot of JUN, in the predicted to be activated transcription regulators in MDA-MB-231 CASTII overexpression. Showed a significant association with survival (P<0.034).

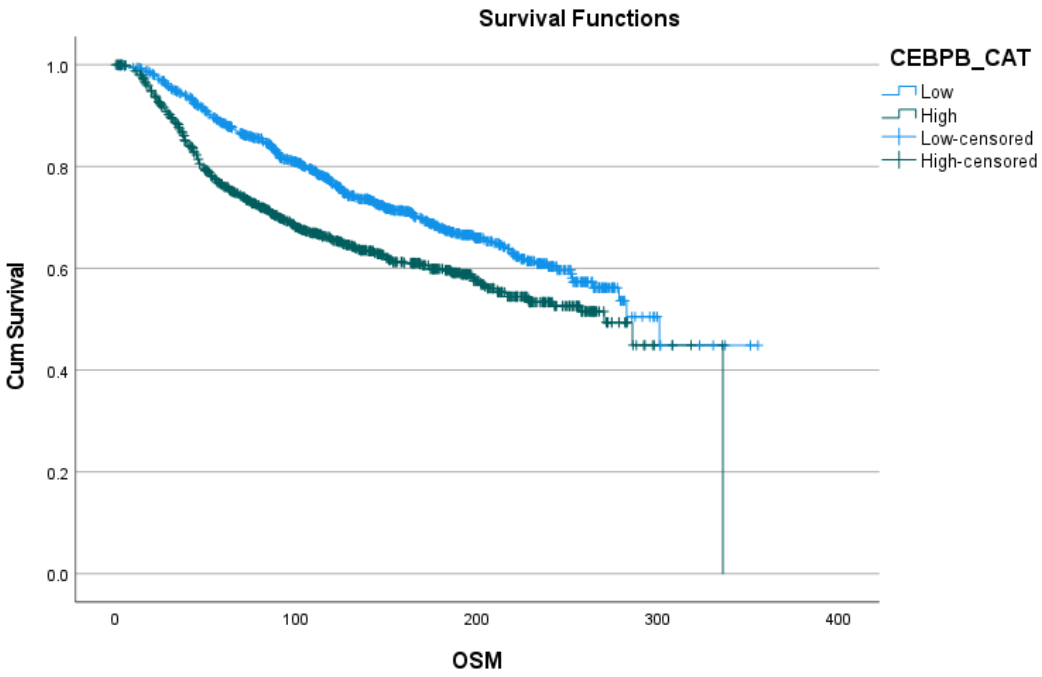

Figure A11. Kaplan-Meier plot of CEBPB, in the predicted to be activated transcription regulators in MDA-MB-231 CASTII overexpression. Showed a significant association with survival (P<0.001).

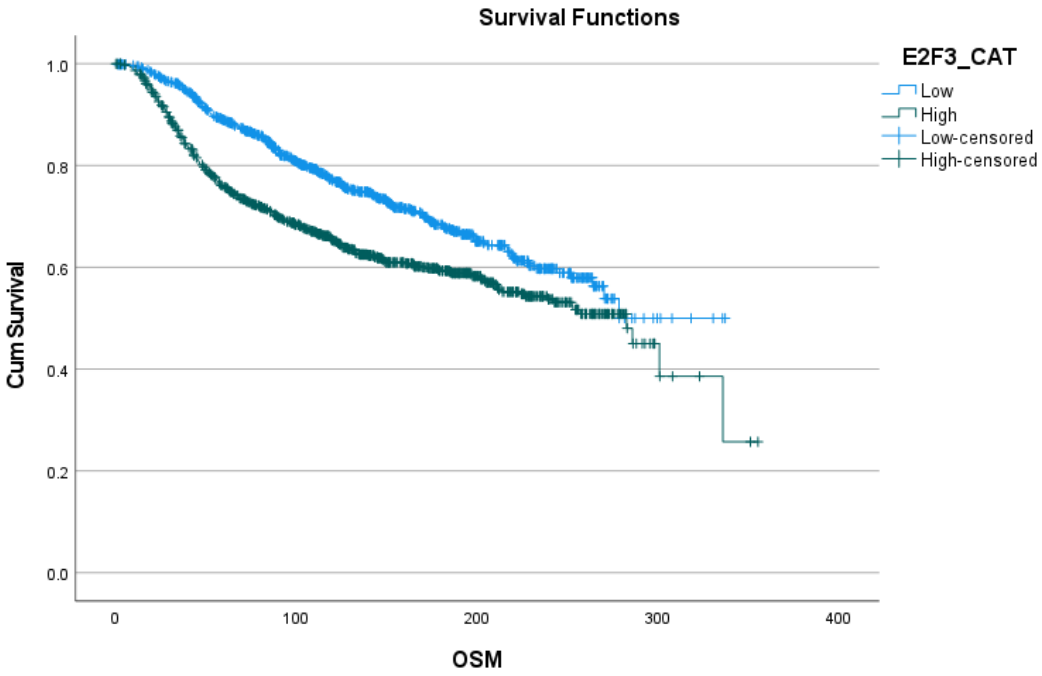

Figure A12. Kaplan-Meier plot of E2F3, in the predicted to be activated transcription regulators in MDA-MB-231 CASTII overexpression. Showed a significant association with survival (P<0.001).

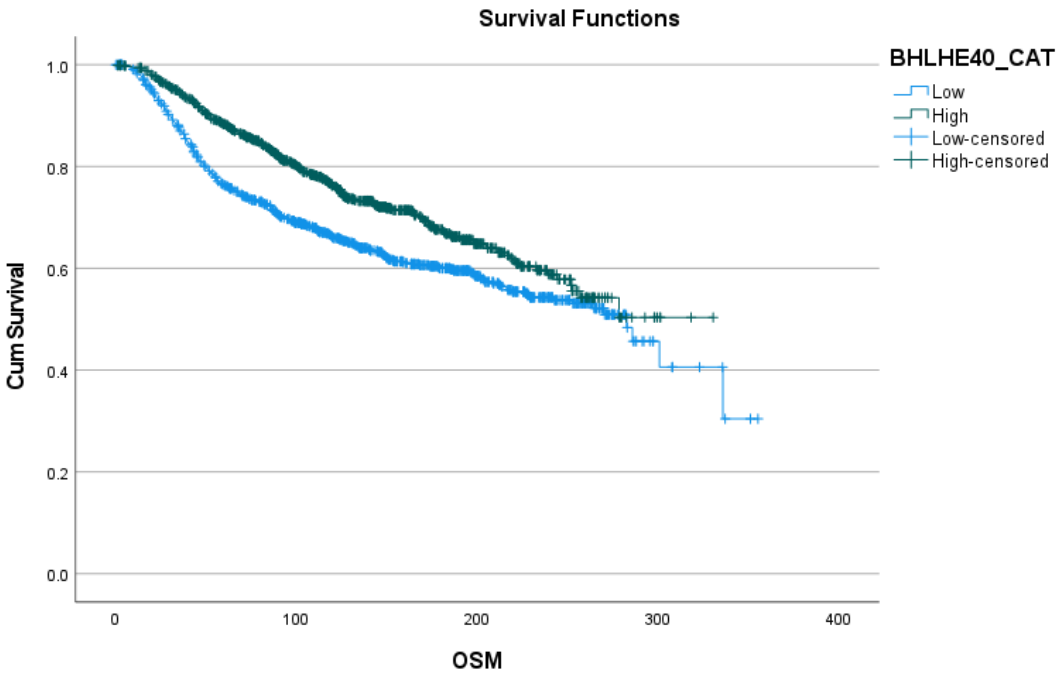

Figure A13. Kaplan-Meier plot of BHLHE40, in the predicted to be activated transcription regulators in MDA-MB-231 CASTII overexpression. Showed a significant association with survival (P<0.001).

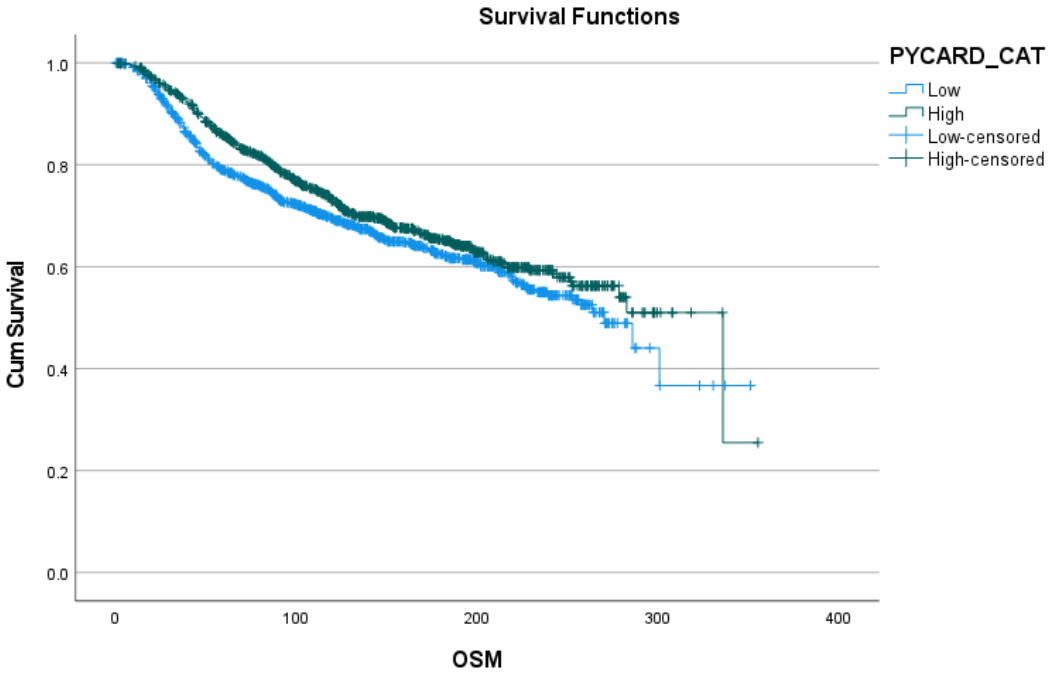

Figure A14. Kaplan-Meier plot of PYCARD, in the predicted to be activated transcription regulators in MDA-MB-231 CASTII overexpression. Showed a significant association with survival (P=0.03).

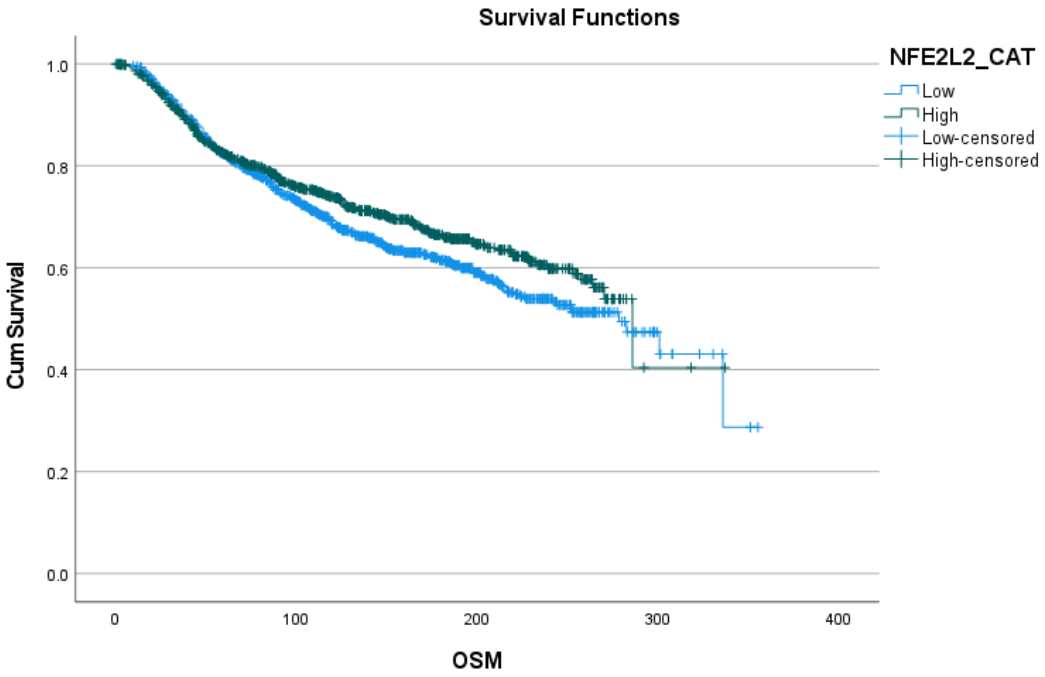

Figure A15. Kaplan-Meier plot of NF2L2E, in the predicted to be activated transcription regulators in MDA-MB-231 CASTII overexpression. Showed a significant association with survival (P=0.48).

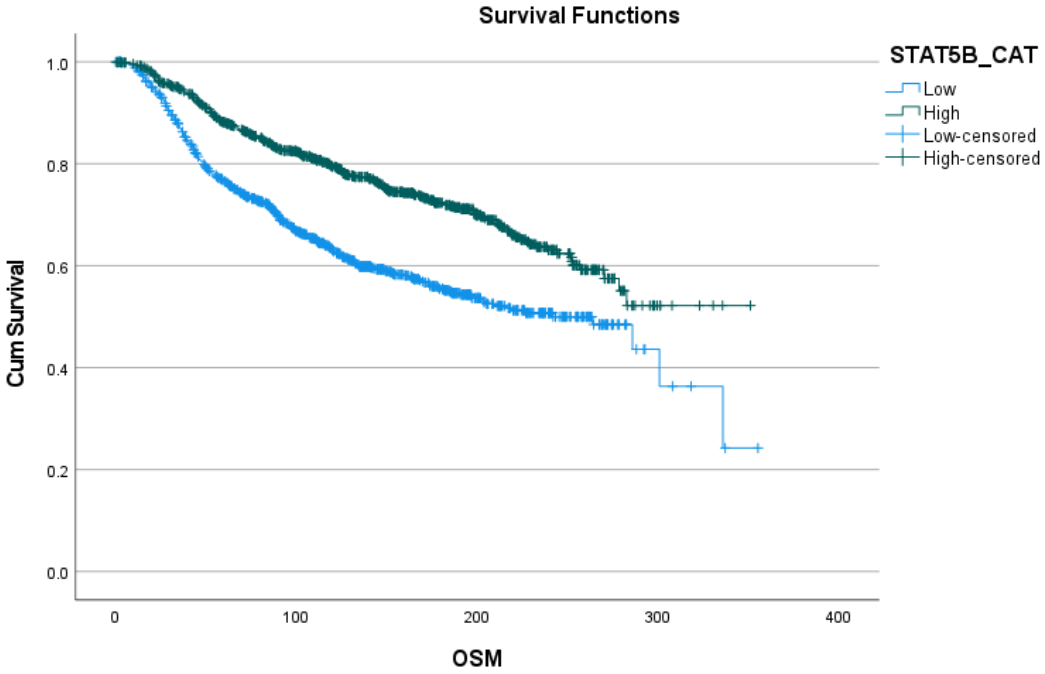

Figure A16. Kaplan-Meier plot of STAT5B, in the predicted to be activated transcription regulators in MDA-MB-231 CASTII overexpression. Showed a significant association with survival (P<0.001).

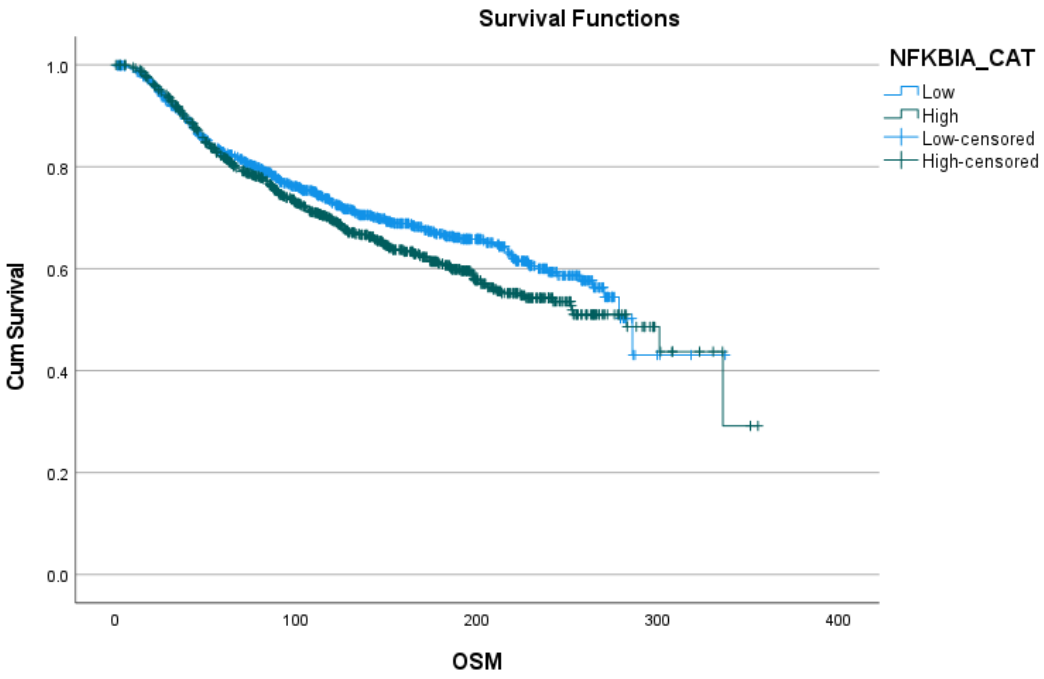

Figure A17. Kaplan-Meier plot of NFKBIA, in the predicted to be activated transcription regulators in MDA-MB-231 CASTII overexpression. Showed a significant association with survival (P=0.046).

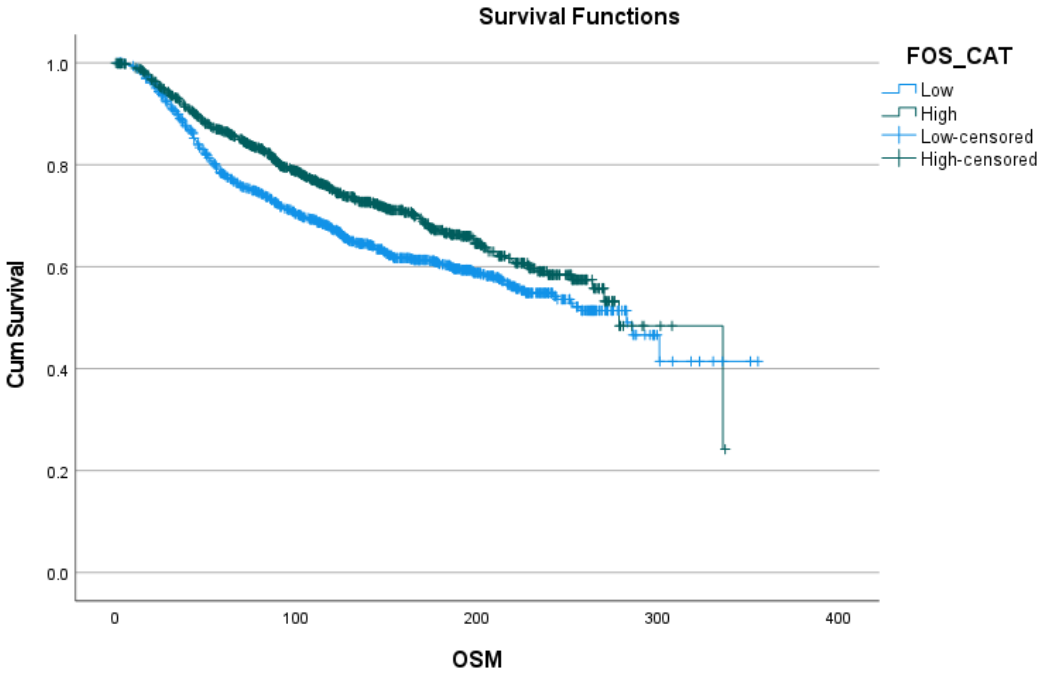

Figure A18. Kaplan-Meier plot of FOS, in the predicted to be activated transcription regulators in MDA-MB-231 CASTII overexpression. Showed a significant association with survival (P<0.001).

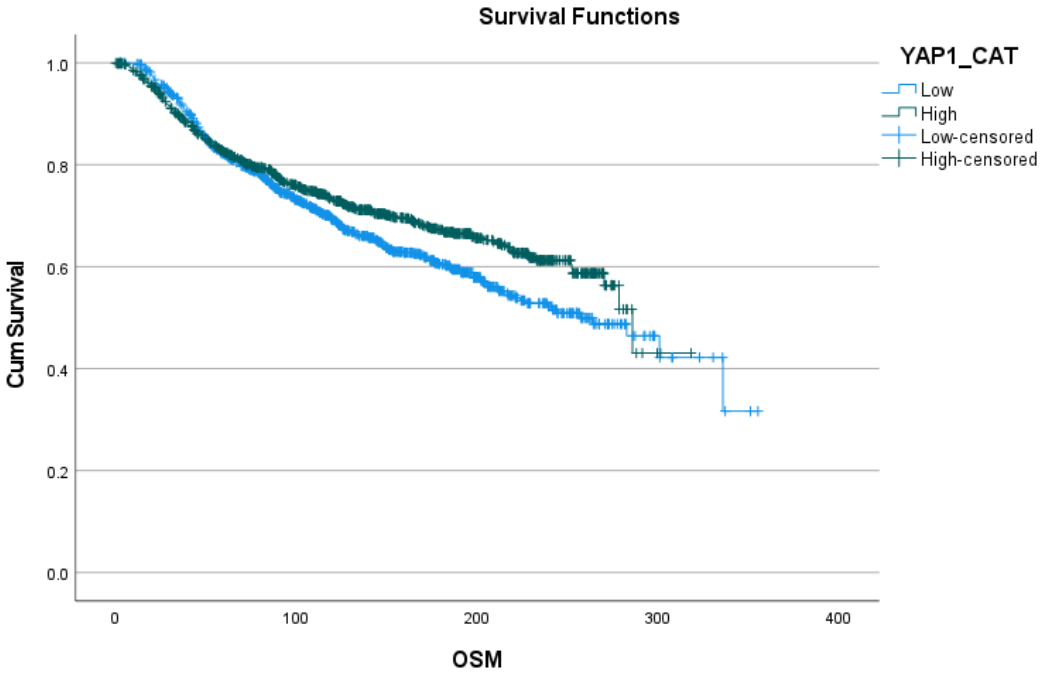

Figure A19. Kaplan-Meier plot of YAP1, in the predicted to be activated transcription regulators in MDA-MB-231 CASTII overexpression. Showed a significant association with survival (P=0.023).

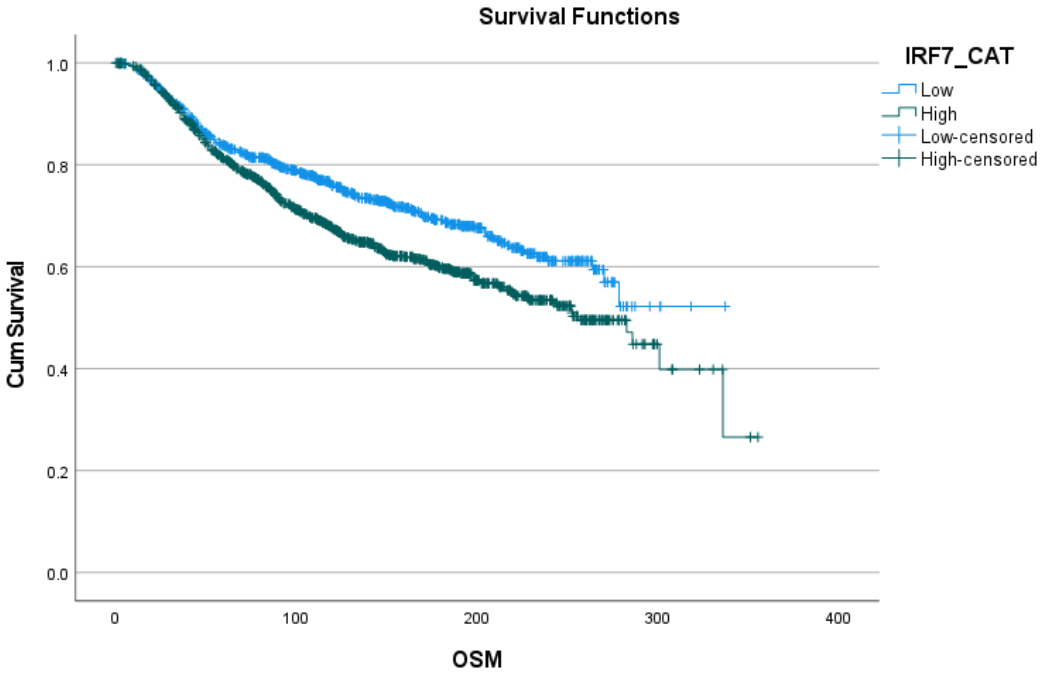

Figure A20. Kaplan-Meier plot of IRF7, in the predicted to be inhibited transcription regulators in T47D CASTII overexpression. Showed a significant association with survival (P<0.001).

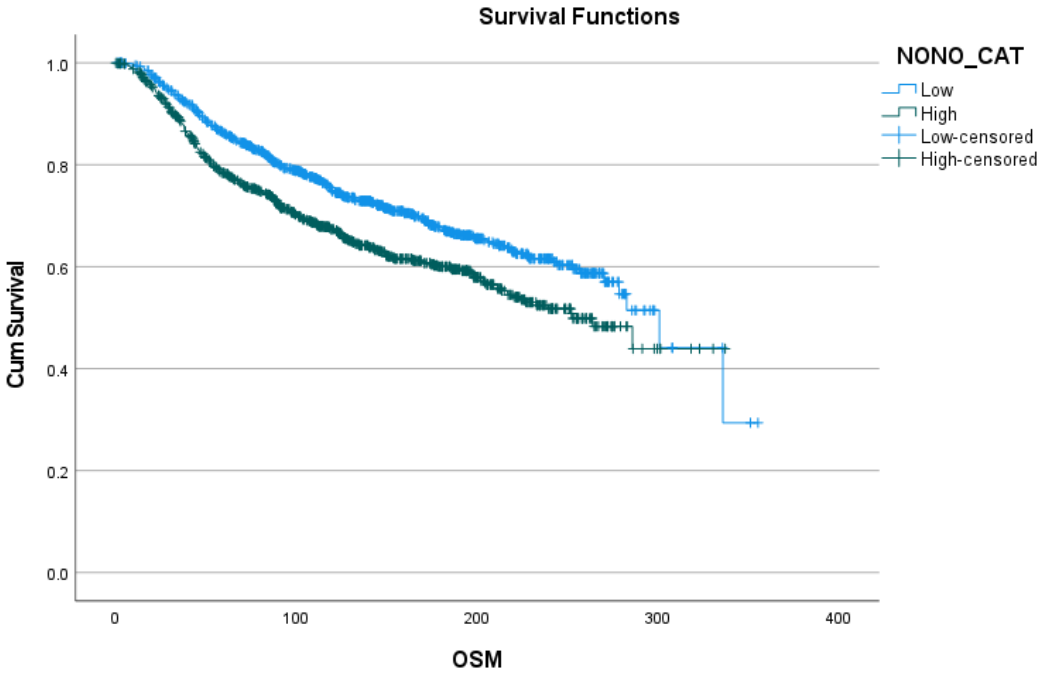

Figure A21. Kaplan-Meier plot of NONO, in the predicted to be inhibited transcription regulators in T47D CASTII overexpression. Showed a significant association with survival (P<0.001).

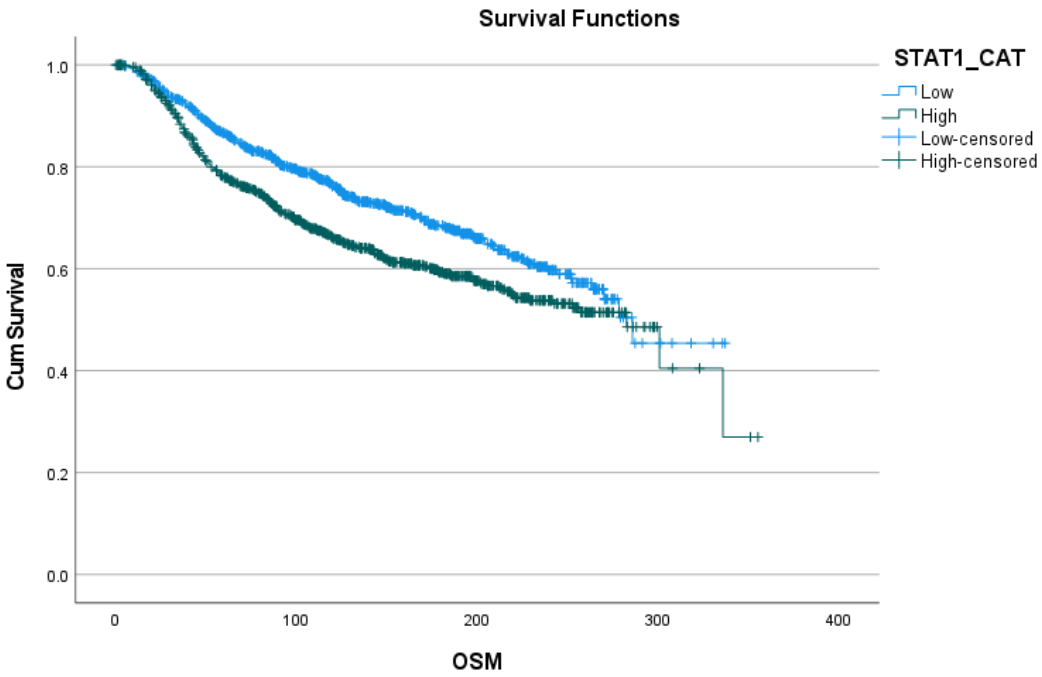

Figure A22.. Kaplan-Meier plot of STAT1, in the predicted to be inhibited transcription regulators in T47D CASTII overexpression. Showed a significant association with survival (P<0.001).

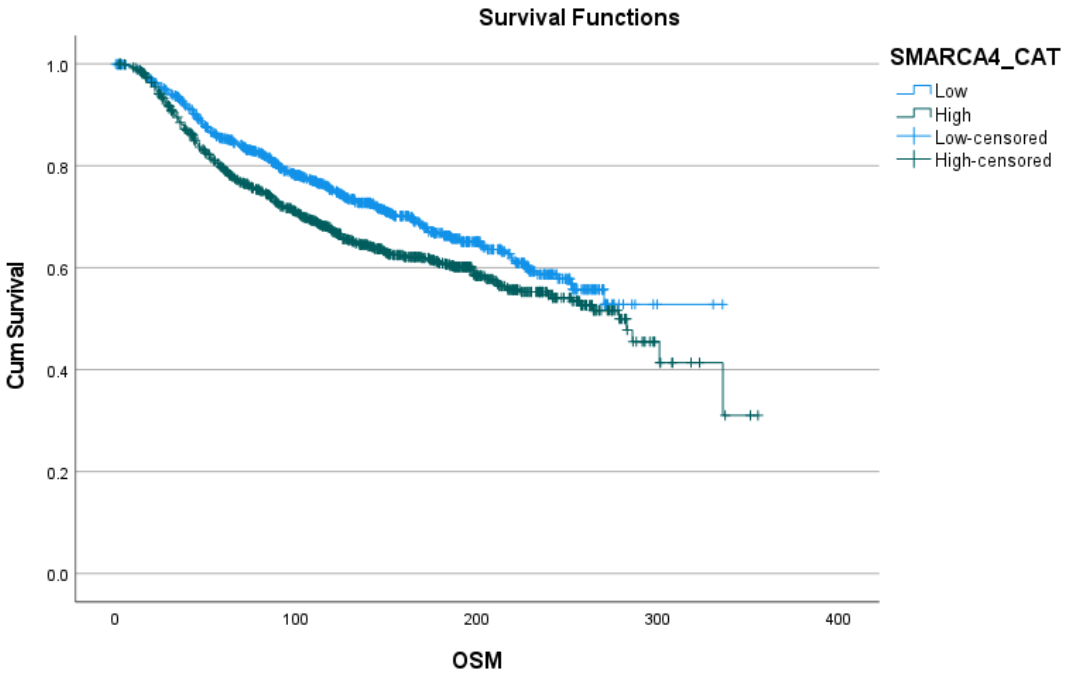

Figure A23.. Kaplan-Meier plot of SMARCA4, in the predicted to be inhibited transcription regulators in T47D CASTII overexpression. Showed a significant association with survival (P=0.001).

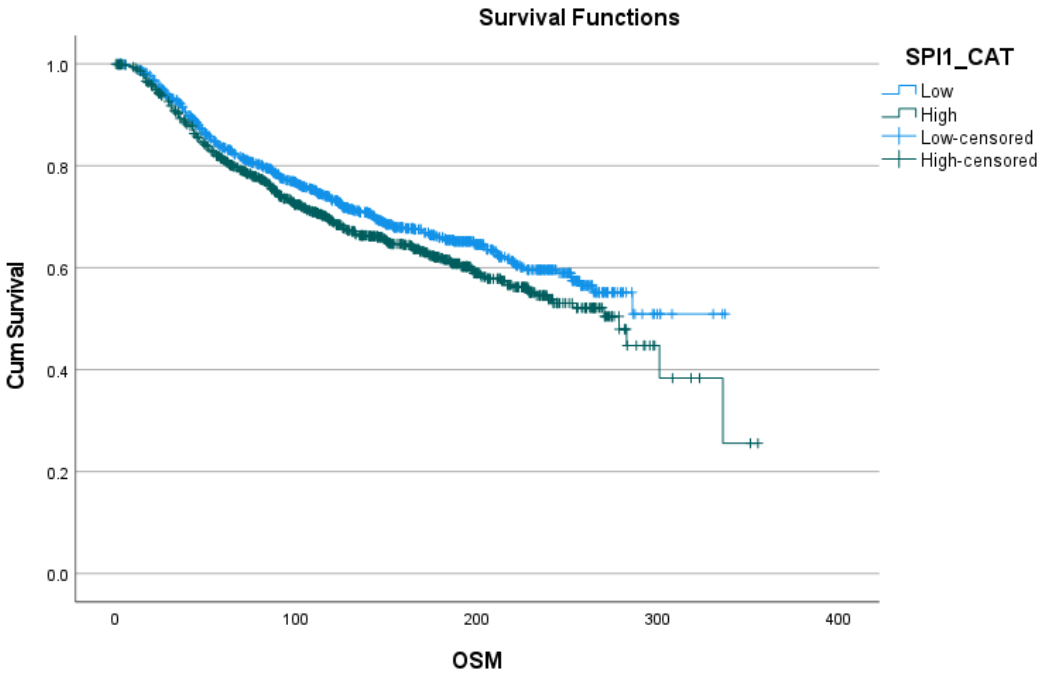

Figure A24.. Kaplan-Meier plot of SPi1, in the predicted to be inhibited transcription regulators in T47D CASTII overexpression. Showed a significant association with survival (P=0.036).

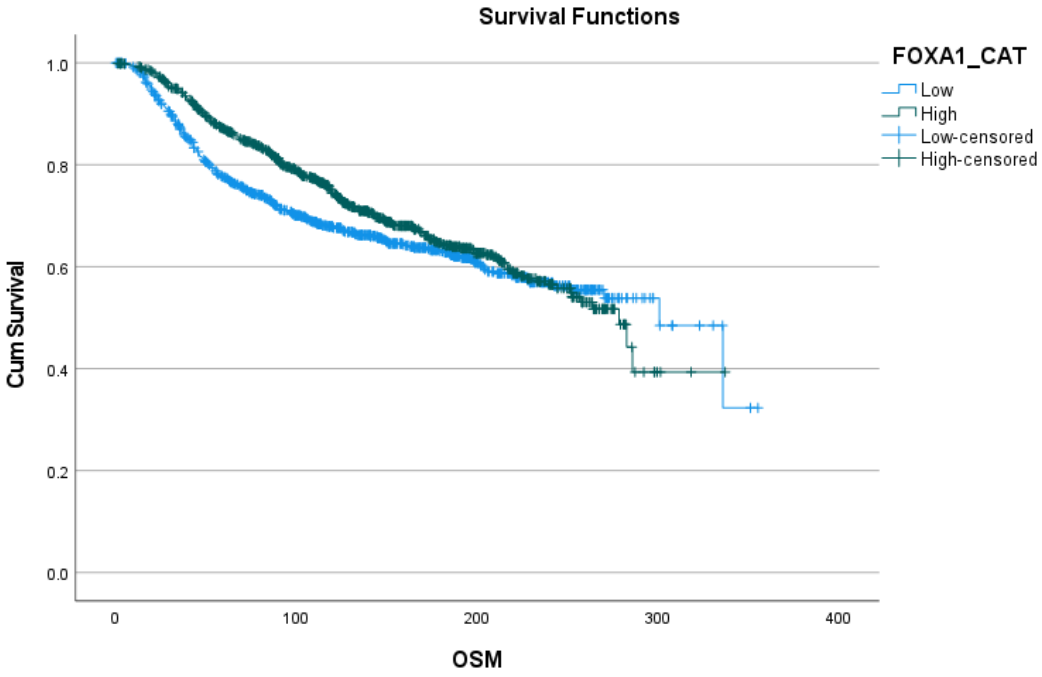

Figure A25.. Kaplan-Meier plot of FOXA1, in the predicted to be inhibited transcription regulators in T47D CASTII overexpression. Showed a significant association with survival (P=0.02).

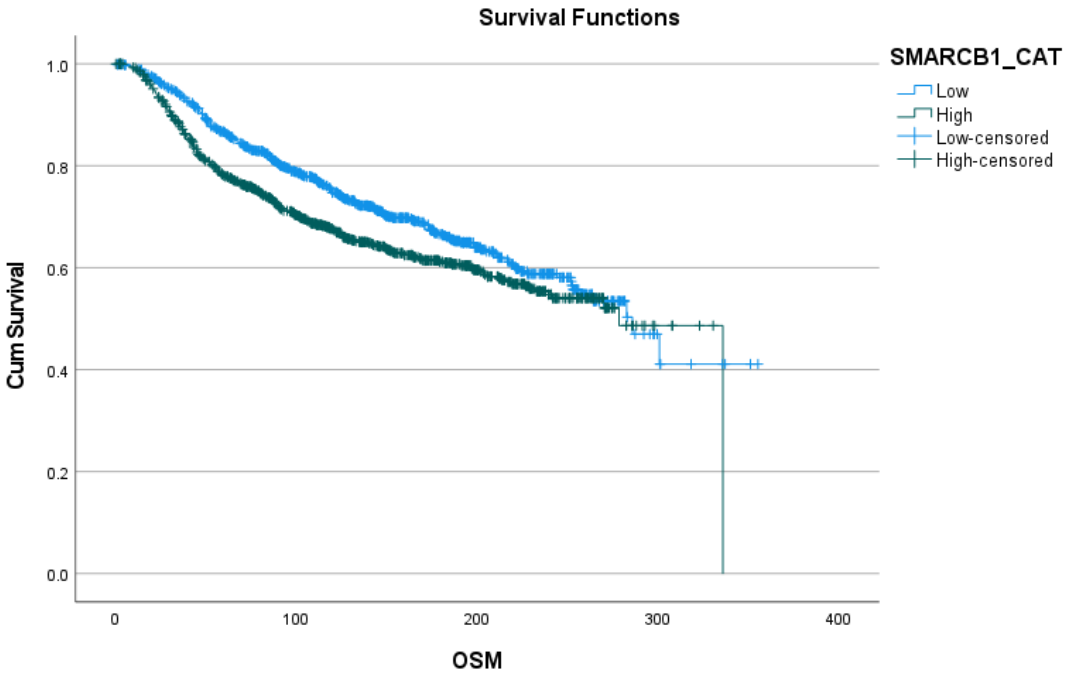

Figure A26.. Kaplan-Meier plot of SMARCB1, in the predicted to be inhibited transcription regulators in T47D CASTII overexpression. Showed a significant association with survival (P=0.002).

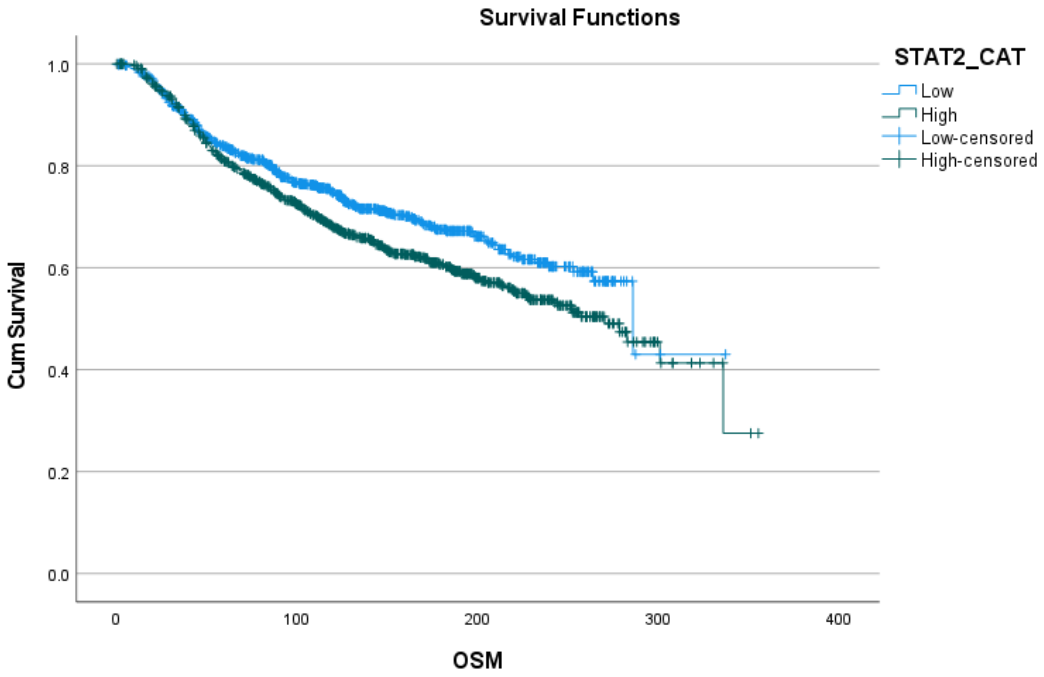

Figure A27.. Kaplan-Meier plot of STAT2, in the predicted to be inhibited transcription regulators in T47D CASTII overexpression. Showed a significant association with survival (P=0.004).

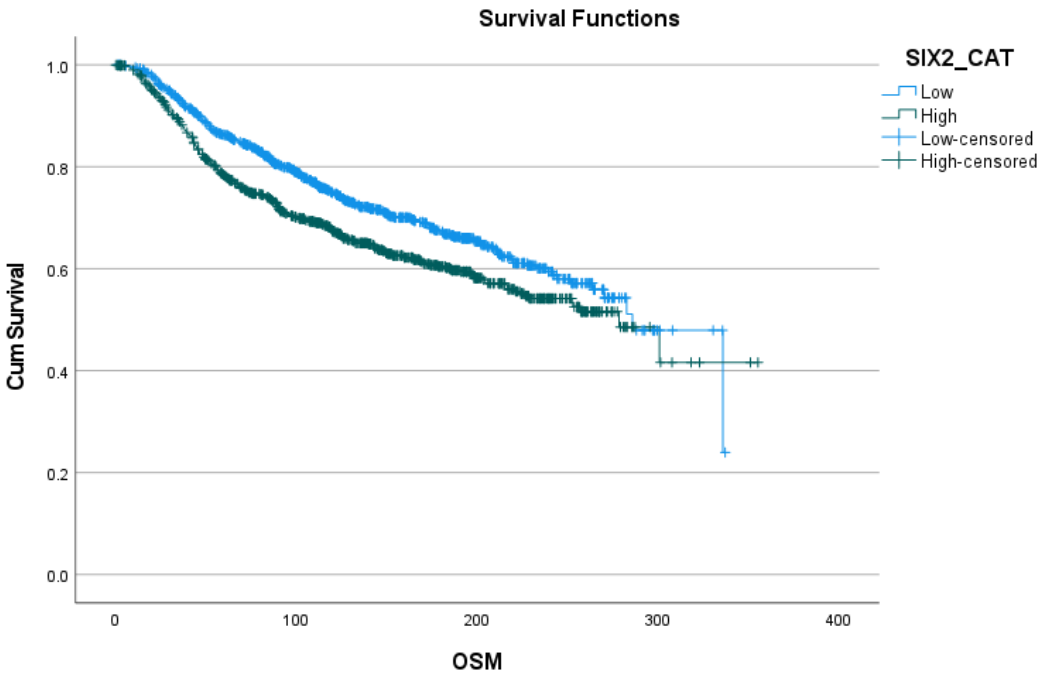

Figure A28.. Kaplan-Meier plot of SIX2, in the predicted to be inhibited transcription regulators in T47D CASTII overexpression. Showed a significant association with survival (P<0.001).

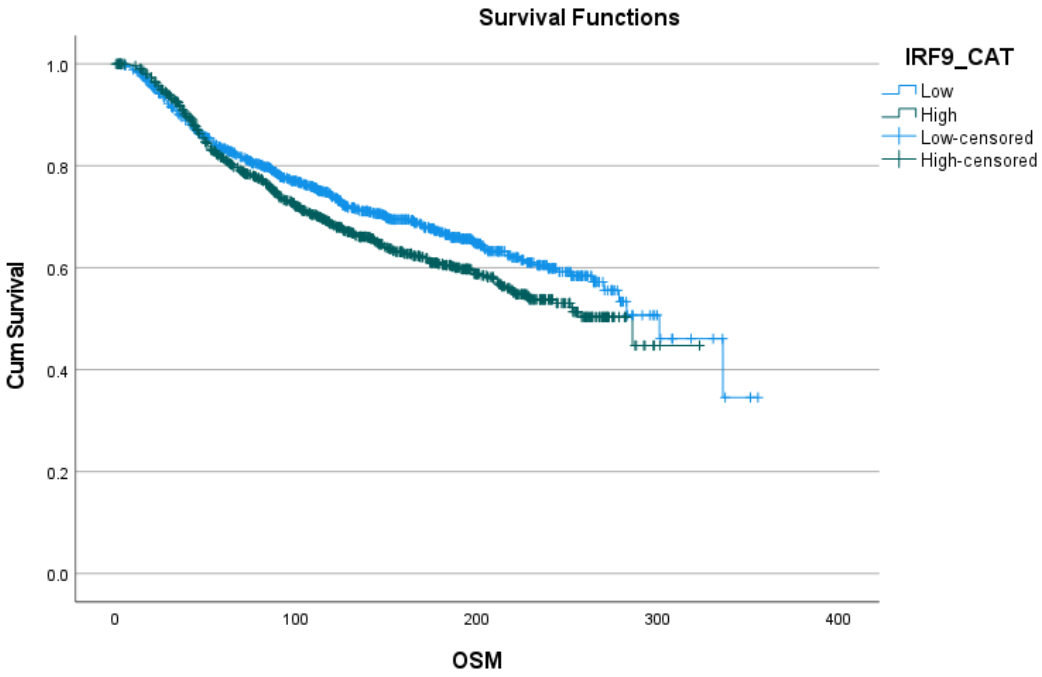

Figure A29.. Kaplan-Meier plot of IRF9, in the predicted to be inhibited transcription regulators in T47D CASTII overexpression. Showed a significant association with survival (P=0.02).

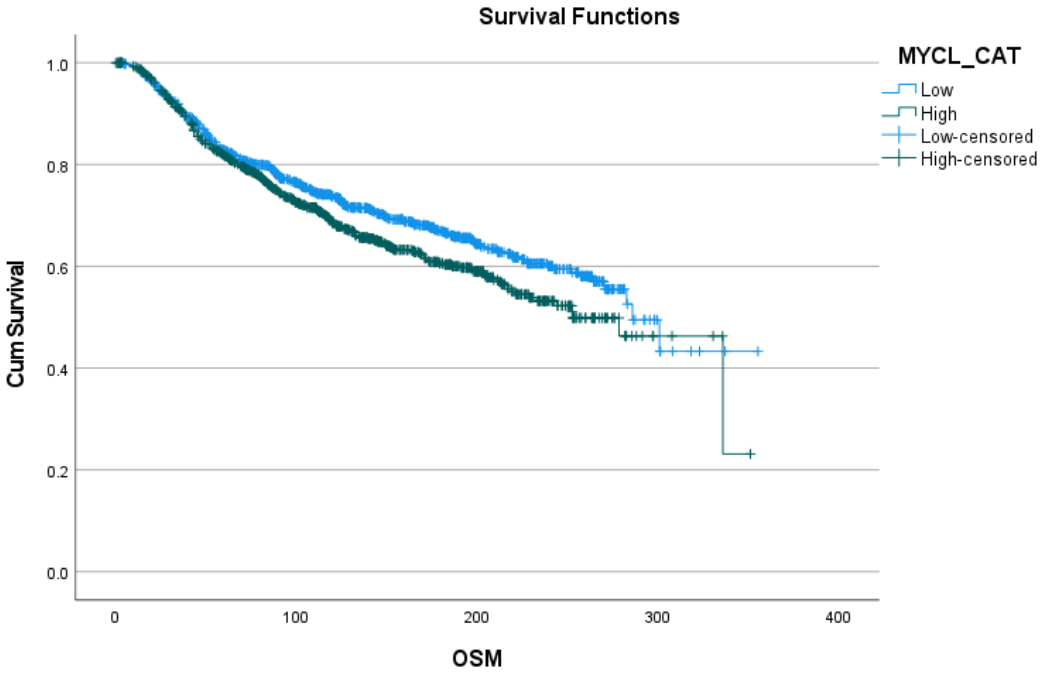

Figure A30.. Kaplan-Meier plot of MYCL, in the predicted to be activated transcription regulators in T47D CASTII overexpression. Showed a significant association with survival (P=0.02).

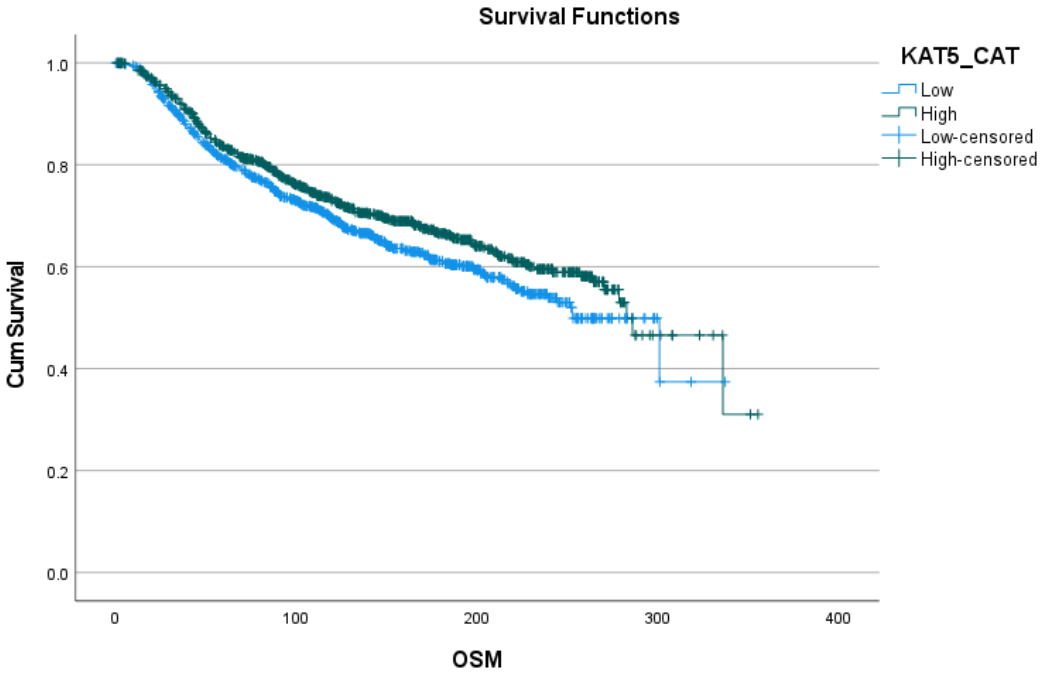

Figure A31.. Kaplan-Meier plot of KAT5, in the predicted to be activated transcription regulators in T47D CASTII overexpression. Showed a significant association with survival (P=0.029).

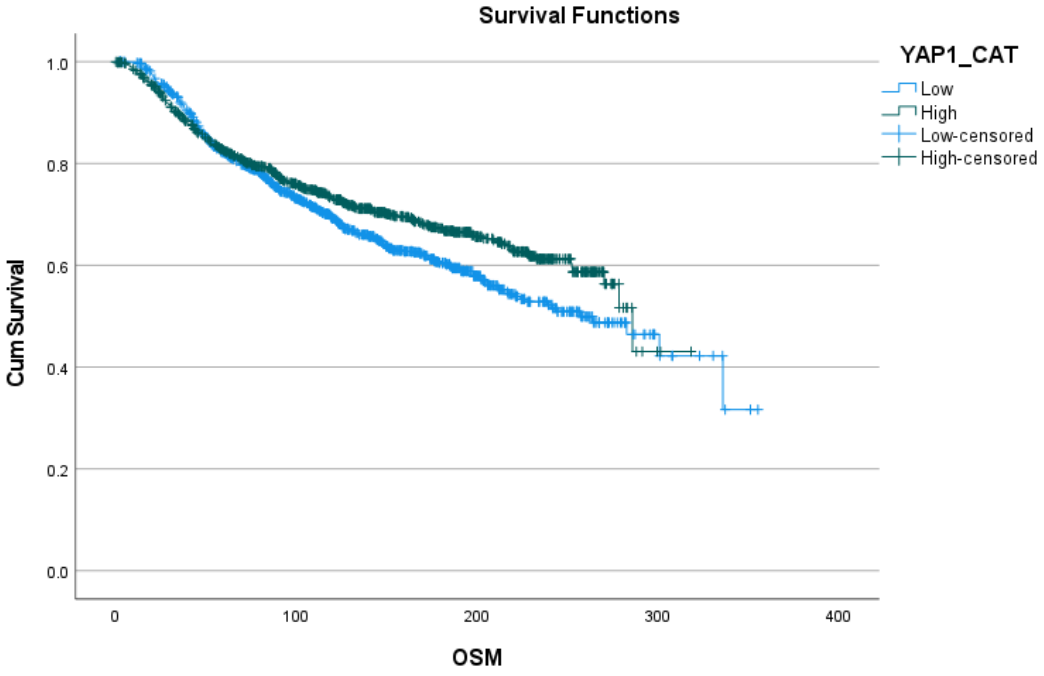

Figure A32.. Kaplan-Meier plot of YAP1, in the predicted to be activated transcription regulators in T47D CASTII overexpression. Showed a significant association with survival (P=0.023).

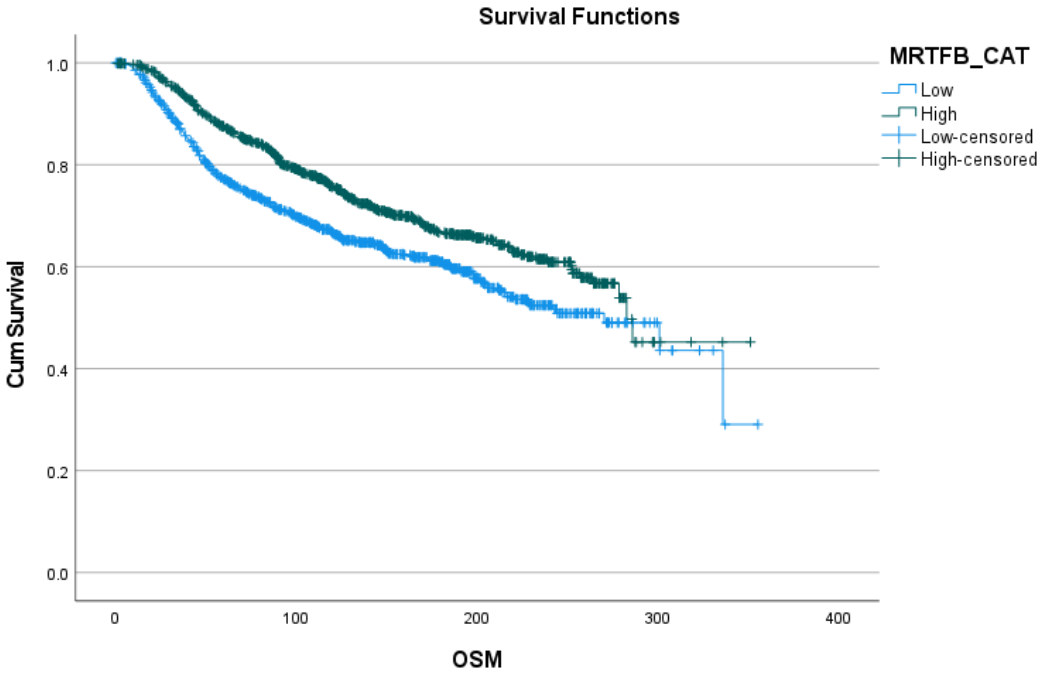

Figure A33.. Kaplan-Meier plot of MRTFB, in the predicted to be activated transcription regulators in T47D CASTII overexpression. Showed a significant association with survival (P<0.001).

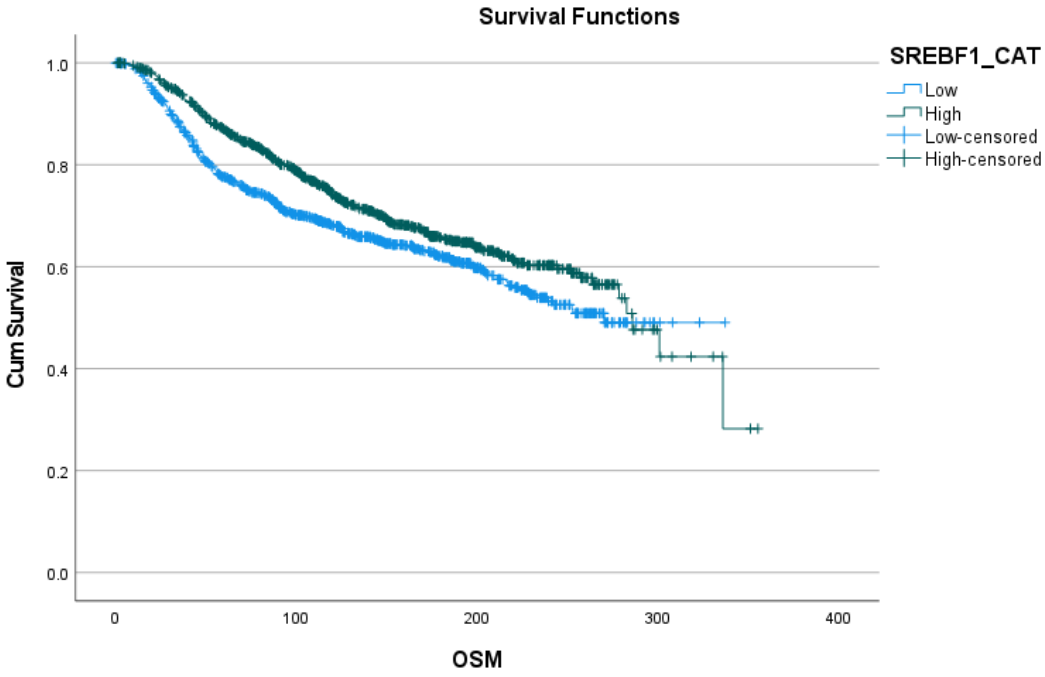

Figure A34.. Kaplan-Meier plot of SREBF1, in the predicted to be activated transcription regulators in T47D CASTII overexpression. Showed a significant association with survival (P=0.001).

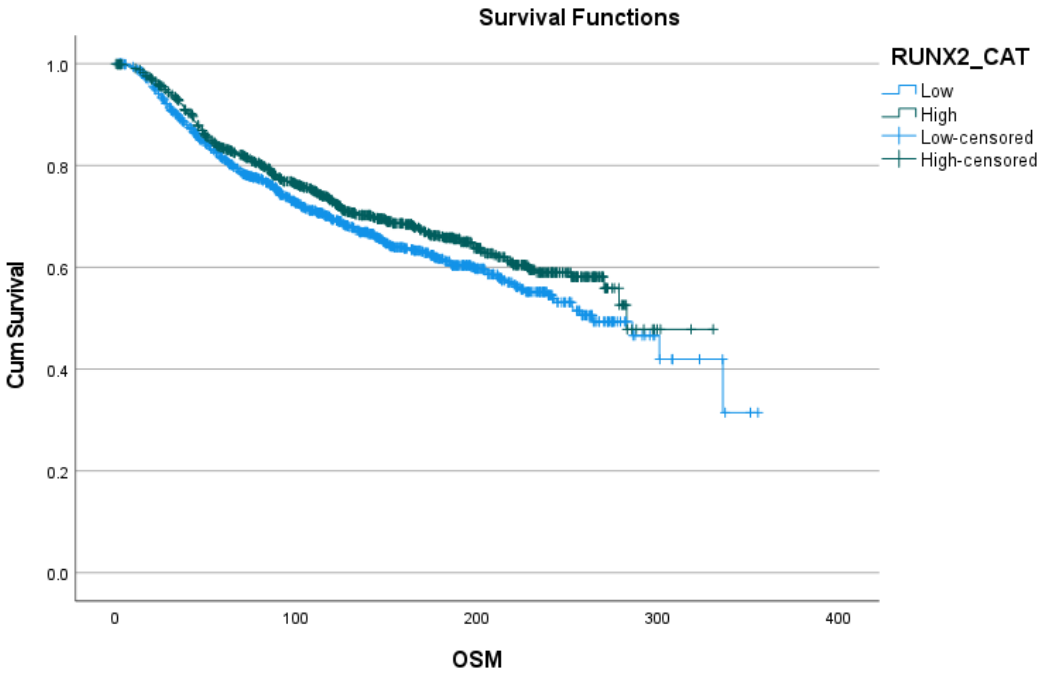

Figure A35.. Kaplan-Meier plot of RUNX2, in the predicted to be activated transcription regulators in T47D CASTII overexpression. Showed a significant association with survival (P=0.045).

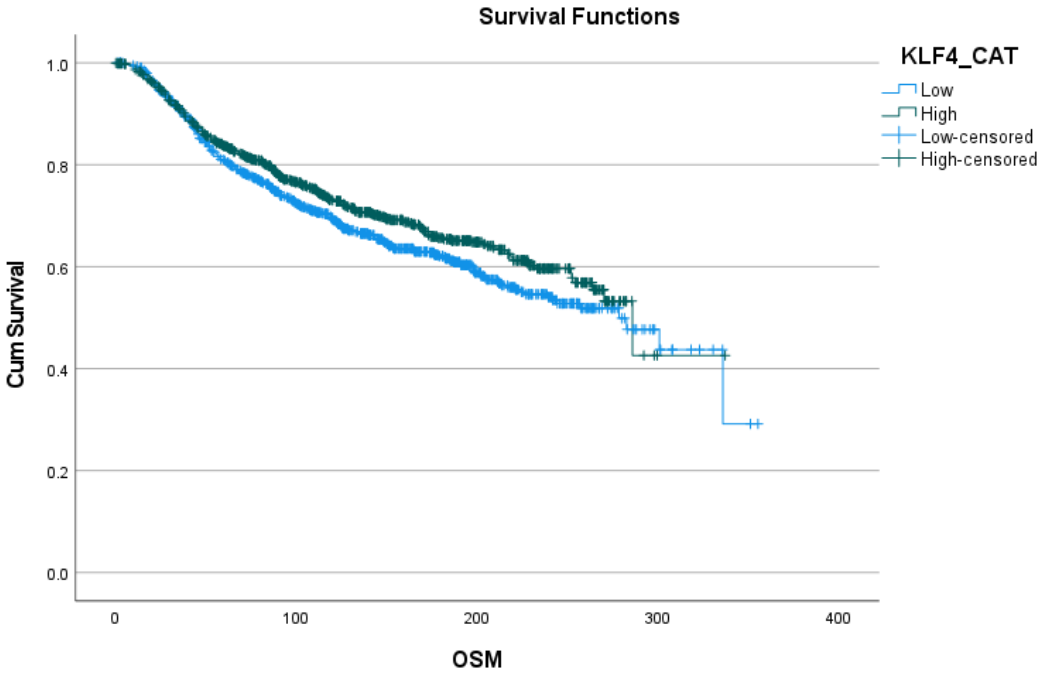

Figure A36.. Kaplan-Meier plot of KLF4, in the predicted to be activated transcription regulators in T47D CASTII overexpression. Showed a significant association with survival (P=0.047).

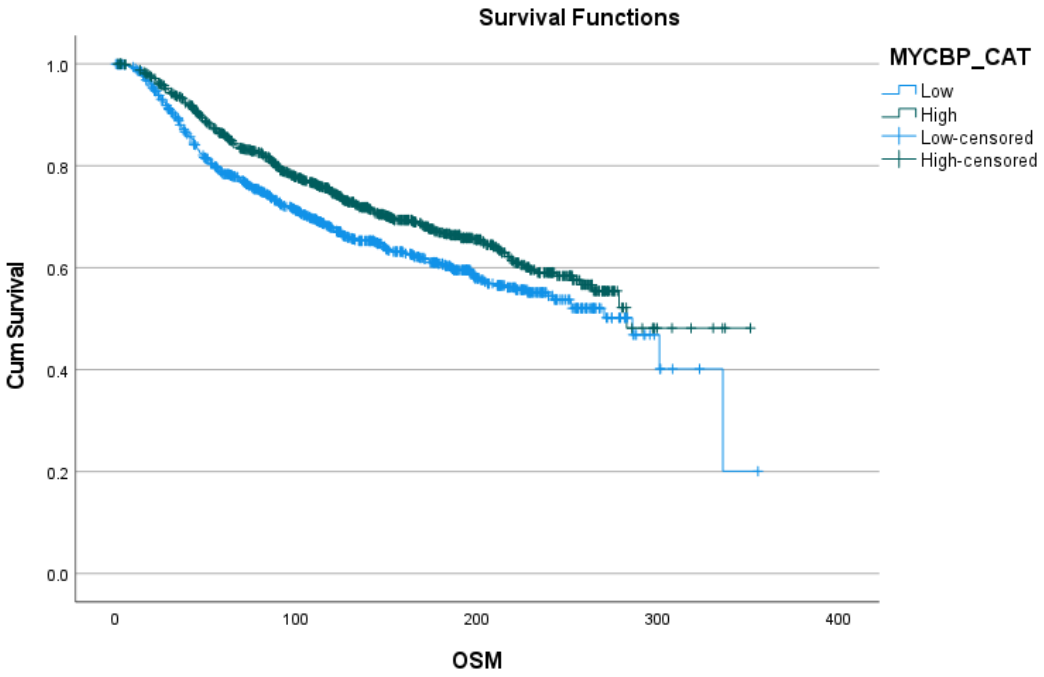

Figure A37.. Kaplan-Meier plot of MYCBP, in the predicted to be activated transcription regulators in T47D CASTII overexpression. Showed a significant association with survival (P=0.001).

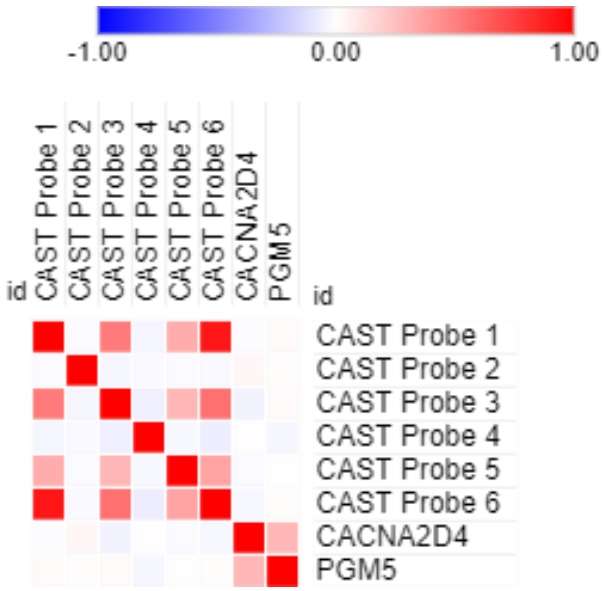

Figure A38. Heatmap of Spearman's Rank Coefficient of top 10 most significant DEGS in CAST II overexpression MDA-MB-231 with data from the METABRIC cohort ($p<0.05$)

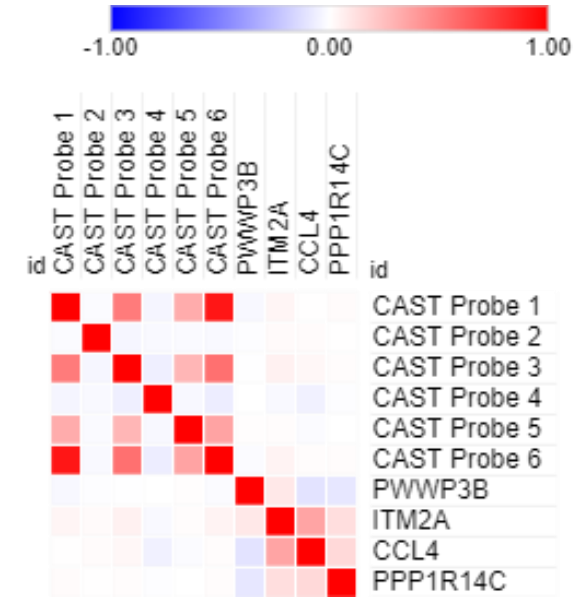

Figure A39. Heatmap of Spearman's Rank Coefficient of top 10 most upregulated t DEGS in CAST II overexpression MDA-MB-231 with data from the METABRIC cohort ($p<0.05$)

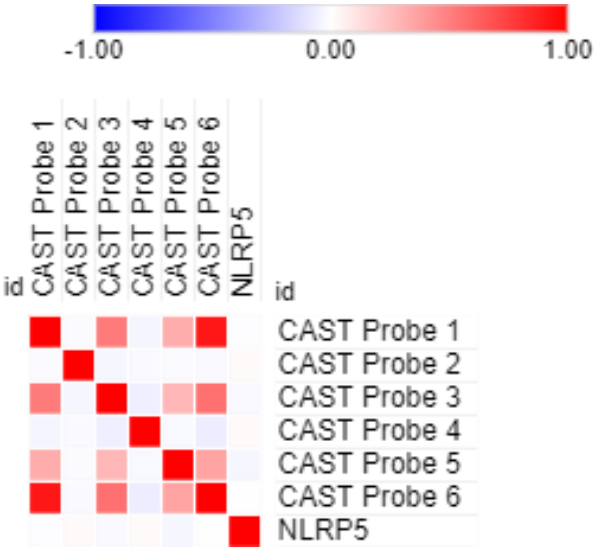

Figure A40. Heatmap of Spearman's Rank Coefficient of top 10 most downregulated DEGS in CAST II overexpression MDA-MB-231 with data from the METABRIC cohort ($p<0.05$)

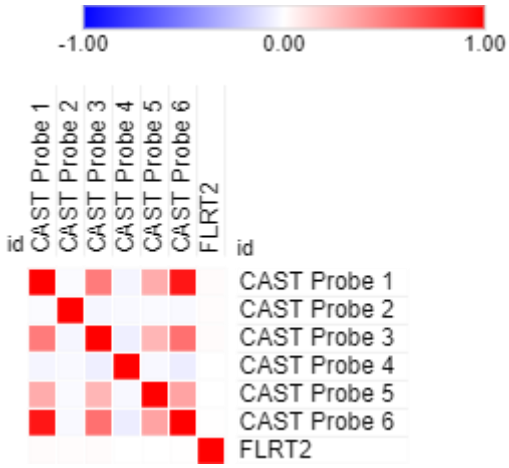

Figure A41. Heatmap of Spearman's Rank Coefficient of top 10 most significant DEGS in CAST II overexpression T47D with data from the METABRIC cohort ($p<0.05$)

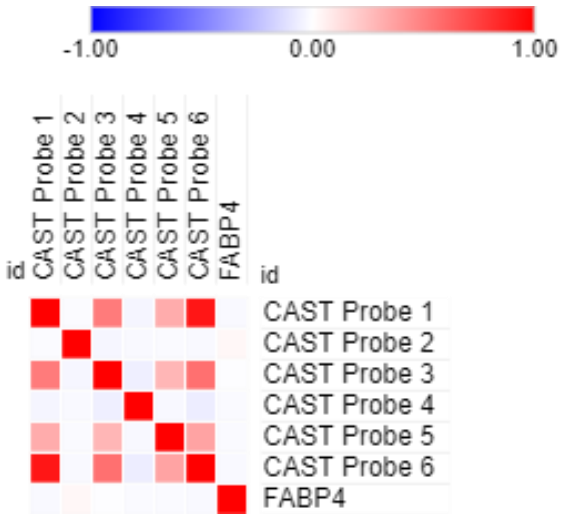

Figure A41. Heatmap of Spearman's Rank Coefficient of top 10 most upregulated DEGS in CAST II overexpression T47D with data from the METABRIC cohort ($p<0.05$)

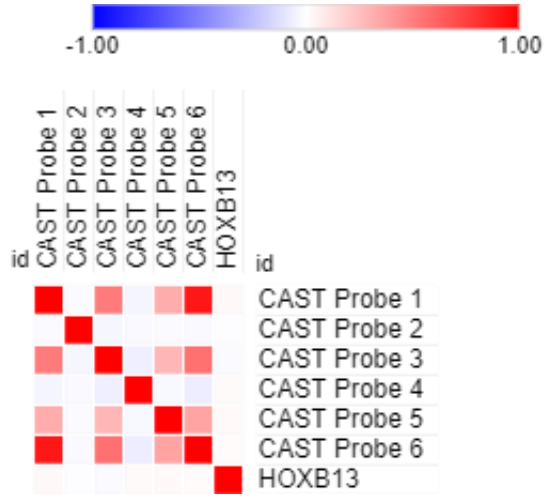

Figure A42. Heatmap of Spearman's Rank Coefficient of top 10 most downregulated DEGS in CAST II overexpression T47D with data from the METABRIC cohort ($p<0.05$)

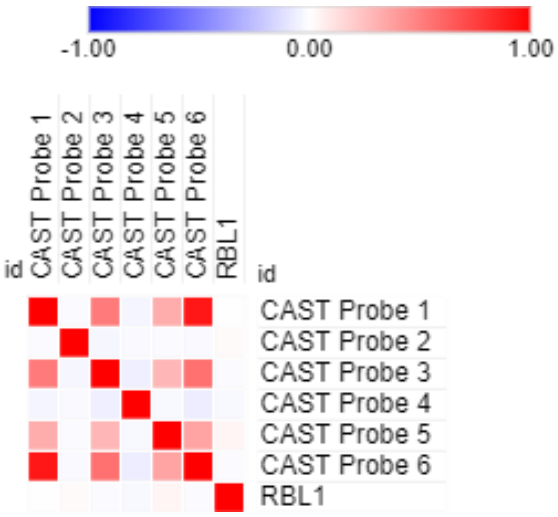

Figure A43. Heatmap of Spearman's Rank Coefficient of predicted to be inhibited transcription regulators in MDA-MB-231 CASTII overexpression cell line with data from the METABRIC cohort ($p<0.05$)

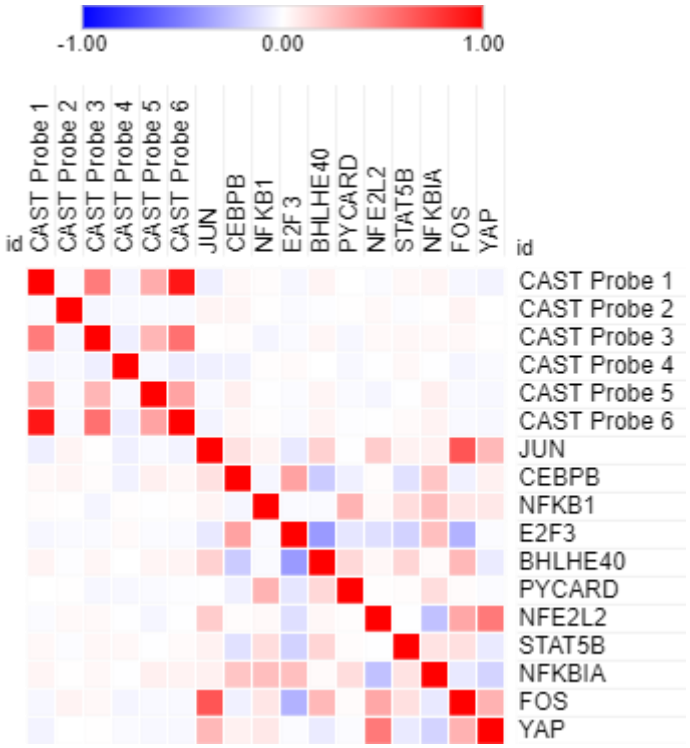

Figure A44. Heatmap of Spearman's Rank Coefficient of predicted to be activated transcription regulators in MDA-MB-231 CASTII overexpression cell line with data from the METABRIC cohort ($p<0.05$)

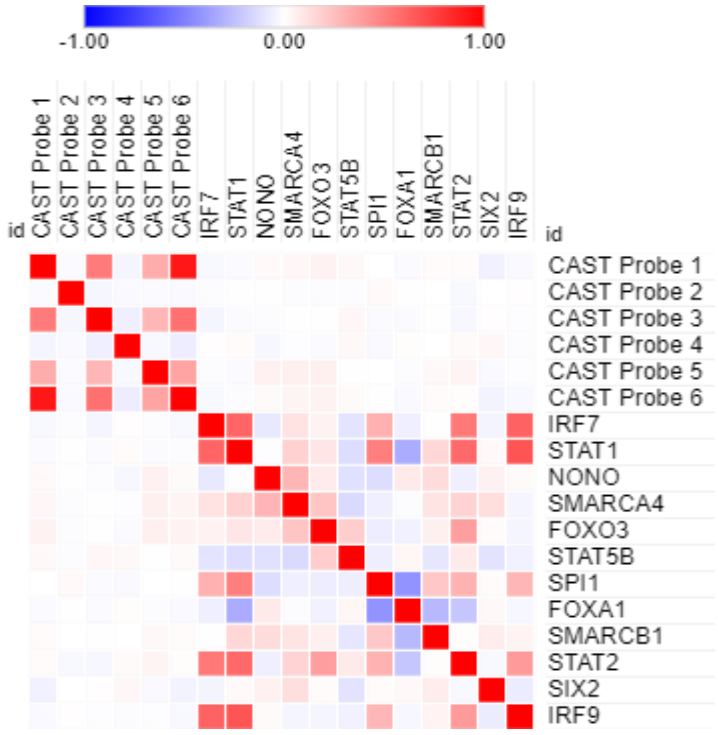

Figure A45. Heatmap of Spearman's Rank Coefficient of predicted to be inhibited transcription regulators in T47D CASTII overexpression cell line with data from the METABRIC cohort ($p<0.05$)

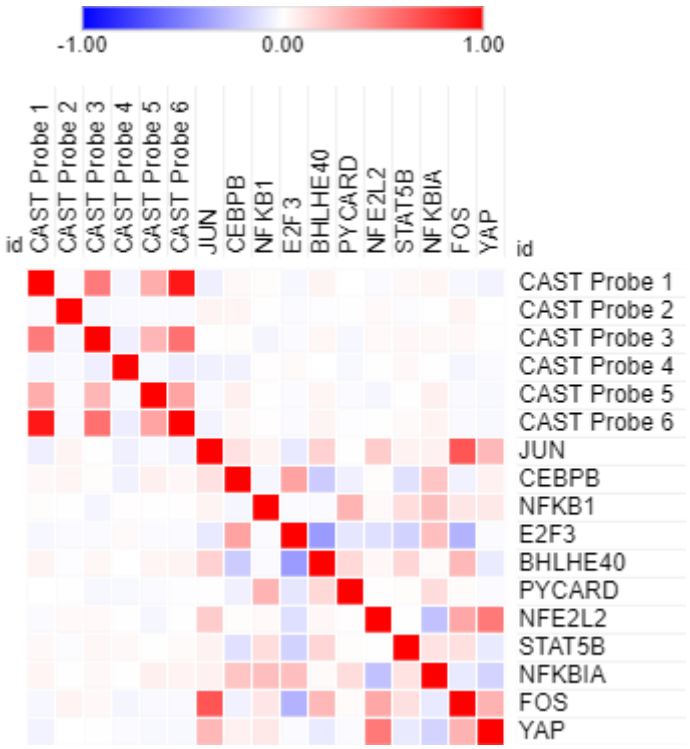

Figure A96. Heatmap of Spearman's Rank Coefficient of predicted to be activated transcription regulators in T47D CASTII overexpression cell line with data from the METABRIC cohort ($p<0.05$)